Modelling sediment and propagule pathways to improve mangrove rehabilitation

A case study of the pilot project in Demak, Indonesia

F. Bisschop

Technische Universiteit Delft

TU Delft

‘There is a reason why mangroves are not already there, find out why...’

(Lewis, 2005)

Modelling sediment and propagule pathways to improve mangrove rehabilitation

A case study of the pilot project in Demak, Indonesia

by

F. Bisschop

to obtain the degree of Master of Science
at the Delft University of Technology,
to be defended publicly on Friday February 3, 2023 at 13:45.

Student number:	4684893	
Project duration:	April 12, 2022 –	
Thesis committee:	Prof. dr. ir. A. J. H. M. Reniers,	TU Delft, chair
	Dr. ir. A. Gijón Mancheño,	TU Delft, daily supervisor
	Dr. ir. S. G. Pearson,	TU Delft, daily supervisor
	ir. B. P. Smits,	Deltares, supervisor

An electronic version of this thesis is available at http://repository.tudelft.nl/.

TU Delft Delft University of Technology

Deltares Enabling Delta Life

Preface

This report describes the results of my thesis research for the master program Hydraulic Engineering at the Delft University of Technology. This research is a modelling study of sediment and propagule pathways of the mangrove coastal system of Demak. The topic is very interesting for me, because it gave me the opportunity to extend my knowledge on the combination of hydraulic and ecological engineering. I really enjoyed working on this research and, I hope I have made a small contribution towards the development of SedTRAILS and the improvement of mangrove rehabilitation.

I would like to thank my graduation committee, who were all always enthusiastic to help me. Ad, the chair of my committee, your extensive knowledge about hydrodynamics and morphology was very valuable. Alejandra, my daily supervisor, thanks for setting up this project, I learned much of your structured guidance, your feedback about my report and your knowledge about the area. Stuart, also my daily supervisor, thanks for helping me with diving into the code of SedTRAILS and setting up a new propagule module. Bob, my supervisor at Deltares, your knowledge about the area and setting up a model in Delft3D was very helpful.

Lastly, I would like to thank my family and friends who kept me motivated throughout my research.

F. Bisschop
Delft, January 2023

Abstract

Mangrove forests are important (sub)tropical intertidal ecosystems providing coastal protection and other ecosystem services like carbon storage and biodiversity. In view of the loss of these forests many rehabilitation projects have started, but unfortunately these efforts often fail. A main cause for coastal erosion is a disrupted (fine) sediment balance due to human interventions. This imbalance prevents establishment of propagules (floating mangrove seeds) at intertidal areas and the early growth of planted mangroves. Coastal solutions such as permeable dams have aimed to stop the erosion, but we need additional systematic methodologies to understand the coastal system.

The objective of this thesis is to extend the physical and ecological understanding of coastal mangrove systems, especially of currents, sediment pathways and propagule pathways, to improve rehabilitation strategies using Demak (Central Java, Indonesia) as study area. Demak's coastline suffers from erosion problems, originating from extensive land use by fish ponds and land subsidence. An idealized morphostatic 3D model was set up in Delft3D-4 to simulate the hydrodynamics of the area, influenced by the interaction between flows due to river discharge, tides and wind. The simulations are used as input for the SedTRAILS particle tracking model to compute sediment and propagule pathways.

The model results support that sediment supplied by alongshore currents and riverine sediment could serve as source for the coastline. The river plume is at the same time obstructing as well as trapping sediment and propagules, because stratification prevents mixing of the sea and river water. However, sediments suspended near the bed could be transported underneath the river plume towards the coast by estuarine circulation. Another lesson learnt is that sediment (suspended in the water column) and propagules (floating around the water surface) do not follow the same pathways, as for propagule dispersal the wind direction is of much larger influence than tidal currents. The simulations confirmed that seasonal variability in wind direction could significantly influence the establishment area and availability of propagules, and old fish pond bunds can increase the establishment area for propagules. Sensitivity analysis show that the timing of propagule release within one tidal cycle (flood-ebb) influences the probability to successfully establish on the nearby coast. A propagule survival module is developed (based on inundation-free period and bed shear stress) as stormy seasons may increase the sediment establishment, but the larger bed shear stresses may lower the survival of propagules.

Although this modelling study is focusing on Demak, there are many other similar mangrove coasts around the world where an idealized model would enable to understand where the sediment and propagules are going and the travel time from source to sink. Permeable bamboo dams would be recommended to add to the model in further research, because they could increase the survival of propagules by reducing bed shear stresses and increase the establishment of propagules by trapping them. In conclusion, this research has made a start in counteracting coastal erosion and improving the success of mangrove forest rehabilitation by studying sediment and propagule pathways, and developing a propagule survival module.

Samenvatting

Mangrovebossen zijn belangrijke (sub)tropische intergetijde ecosystemen die de kust beschermen en andere ecosysteemdiensten zoals koolstofopslag en biodiversiteit leveren. Gezien het verlies van deze bossen zijn veel herstelprojecten gestart, maar helaas mislukken deze inspanningen vaak. Een belangrijke oorzaak van kusterosie is een verstoorde (fijn) sediment balans als gevolg van menselijke ingrepen. Dit verstoorde evenwicht verhindert de vestiging van propagulen (drijvende mangrove zaden) in intergetijdengebieden en de eerste groei van aangeplante mangroves. Kustoplossingen zoals doorlaatbare dammen hebben als doel de erosie te stoppen, maar we hebben aanvullende systematische methoden nodig om het kustsysteem te begrijpen.

Het doel van deze thesis is om het fysische en ecologische begrip van mangrovesystemen aan de kust uit te breiden, met name van stromingen, sedimentpaden en propagulepaden, om herstelstrategieën te verbeteren met Demak (Midden-Java, Indonesië) als studiegebied. De kustlijn van Demak kampt met erosieproblemen, veroorzaakt door extensief landgebruik door visvijvers en bodemdaling. Een geïdealiseerd morfostatisch 3D-model is opgezet in Delft3D-4 om de hydrodynamica van het gebied te simuleren, beïnvloed door de interactie tussen stromingen als gevolg van rivieren, getij en wind. De simulaties worden gebruikt als input voor het SedTRAILS particle tracking model voor het berekenen van sediment- en propagulepaden.

De modelresultaten bevestigen dat sediment dat wordt aangevoerd door kuststromingen en de rivier als bron voor de kustlijn kunnen dienen. De rivierpluim houdt zowel sediment en propagulen tegen als vast, omdat de stratificatie vermenging van het zee- en rivierwater verhindert. Sedimenten in suspensie nabij de bodem kunnen echter door de estuariene circulatie onder de rivierpluim door naar de kust worden getransporteerd. Sediment (in suspensie in de waterkolom) en propagulen (drijvend rond het wateroppervlak) volgen niet dezelfde paden, aangezien voor de verspreiding van propagulen de windrichting van veel grotere invloed is dan de getijdenstroming. De simulaties bevestigen dat een seizoensgebonden windrichting het vestigingsgebied en de beschikbaarheid van propagulen aanzienlijk kan beïnvloeden, en dat oude visvijverdammen het vestigingsgebied voor propagulen kunnen vergroten. Gevoeligheidsanalyses tonen aan dat het tijdstip binnen een getijdecyclus (vloed-ebb) waarop propagulen worden losgelaten de kans van succesvolle vestiging op de nabijgelegen kust beïnvloedt. Er is een overlevingsmodule voor propagulen ontwikkeld (gebaseerd op inundatievrije periode en bodemschuifspanning), aangezien stormachtige seizoenen de vestiging van sediment kunnen vergroten, maar de grotere bodemschuifspanning de overlevingskans van propagulen kan verkleinen.

Hoewel deze modelstudie is gefocust op Demak, zijn er vele andere soortgelijke mangrovekusten in de wereld waar een geïdealiseerd model het mogelijk zou maken te begrijpen waar het sediment en de propagulen naartoe gaan en hoeveel tijd het kost van bron tot eindpunt. Doorlatende bamboo dammen zouden in verder onderzoek aan het model kunnen worden toegevoegd, omdat deze de overlevingskans van propagulen zouden kunnen vergroten door de bodemschuifspanning te verkleinen en de vestiging van propagulen kunnen vergroten door ze vast te houden. Concluderend, dit onderzoek een begin heeft gemaakt het tegengaan van kusterosie en het verbeteren van het succes van het herstel van mangrovebossen door het bestuderen van de paden van sediment en propagulen en het ontwikkelen van een overlevingsmodule voor propagulen.

Contents

1

Introduction

This chapter introduces the research by giving the context, problem statement, objective, research questions including hypotheses and the methodology.

1.1. Context

Mangrove forests are important (sub)tropical intertidal ecosystems providing coastal protection and other ecosystem services like carbon storage and biodiversity (van Eekelen and Bouw, 2020). They are found along muddy coastlines with relatively low wave energy between 30˚N and 30˚S latitude (Giri et al., 2011), see Figure 1.1. In these areas mangroves can reduce water levels during storm events (Gedan et al., 2011). In addition, the dense root systems above the bottom level dissipate wave energy, favouring sediment accretion. This protects against shoreline erosion (Thampanya et al., 2006). This vertical sediment accretion could compensate partly or totally the rates of relative sea level rise, which is a major problem in many mangrove areas. In the current situation of climate change and the subsequent rising sea levels, these protection services of mangroves become even more important for flood risk reduction (Winterwerp et al., 2013).

The annual economic value of mangroves, estimated by the cost of the products and ecosystem services they provide, is around 200,000 to 900,000 USD per km^2 per year (Wells and Ravilious, 2006). Despite their importance, mangrove forests have lost around 1-2% per year of their area from 1980 to 2000, which slightly decreased to 0.7% from 2000 to 2005 (FAO, 2007). There are several reasons for these degradations and losses: conversion of mangrove forests into fishponds, cutting mangrove trees for wood, development of infrastructure, urbanization and groundwater extraction including land subsidence (Winterwerp et al., 2020). Therefore, many rehabilitation projects have started, but unfortunately these efforts often fail. The survival of planted mangroves was for example only 5-10% in a large project of 44 thousand hectare in the Philippines (Primavera and Esteban, 2008).

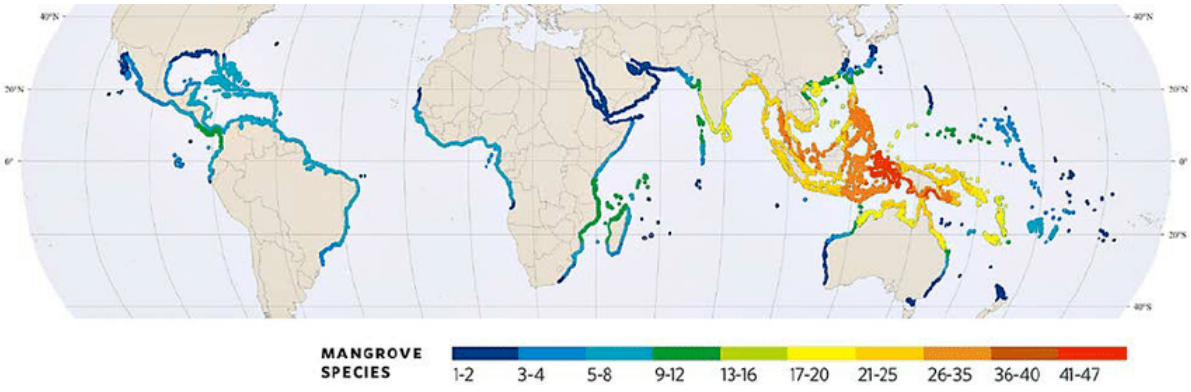

Figure 1.1: World map of the mangrove distribution zones and the number of mangrove species along each region (Michel, 2014).

Many researchers of the ecosystem restoration movement (Lewis, 2005; Winterwerp et al., 2014) think that those mangrove efforts failed, because practitioners ignored the state of the mangrove habitat. The main premise of the ecosystem restoration movement is that if mangroves are not returning naturally, it is because their habitat requirements are not satisfied, and those requirements should be restored first. For instance, in some places the hydrology has to be recovered by earth excavations or fillings (Turner and Lewis, 1997). In the specific case of eroding coastlines, where erosion should be stopped to have mangrove establishment, one of main causes is a disrupted (fine) sediment balance due to human interventions. This imbalance prevents establishment of propagules (floating mangrove seeds) at intertidal areas and the early growth of planted mangroves (Stanley and Lewis, 2009).

The problem of this erosion preventing the mangroves from establishing, has been addressed by building temporary permeable dams that promote sediment accumulation near the coast (Winterwerp et al., 2013). Another option would be to use hard structures, but at fine-sediment coastlines, reflection and scour often result failure of these structures. Permeable dams can cause accretion, the coastal protection pilot project in Demak (Central Java, Indonesia) is an example of where they are applied at an eroding shoreline. The dams caused on average 20-30 cm of vertical accretion in Demak, but this amount was insufficient to stop coastline retreat and cause long-term mangrove restoration (Winterwerp et al., 2020). However, the dams significantly increased the survival of already established mangrove seedlings compared to sites more exposed to waves (van Bijsterveldt et al., 2022). At the start of the project in Demak the extent of subsidence rates in the area was not known and not accounted for in the designs. Although if subsidence is a large factor, it is still not known how to account for in future designs. The dam designs themselves were also quite empirical in general. Concluding, it is necessary to extend the understanding of the physical processes behind the erosive sediment transport, to develop better strategies to restore mangroves.

A better understanding of the disrupted (fine) sediment balance would therefore be useful for decision-makers trying to intervene in the eroding coastal system. An idealized model of a mangrove coastline would enable coastal managers to understand where the sediment and propagules are going and how long it takes to travel from source to sink. Quantifying these sediment fluxes is essential for sustainable coastal management (Hendriks et al., 2020; Pearson et al., 2020). The Demak pilot area in Indonesia is very suitable for this idealized model, since the area is well-known. Several field campaigns and modelling studies were done in the area (Bijsterveldt et al., 2020; Tas et al., 2020; Van Domburg, 2018; Smits, 2016). Demak's coastline suffers from erosion problems, originating from extensive land use by fish ponds and land subsidence. The area extends from the Semarang City to the Wulan River, in between there are inundated fish ponds, which have replaced the earlier mangrove forest.

Developing a idealized model of Demak can be very useful to understand the current, sediment pathways and propagule pathways, which are influenced by the interaction between flows due to the Wulan river discharge, tides and wind. In such a idealized model, one can look at the coastal system in a relatively simple way, including the physical behaviour of different processes and increasing the system complexity by adding them sequentially. Understanding these physical processes will be critical in counteracting coastal erosion and improving the success of mangrove forest rehabilitation.

1.2. Problem Statement

Mangrove establishment at eroding coastlines is hindered by the continuous loss of habitat, and the increasing water depths. Coastal solutions such as permeable dams have aimed to stop erosion, but we lack additional systematic methodologies to understand the coastal system, especially with respect to morphodynamic and ecological processes, and evaluate the potential effect of dams on the morphodynamics. At the eroding coastline of Demak dams were build, but tools to predict their morphodynamics are lacking. Thus before mangrove propagules will be able to re-establish at this coast, the sediment balance has to be restored, which requires additional knowledge of the sediment pathways from source to sink. To conclude, the problem is the limited knowledge of the sediment and propagule pathways along mangrove coastlines.

1.3. Objective

The objective of this thesis is to extend the physical and ecological understanding of coastal mangrove systems, especially of currents, sediment pathways and propagule pathways to improve rehabilitation strategies using Demak as study area. The currents, sediment pathways and mangrove propagule pathways are influenced by the interaction between flows due to the river discharge, tides and wind. This objective is presented in the following research question:

What can we learn from modelling sediment and propagule pathways to improve mangrove rehabilitation strategies?

This research question will be answered using the following sub-questions in four phases:

Phase A - Currents:

1a. How are currents influenced by the interaction of barotropic forcings (tidal flows, river discharge and wind) and geometric features (protruding delta and basins)?

1b. How are currents influenced by the interaction of tidal flows and river discharge, including baroclinic forcing?

Phase B - Sediment Pathways:

2a. How are sediment pathways and connectivity influenced by the interaction of barotropic forcings (tidal flows, river discharge and wind) and geometric features (protruding delta and basins)?

2b. How are sediment pathways and connectivity influenced by the interaction of tidal flows and river discharge, including baroclinic forcing?

3. What are the similarities and differences between the muddy and sandy sediment pathways?

Phase C - Propagule Pathways:

4. How are mangrove propagule pathways and connectivity influenced by the interaction of tidal flows and river discharge?

5. How is the survival of mangrove propagules at the establishment area influenced by the 'Windows of Opportunity'?

6. What are the similarities and differences between the sediment and propagule pathways?

1.4. Hypothesis

The hypothesis of this research is that we can have a better understanding of the physical processes affecting the Demak coastline by modelling sediment transport pathways and thereby can improve mangrove rehabilitation strategies to a certain extent. For each sub-question, the hypotheses are formulated and supported by Figure 1.2, which shows a conceptual overview of important site conditions affecting the Demak coastline:

1.
   - Wet season: It is expected that there is a river water plume staying along the coastline, due to stratified currents by the large river discharge and winds from offshore.
   - Dry season: It is expected that river and coastal waters mix, due to relatively large tidal influence in comparison to the low river discharge and winds from onshore.

2.
   - Wet season: It is expected that riverine sediments stay along the coastline and sedimentation takes places in tidal basins.
   - Dry season: It is expected that mixed river sediments are transported offshore and there is some deposition of sediment still suspended from the wet season in tidal basins.

3. It is expected that the finer muddy sediments are more mobile and transported higher up in the water column than the sandy sediments, which results in different pathways. Furthermore, mud is abundant in the area and sand availability is spatially very restricted.

4. • Wet season: It is expected that propagules stay along the coastline, due to stratification and offshore wind.
   • Dry season: It is expected that onshore wind and tidal mixing push propagules to offshore waters.
5. • Wet season: It is expected that survival of mangroves propagules is relatively low due to larger waves and erosive forces.
   • Dry season: It is expected that survival of mangrove propagules is relatively high due to the calmer conditions.
6. It is expected that the fine (O(m^{-7}-m^{-4})) but heavier (2650 kg/m^3) sediments are mainly dependent on current velocities in the water column relatively closer to the bed, while larger (O(m^{-2}-m^{-1})) but lighter floating propagules on velocities near the water surface, which results in different pathways.

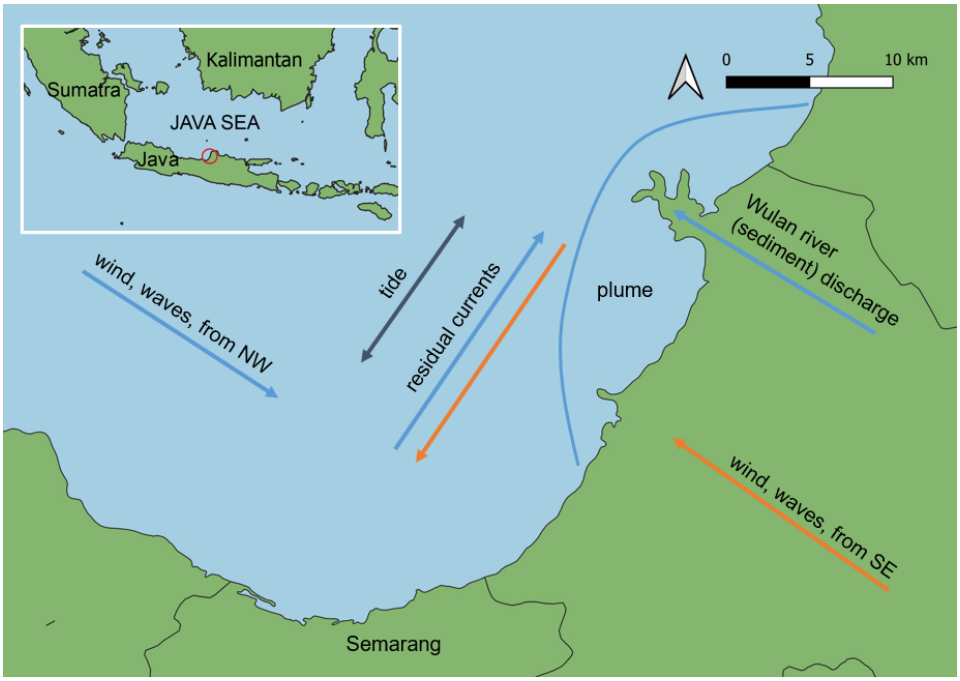

Figure 1.2: Visualization of the important site conditions affecting the Demak coastline during the wet season (blue) and dry season (orange).

1.5. Methodology

To answer the research question and corresponding sub-questions, the following steps are performed. First a literature study is executed to describe the different physical processes at eroding mangrove coastlines, especially for the ecology, hydrodynamics, morphodynamics and erosion-mitigation measures (Chapter 2). The coastal characteristics of the Demak area, from Semarang to the Wulan River are described in Chapter 3. Furthermore, it is investigated how the models Delft3D-4 and SedTRAILS work and which processes have to be included. From here a idealized morphostatic model of the Demak area is set up in Delft3D-4, the geometry of the coastal area and processes are simplified (Chapter 4). This model simulates the hydrodynamics, which are used as input in the particle tracking model SedTRAILS to simulate sediment and mangrove propagule pathways. A new module is developed in SedTRAILS for propagule pathways including the survival, as SedTRAILS is originally intended for sediment. The results of the simulations are analyzed (Chapter 5) and the influence of the interaction between the flows due to river discharge and tidal flow is discussed, as well as verification of the model results by expert judgement. Finally, the important conclusions of the research are summarized including recommendations for further research (Chapter 7).

2

Literature

This first chapter describes a literature study about the physical processes at eroding mangrove coastlines, especially on the ecology, hydrodynamics, morphodynamics and solutions.

2.1. Mangrove Ecology

This section elaborates on the ecosystem services, dispersal and establishment of mangrove forests.

2.1.1. Ecosystem Services

Mangroves are a group of salt-water tolerant trees and shrubs in the intertidal zone. They are found at (sub)tropical muddy coasts with relatively low wave energy between 30˚N and 30˚S latitude (Giri et al., 2011). Mangroves are especially adapted to coastal environments, including high salinity, flooding, muddy sediments and a lack of oxygen at their roots. Mangroves have dense roots above bottom level, which capture sediment and dissipate wave energy. In this way a natural coastal barrier is created, which reduces erosion (Thampanya et al., 2006) and limits flooding of the hinterland (Gedan et al., 2011).

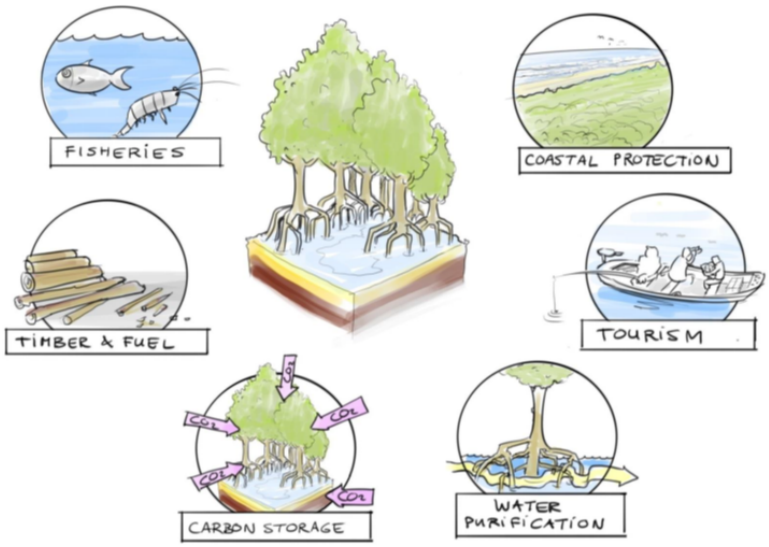

Figure 2.1: Ecosystem services of mangrove forests (EcoShape, 2015).

Besides sediment stabilization and flood protection mangroves provide many more ecosystem services (see Figure 2.1). For instance, they provide local communities with seafood production, timber (Rönnbäck, 1999) and tourism. Mangrove forests store carbon and are even one of the most carbon-rich forests in the world, thereby regulating carbon dioxide levels (Donato et al., 2011). They store and

recycle nutrients and pollutants by filtering water and providing good water quality. Mangroves also induce sedimentation by organic matter production and hereby maintain soil fertility (Thongjoo et al., 2018). In addition, they are a barrier against salt water intrusion. Finally, a healthy mangrove forest ecosystem provides for a lot of biodiversity as habitat (nursery, breeding and feeding ground) and even supports other coastal ecosystems. The annual economic value of mangroves, estimated by the cost of the products and ecosystem services they provide, is around 200,000 to 900,000 USD per km^2 per year (Wells and Ravilious, 2006). Summarizing, mangrove forests are important (sub)tropical intertidal ecosystems providing coastal protection and other ecosystem services (van Eekelen and Bouw, 2020).

2.1.2. Propagules

Floating mangrove seeds (Figure 2.2) are technically called propagules, because they germinate while they are still on the tree. In general most plant seeds germinate when there are dispersed, whereas the adaptation of mangrove propagules helps them establish quickly when dropped to the soil (Moore, 2009). Before settlement, propagules disperse via currents within and between populations, increasing biological connectivity (der Stocken et al., 2019a). Dispersal is an essential process that determines the potential of a species to colonize new habitats suitable for establishment (der Stocken et al., 2019b). When the propagule establishes in the ground and grows to a small plant, it is called seedling, and then growing further to a young tree or sapling.

Figure 2.2: Stages of development for propagules, from germinating seed (bottom) to rooted seedling (top), O(1-30cm) (Moore, 2009).

2.1.3. Dispersal

In this research we focus on the dominant transport mechanism of buoyant mangrove propagules: near- and alongshore dispersal O(10km), in other words short distance dispersal (SDD). Triest et al. (2018) found that rivers act as physical barriers for SDD affecting connectivity. Transport across oceans by eastern and western boundary currents and large gyres O(100-1000 km) is called long distance dispersal (LDD) (der Stocken et al., 2019b). LDD allows mangroves shifting their geographic ranges to follow changing climate conditions, for instance poleward expansion of mangroves has been observed (Cavanaugh et al., 2014; Saintilan et al., 2014). For LDD the chances increase of loss during dispersal or arriving at unsuitable site (der Stocken et al., 2019a). Floating periods of propagules depend on dispersal (tidal flow, freshwater discharge and wind), trapping (retention by vegetation and tidal flats) and seed properties (numbers, size, shape, buoyancy and viability) (Nitto et al., 2013; der Stocken and Menemenlis, 2017; Stocken et al., 2015a).

The buoyancy and viability period of a propagule determines the maximum period available for successful dispersal, there is a lot of variation of this period even within species (Appendix C). Some species have even no buoyancy, other may float for around 300 days and some can be become buoyant again after stranding. In general a weeks to several months can be assumed for buoyancy and viability periods are in the order of months (der Stocken et al., 2019b). After 1 to 5 weeks they often develop roots for anchoring. Propagules of small size have a higher chance of transport over longer distances, while larger propagules are more easily become trapped by other mature mangrove roots locally (der Stocken et al., 2019a). Apart from the maximum period, mangrove propagules also have a minimum period for dispersal, which is determined by the obligate dispersal period (ODP). This ODP is the period after abscission when a propagule is not yet able to initiate root growth or to germinate (Rabinowitz, 1978).

Phenology or the timing of recurring biological events (Lieth and of Biological Sciences., 1974), is often neglected in propagule dispersal research (der Stocken et al., 2017). Although timing of propagule release significantly alters the resulting deposition area of dispersal (Savage et al., 2010). Alleman and Hester (2011) found that mangrove trees tend to produce higher numbers of propagules in years after hurricanes, a sort of compensating mechanism for the storm damage to the trees. Their results suggest that trees individually vary the amount of energy they invest in reproduction in consecutive years. Even within year there are seasons where mangroves produce more propagules than other seasons (der Stocken et al., 2017). This research found significant correlations between mangrove propagule release and rainfall, with 72% of data reporting propagule release during the wet season, except in the southernmost latitudes. In the equatorial zone (10°N–10°S), propagules fall from parent trees throughout most of the year without pronounced production peaks. At latitudes higher than the equatorial zone, propagule release was also significantly correlated with temperature. Their results (der Stocken et al., 2017) show phenological complementairy between the northern and southern hemisphere, with a peak in propagule release in summer. However, it must be taken into account that due to the complex environmental determinants that govern phenology in mangroves, the phenology of propagule release can be highly species and location specific (der Stocken et al., 2019a). Altogether, the individual, yearly and seasonally variations in the amount of propagules affect the distribution.

To conclude, dispersal forces, trapping factors and seed properties determine the period in which propagules can be transported to a coastal habitat suitable for establishment. Therefore, floating periods in combination with prevailing currents and wind determine spatial scales of dispersal, geography of mangrove species, and genetic diversity.

2.1.4. Establishment

After dispersal the propagules need to establish somewhere. Balke et al. (2011) has formulated three thresholds needed for successful mangrove restoration by understanding the processes of propagule establishment (phase 1 to 3 in Figure 2.3):

1. “stranded propagules need an inundation-free period to rapidly develop roots that are long enough to withstand displacement by flooding,

2. roots need to become long enough to withstand seedling dislodgement by hydrodynamic forces from waves and currents, with the required root length being proportional to the force that needs to be resisted,

3. even longer roots are needed to survive high energy events that cause sheet erosion and can thereby induce seedling dislodgement.”

van Bijsterveldt et al. (2022) added phase 0 and 4 to these windows of opportunity of Balke et al. (2011). This research focuses on phase 0, the propagule availability: sources of propagules and which locations are connected to these sources. These windows of opportunity can be extended by for instance: digging a creek in a fish pond and thereby re-establishing propagule connectivity and initiating mangrove growth (phase 0). Another example is placing permeable dams, increasing bed level by sediment trapping (phase 1) as well as decreasing wave stresses (phase 2).

In many rehabilitation projects mangrove establishment is artificially done by replanting mangroves, but this is not necessary if mangrove propagules are already available in the area and the environmental conditions are favorable. In many cases there is already an abundant supply of mangrove propagules (phase 0), which will establish naturally if phases 1 to 4 are satisfied. If there are no growth limitations

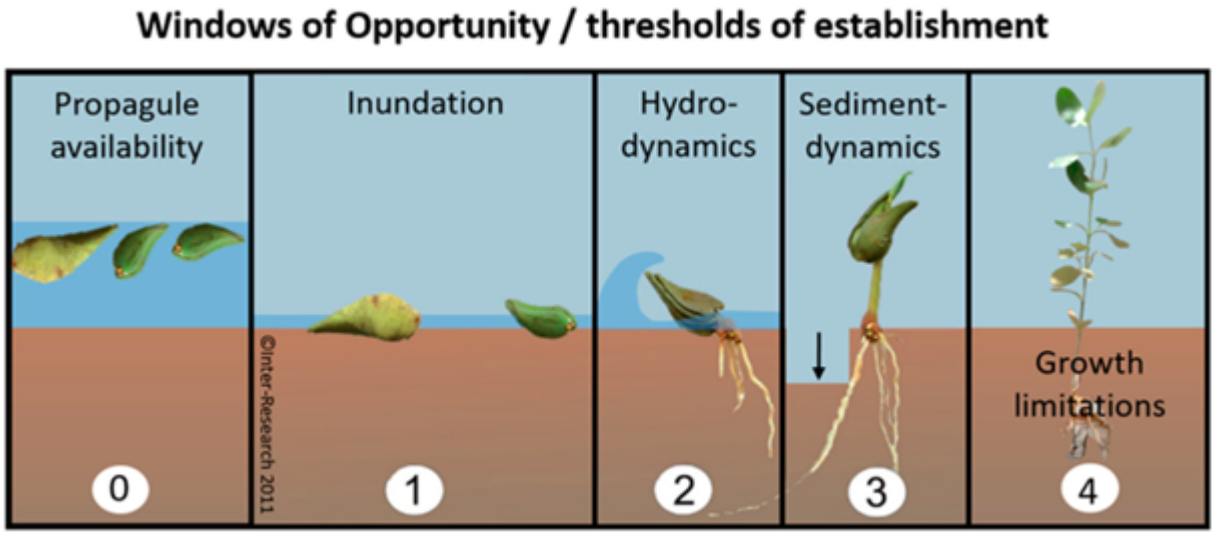

Figure 2.3: Windows of opportunity that propagules should encounter (or threshold of establishment that propagules should overcome) before they can colonize a site (van Bijsterveldt et al., 2022; Balke et al., 2011).

(phase 4) propagules establish and mangrove growth can be rapid, reaching heights of 2 m in two years. Altogether, in limited cases mangrove propagule supply is a constraint and there mangrove planting can be considered (Winterwerp et al., 2013). Identifying locations where supply is constrained could help focusing planting efforts. This research investigates on the availability of propagules (phase 0), by assessing propagule pathways, sources and sinks.

Furthermore, Bijsterveldt et al. (2020) studied the processes controlling natural mangrove establishment in landward direction (into the fishponds) and seaward direction also using the area of the Demak coastline. Expansion in landward direction is positively related to emergence time and sediment stability, which both depend on the bed level and drainage. In this case there was no effect of the soil chemistry. On the other hand expansion in seaward direction is related to the foreshore morphology. Mangroves only expand if a mudflat is present, while they retreat if a mudflat is absent and the profile is concave (see Figure 2.5a). Concluding, landward establishment can be improved by drainage to enhance sediment stability, accretion and seaward establishment can be promoted by foreshore morphology restoration.

2.2. Erosion-mitigation measures

This section describes possible measures against erosion of the coastline are implementing hard structures or rehabilitation of mangroves.

2.2.1. Hard Structures

One could argue to implement hard structures, such as dikes, dams, breakwaters or vertical walls, as a solution to protect against erosion. However, these hard structures often work counterproductive (Ismanto et al., 2017), as the onshore sediment transport from large waves is reduced by these structures and sometimes they even aggravate the erosion (Winterwerp et al., 2005). In general the erection of hard structures affects the sediment balance with two different processes:

- Hard structures in front of the coast reduce onshore water flux (tidal prism), as the area behind these structures is closed off from tide. This reduced onshore water flux decreases the onshore flux of fine sediment.
- Hard structures in front of the coast induce wave reflection (Winterwerp et al., 2020). Due to this reflection wave heights increase close to the structures, causing local scour of the sediment. This scouring can even lead to instability of the structure.

Muddy coasts have an extra problem in comparison to sandy coasts, regarding to hard structures. Soft muddy sediment is fine, contains a lot of water, has a low permeability and obtains strength by cohesion between clay particles. The internal binding of solid mud can be broken by waves, the resulting fluid mud leads to failure of structures. All these processes together set in motion more and more erosion, this positive feedback effect is described in subsection 2.4.1 (Winterwerp et al., 2013). Concluding, hard structures are not a sustainable solution for eroding mangrove coastlines.

2.2.2. Mangrove Rehabilitation

Despite the importance of mangrove ecosystems, the amount of mangrove shorelines is declining. Annual losses were around 1-2% from 1980 to 2000 and slightly decreased to 0.7% from 2000 to 2005 (FAO, 2007). There are several reasons for these losses: conversion of mangrove forests into fishponds, cutting mangrove trees for wood, development of infrastructure, urbanization and groundwater extraction including land subsidence (Winterwerp et al., 2020). Many rehabilitation projects have started, but unfortunately these mangrove planting efforts often fail. The survival of planted mangroves was for example only 5-10% in a large project of 44 thousand hectare in the Philippines (Primavera and Esteban, 2008).

To overcome failure of mangrove planing, interests have been shifting increasingly towards restoration of mangrove habitat to promote natural recruitment, rather than using active planting of mangrove propagules or seedlings (van Bijsterveldt et al., 2022). Many researchers of the Ecological Mangrove Restoration (EMR) movement (Lewis, 2005; Winterwerp et al., 2014) think that these mangrove efforts failed, because practitioners ignored the state of the mangrove habitat. Their idea is that if mangroves are not returning naturally, there is something wrong with the habitat requirements of the mangroves, and those requirements should be restored first. Lewis (2005) and Winterwerp et al. (2013) proposed five principles that bear in mind the ecology and dynamics of natural mangrove systems, learnt from rehabilitation projects:

1. “Understand the ecology of the mangrove species at the site, in particular the patterns of reproduction, propagule distribution, and successful seedling establishment.”

2. “Understand the hydrologic patterns (in particular the depth, duration and frequency of tidal inundation) that control the distribution and successful establishment and growth of (targeted) mangrove species.”

3. “Assess modifications of the original mangrove environment that currently prevent natural regeneration (recovery after damage).”

4. “Restore hydrology and other environmental conditions that encourage natural recruitment of mangrove propagules and successful plant establishment.”

5. “Only consider actual planting of propagules, collected seedlings, or cultivated seedlings after determining (through steps 1–4) that natural recruitment will not provide the quantity of successfully established seedlings, rate of stabilization, or rate of growth of saplings established as objectives for the restoration project.”

These principles explain why mangrove restoration is relatively unsuccessfull at eroding mangrove coastlines. Lewis (2005) emphasized that planting mangroves on any convenient bare mudflat is not wise, as ‘there is a reason why mangroves are not already there, find out why’. For instance, in some places the hydrology has to be recovered by earth excavations or fillings (Turner and Lewis, 1997). In the specific case of eroding coastlines, where erosion should be stopped to have mangrove establishment, one of main causes is a fine sediment balance disturbed by human interventions. This imbalance prevents the planted mangroves or propagules (floating seeds) from re-establishing (Stanley and Lewis, 2009). The coastal protection pilot project in Demak belongs to this type of eroding coastlines. Mangroves can be planted along these erosive coasts, but several factors may damage them: erosion increases the water depth, so more area may become unavailable for mangrove establishment. Larger water depths also involve larger waves, causing large forces in small seedlings, which topple over and are swept away (Winterwerp et al., 2016). Moreover, erosion in an area with seedlings may mean that seedlings are unburied during a storm. Large trees may also become unstable if their location is eroded.

The problem of this erosion preventing the mangroves from establishing has been addressed by building permeable dams that promote sediment accumulation near the coast (Winterwerp et al., 2013). Permeable dams made for example out of bamboo poles and brushwood filling, can enhance the trapping of fine sediments in the intertidal zone (Winterwerp et al., 2020). Other advantages of these dams are the reduction of wave heights and long-shore currents. By installing these permeable dams a buffer zone is created, which is still freely accessible for the tide. This is important, because the tide provides the onshore sediment flux for this buffer zone. However, brushwood filling decays, compacts rapidly and needs to be refilled regularly. Hence the required large quantities of brushwood form a large part of the total construction costs. These maintenance problems can be prevented by construction of permeable dams out of vertical bamboo poles only, without brushwood filling (Gijón Mancheño et al., 2021). Since waves at mangrove coasts behave as shallow water waves, which induce horizontal orbital movements only, the orientation of energy-dissipating elements in permeable dams becomes irrelevant (Winterwerp et al., 2020). Permeable dams caused around 20-30 cm of accretion in Demak, but this amount was insufficient to stop coastline retreat and cause long-term mangrove restoration. At the start of the project in Demak the extent of subsidence rates in the area was not known and not accounted for in the designs. Although if subsidence is a large factor, it is still not known how to account for in future designs. The designs themselves were also quite empirical in general. Concluding, it is needed to extend the understanding of the physical processes behind the erosive sediment transport, to develop better strategies to restore mangroves.

Another problem during mangrove rehabilitation is the planting of mangrove too low in the intertidal zone, despite good intentions (Primavera and Esteban, 2008). When planted too low in the intertidal zone, they influence and affect other ecosystems, such as seagrasses and mudflats, those ecosystems are essential areas for (shell)fish, but also for threatened species such as sea turtles. Hence planting projects may counteract and destroy other coastal ecosystems. Even when all conditions to rehabilitate mangrove forests have been met, other local stress factors may influence establishment and survival of mangrove vegetation. In South-East Asia the large quantity of household waste, like plastics, is a significant problem (Winterwerp et al., 2020).

2.3. Hydrodynamic Conditions

Mangrove forests are influenced by hydrodynamic forcings such as tides, waves, sea level rise and estuarine circulation.

2.3.1. Tide

In general, mudflat foreshores with small water depths have small longshore tidal currents. Except in deeper water, where longshore currents are likely to dominate the sediment transport (Hir et al., 2000; Winterwerp et al., 2016). Rising tides mainly induce cross-shore currents on the foreshore. The tidal volume filled every tidal cycle is large, as the mildly sloping foreshore results in large storage areas. The rising tide is thus important for the onshore transport of fine sediments (Pritchard et al., 2002).

The study of Sidik et al. (2021) highlights the importance of restoring tidal flows in abandonded fish ponds. Tidal flows supply sediments to the ponds, where they can accumulate and increase in bottom level. Furthermore, tidal flows can facilitate the dispersal of mangrove propagules to the ponds, contributing to subsequent mangrove development. Oh et al. (2017) found that the tidal inundation period (related to the surface elevation of the ponds) is one of the key factors for the establishment of the propagules.

$$c = \sqrt{g(h + \eta)} \tag{2.1}$$

Fish ponds can be compared to tidal basins, which partly dry and flood again during the tidal cycle. Tidal basins usually trap sediments and organic matter brought in by the tide, thus serving as material sinks (Kjerfve and Magill, 1989). The small water depths (h) cause the high tide ($+\eta$) to have a higher propagation velocity (c) than the low tide ($-\eta$) (see Equation 2.1). Since the high tide (the wave crest) propagates faster than the low tide (the trough), the rising period is smaller than the falling period. Friction gives an additional slowing down of the low tide with respect to the high tide, since the low tide 'feels' the bottom more (Friedrichs and Madsen, 1992). In absence of other forces or river discharge, the averaged net tidal discharge should be zero, even though the tidal current is asymmetric. A shorter flood duration therefore means that maximum flood velocities exceed maximum ebb velocities.

If maximum flood velocities are higher than ebb velocities, net sediment transport in flood direction is expected, since sediment transport (S) non-linearly responds to the velocity (u), see Equation 2.2. If ebb velocities are higher, it results in a net export of sediment. Asymmetry of the horizontal tide is important for sediment transport, but is mainly dominant for medium to coarse sediment. As mangrove coasts consists mainly of fine sediment the tidal slack asymmetryi may be more important (Bosboom and Stive, 2021).

$$S(t) \propto u|u|^{n-1} \tag{2.2}$$

The tidal slack asymmetry affects the net transport of fine sediment in inlets and basins. Fine sediments deposit if the slack duration is long enough, because fines need time to settle. Unequal slack durations induce this asymmetry. For instance, if the duration of HW slack (before ebb) is longer than the duration of LW slack (before flood), stronger sedimentation occurs just before flow reversal to ebb. Hence during ebb less fine material is in suspension than during flood, leading to a net transport of fines in flood direction. The situation can also be the other way around for offshore net transport of fines (Bosboom and Stive, 2021).

Maanen et al. (2015) studied how mangroves influence tidal channel evolution, using a model that accounts for the effect of the mangroves on the tidal flow, sediment dynamics and the effect of the hydrodynamics on the mangrove growth. It was found that mangroves enhance the initiation and branching of tidal channels. Flow concentrates in between the vegetated areas, because mangroves give the flow extra resistance. The enhancement of branching is also the result of an increase in erosion threshold due to the vegetation. On the other hand the higher erosion threshold in combination with sedimentation by organic matter production results in a reduction in landward expansion of channels. The accretion caused by mangroves can reduce the tidal prism and retreat of the tidal network. Even during sea level rise, mangroves can enhance the bottom level to retain a position in the upper intertidal zone by hindering branching and erosion at the landward side. The conclusion is that tidal channels are more branched, but less developed at the landward side in comparison to a situation without mangroves.

2.3.2. Waves

Mangroves only grow along coastlines where wave energy is low or where mangrove wetlands are protected against high waves by tidal flats, cheniers or corals (Selvam and Karunagaran, 2019). For example, a foreshore with very gently sloping tidal flats consisting of mud and sand. Before waves arrive at this coast, they have to travel over these long tidal flats, which causes refraction of waves towards perpendicular approaching the shore. During this process, waves are dampened more by viscous mud dissipation than by wave breaking (Borsje, 2019; Wells and Kemp, 1986).

Waves induce bed shear stresses, which vary over time and reverse with the direction of the orbital velocities. In shallow water the contribution of the waves to the magnitude of the bed shear stress is often more important than the contribution of currents. The absolute magnitude of the bed shear stress is positively related to the stirring of sediment, thus the direction of the bed shear stress does not matter for the amount of stirring (Bosboom and Stive, 2021). The bed shear stress by waves is therefore important to include in the total bed shear stress, to compute sediment transport patterns. Apart from sediment mobilization by stirring, waves influence sediment transport due to wave-induced currents, however these are not included in the model.

The erosion rate of mangrove coastlines mainly depends on the wave characteristics (Hir et al., 2000). Even small capillary waves can stir up the fine sediments. However, larger waves tend to stir up sediments further offshore and these sediment are transported to the coast by the rising tide. Thus generally, small waves erode sediment, whereas larger waves both erode and supply sediment (Winterwerp et al., 2013). Since the waves are largest during the wet season, it is expected that the largest amount of coastal erosion as well as accretion takes place during the wet, stormy season (Winterwerp et al., 2020).

2.3.3. Relative Sea Level Rise

Mariotti and Fagherazzi (2010) have done research on the influence of sea level rise on salt marshes, which is also partly applicable for mangrove forests. Depending on the sediment supply and sea level a marsh can accrete or erode. A low rate of sea level rise reduces the depth of the tidal flat increasing wave dissipation. Sediment deposition is thus favored, and the marsh boundary progrades. A high rate

of sea level rise leads to a deeper tidal flat and therefore higher waves that erode the marsh boundary, leading to erosion.

Moreover, Saintilan et al. (2020) specifically investigated the effects of the increasing rate of relative sea level rise on coastal mangrove forests, because of their importance for coastal protection. They reviewed data on mangrove accretion between 10,000 to 7000 years ago, when the rate of relative sea level rise was high as a result of glacial ice melt. Mangrove forests expanded between 9800 and 7500 years before present, resulting in thick vertically accreting layers of organic sediments at a rate primarily driven by the rate of sea level rise. Their analysis suggests an upper threshold of 7 mm/yr, which is the maximum rate of relative sea level rise associated with vertical mangrove development. Above this rate, mangroves fail to keep up with the changes. Based on the projected rates of global sea level rise, they predict that there will be a gap between accretion and sea level rise in the next 30 years, although locally this can be already happening.

Concluding, the persistence of mangroves implies an ability to cope with moderately high rates of relative sea-level rise. However, many tropical coasts also experience large subsidence rate, which augments relative sea-level rise. Moreover, human pressures threaten mangroves, resulting in a continuing decline in their extent (Woodroffe et al., 2016).

2.3.4. Estuarine Circulation

If rivers are discharging into the sea, estuarine circulation can be important for mangrove coasts depending on tidal and river influence. Estuarine or gravitational circulation takes place in transitional regions between salt and fresh water. Landward of this transitional region river forces will dominate and seaward the tidal forces. Saline seawater has a higher density than fresh river water, leading to baroclinic pressure differences. Near a river outflow, this sea and river water will meet each other. The barotropic and baroclinic pressure differences together will result in total pressure differences, that drive the estuarine circulation. Less dense river water overrides the sea water, while sea water will intrude beneath the river water. At the seabed, the net flow is thus in landward direction and at the surface in seaward direction (see Figure 2.4). If the tidal influence is larger than river influence, stratification is weak and coastal waters are well-mixed over the water column. However, if the river influence is more important, stratification is strong and a salt wedge develops along the coast. This may vary seasonally and as a function of the spring-neap tidal cycle (Bosboom and Stive, 2021).

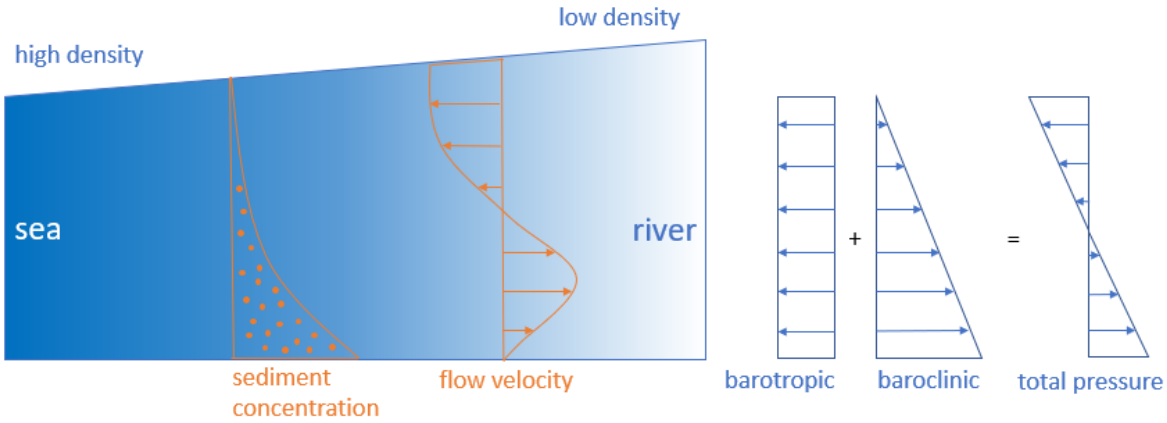

Figure 2.4: Estuarine circulation is forced by both baroclinic as barotropic pressure differences, because of interaction between fresh river and salty sea water at the coast (Bisschop, 2022).

Next to the tide, wind can also cause mixing of the water column and thereby reduces stratification, whereas high temperatures and evaporation enhance stratification (Wolanski, 1992). Physical processes can largely differ between the wet and dry season. In the dry season when river discharges are much lower and temperatures are higher, evaporation causes high salinity waters at the coast. In this situation mangrove swamps behave like an evaporation pond and thus estuarine circulation is inversed (Wattayakorn et al., 1990).

This estuarine circulation has some consequences for the sediment transport, as sediment concentrations are not uniform over the water column. Suspended sediment concentrations are high near the bottom, hence sediment is transported to the coastline by estuarine circulation. If clay particles are present in the river water, high concentrations of fine sediments could be found at the transitional region, because salt sea water stimulates flocculation of clay particles (Eisma, 1986).

Particulates, sediments and dissolved nutrients outwelled from mangrove forests into coastal waters can be retained in a coastal boundary layer formed by estuarine circulation (Wolanski, 1992). This coastal boundary layer water can be trapped along the shore for long periods, if the mangrove shoreline is straight and coastal waters are shallow. While headlands inhibit coastal trapping, because they enhance mixing. Nutrient-rich coastal waters of the boundary layer may be ejected offshore as tidal jets peeling off headlands and locally enriching offshore waters. Longshore currents can ensure coastal trapping of steady river plumes up to hundreds of km (Murray and Young, 1985).

2.3.5. Wind

As bed slopes in front of muddy coastlines are mild, there is a considerable shallow area in front of the coast, where wind is likely to affect currents (Equation 2.3). Wind-generated currents are characterized by high flow velocities at the water surface, which rapidly decays towards the bottom (Bosboom and Stive, 2021). Sediment concentrations are low in this surface layer, thereby wind is not that important for sediment transport.

$$\rho g h \frac{d\eta}{dx} = \tau_{\text{wind},x} \tag{2.3}$$

In contrast to sediment transport, propagule dispersal is more influenced by wind, as buoyant propagules float in the upper layer of the water column near the surface. Stocken et al. (2013, 2015b) found that dispersal is governed by the interaction between hydrodynamic and wind conditions, and depends on the physical characteristics of the propagules as density, shape and orientation. Low densities enable propagules to float on top of the water surface and exposes propagules to wind action. While the high-density floating propagules are less exposed, as a large part is submerged and only a small part sticks above the water surface. Their results also suggest that shape has a significant effect, propagules with large surface areas are more affected by wind than spherical propagules with smooth surfaces. A differential effect of wind was found within elongated propagules, which directly follows from the floating orientation of the propagules. While the dispersal path of vertically floating propagules was influenced by the strength and direction of the water currents and to a lesser extent by wind conditions, the dispersal path of horizontally floating propagules was influenced by both strength and direction of the water currents and wind forces. The studies of Stocken et al. (2013, 2015b) illustrate that different propagule types have a different likelihood of reaching offshore waters depending on prevailing wind and hydrodynamics. This has important implications for variations in dispersal patterns and the likelihood of reaching suitable habitat patches within the floating period.

2.4. Morphodynamic Conditions

Mangrove coastlines consisting of a mixture of mud and fine sand, are depending on a balance of erosion and sedimentation. Moreover their morphodynamics are influenced by cheniers and fluid mud layers.

2.4.1. Erosion and Sedimentation

The change of the position of a mangrove coastline (cl) over time (t) can be conceptually described by the following equation consisting of a sedimentation and erosion rate (Winterwerp et al., 2005):

$$\frac{\mathrm{d}cl}{\mathrm{d}t} = \text{ sedimentation rate } - \text{ erosion rate} \tag{2.4}$$

The sedimentation rate is mainly depending on the tide, sediment trapping by vegetation and consolidation of sediment. While the erosion rate is depending on waves, as described in subsection 2.3.2. Generally the erosion and sedimentation fluxes are large, whereas the difference between the two fluxes is small. So small changes in one of the fluxes can make a big difference by shifting from prograding coastline to a degrading one.

This sedimentation and erosion balance can be disturbed by extensive land-use as fish ponds, leading to the start of a positive feedback effect of more and more coastal erosion (Figure 2.5b). The initial response to this change in land-use is a decrease in sediment flux to the coast, followed by a local increase in wave height. The erosion by these higher waves is not compensated by the onshore sediment transport and the coastline starts to retreat. Mangroves are lost into the sea, which further reduces the sedimentation rates, as less mangroves remain to capture sediment. This retreating coastline results in a concave-up profile as shown in Figure 2.5a and wave effects start to dominate. With this profile the water depth in front of the mangrove coastline increase further, followed by further wave penetration, which enhances erosion further.

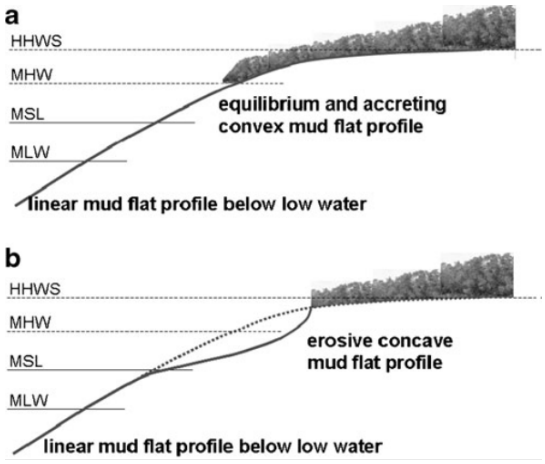

(a) Accreting (convex) and eroding (concave) mudflat profiles (Winterwerp et al., 2013).

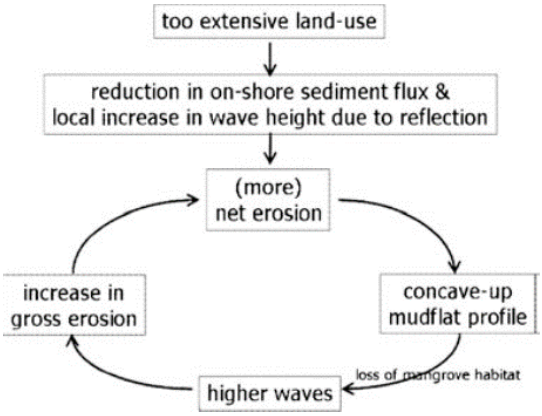

(b) Processes of the positive feedback effect, resulting in more and more coastal erosion (Winterwerp et al., 2013).

Figure 2.5: The positive feedback effect of mangrove coastline erosion including mudflat profiles.

Not only the pathways of the sediment are important, also the sediment concentrations are affecting the actual sedimentation rates (Winterwerp et al., 2020). Suspended sediment concentrations are generally larger during wet season in monsoon climate. Monsoons are not only determined by rain, but also strongly linked to a particular wind and wave climate. Figure 2.6 illustrates the large sedimentation and erosion rates during the wet season (Cuong and Brown, 2012), from these observations several conclusions can be made. Sediment transport especially takes place during the wet season, as during this season waves stir up fine sediments from the bed, which are carried onshore by the tide. As waves also erode, the entire deposit in the control plot was lost again. In plots with permeable dams, the dams did prevent erosion of sediment deposited behind them. To conclude, coastal sedimentation and erosion both take mainly place during the wet season. It is the challenge to reduce erosion rates, while maintaining or enhancing sedimentation rates at the same time (Winterwerp et al., 2020).

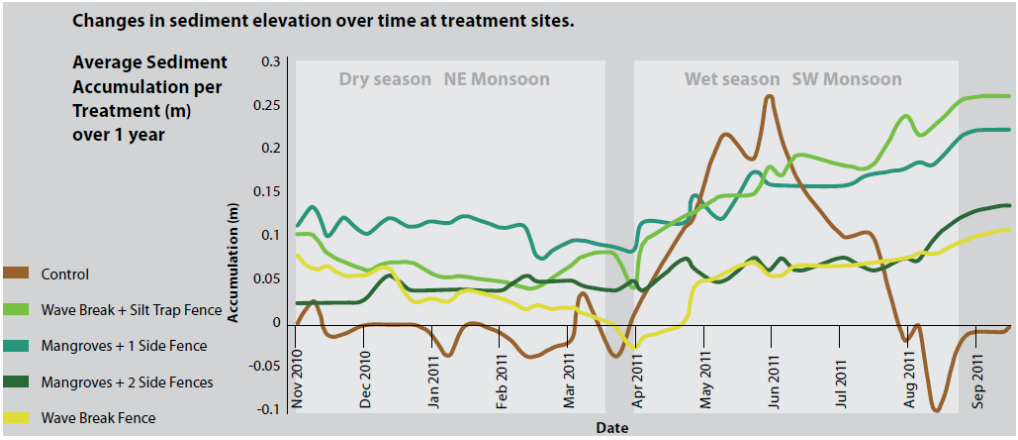

Figure 2.6: Sediment accumulation in Vietnam (Cuong and Brown, 2012).

2.4.2. Sediment Characteristics

Mangrove coastlines are characterized by sediment mixtures of mud and fine sand and therefore bed slopes are very mild around 1:1000 (Robertson and Alongi, 1992; Winterwerp et al., 2016). The size and properties of mud and sand are different. Sand particles are individual quasi-spherical grains ($d = 63 - 2000\mu m$) and have densities (ρ_{sand}) around $2650 kg/m^3$. Whereas mud is a mixture of clay, silt, organic matter, water and sometimes fine sand. Mud, especially the clay particles ($d < 2\mu m$), can flocculate and bond with organic matter (Eisma, 1986). Resulting in irregularly shaped flocs varying in size ($d = 10 - 1000\mu m$), having relatively low densities ($\rho_{floc} = O(1100 - 2000 kg/m^3)$) and lower settling velocities than sand (Many et al., 2019). Studies on erosion behaviour indicate that a sand-mud mixture exhibits cohesive mixture when the mud contents above 30% (van Ledden et al., 2004). Furthermore, the large water content of the fine sand-mud mixture lowers the bearing capacity in comparison to more coarse sediment and decreases permeability significantly, increasing the risk for liquefaction.

The spatially heterogeneous distribution of sand and mud is a function of morphology, supply and hydrodynamic conditions. Due to episodic (storms and floods) and persistent (tides) forcing and human influences, coastal sediments are very dynamic. Mud fractions are generally higher more onshore as mud particles can only settle in low energetic areas, while sand fractions decrease at these small water depths as sand can not be mobilized. Although the sediment composition at a specific location may vary in particle size and mineralogy, for example cheniers are of coarser sand. Bed sediments are mobilized and transported, through bed load (particles in contact with the bed, such as sliding or rolling) or suspended load (particles diffused in the water column by turbulence) (Pearson et al., 2021b). This research concerns transport in suspension, dealing with mud and very fine sand. The morphological changes resulting from these transports are not taken into account, as the model is morphostatic.

2.4.3. Cheniers

Cheniers (Figure 2.7) are dynamic ridges of coarse-grained sediment consisting of sand and shells on a muddy substrate formed by wave forcing (Tas et al., 2022). Cheniers are important for stabilizing muddy coastlines, as they prevent sediments from being transported offshore, resulting in deposition in the shallow areas between the coast and chenier.

Figure 2.7: Two cheniers at the coastline of Demak and behind them some small patches of mangrove forest are visible (Tas et al., 2020).

Tas et al. (2020) showed that both tides and waves are capable of transporting the sediment of the chenier system. During calm conditions and emergence of the chenier crest, tides generate sediment transport in landward direction. This is because the ebb currents prefer to flow around instead of over the chenier and the tide generates substantial sediment transport in very shallow water only. While during periods with higher waves and submergence of the chenier, waves generate substantial sediment transport. The cross-shore chenier dynamics are sensitive to the timing of tide and waves and most sediment transport takes place when high water levels coincide with high waves. During calm hydrodynamic conditions cheniers migrate relatively fast in landward direction, around 0.5 to 8 m/day. Because of small water depths during the dry season at the top of the chenier, even small waves can have an effect on sediment transport. This dynamic behaviour of cheniers is not included in this research as the model is morphostatic.

2.4.4. Fluid Mud

At many mangrove coasts, soft, fluid mud layers are found of different thicknesses. Mud is a mixture of clay, silt, organic matter, water and sometimes fine sand. In Demak, soft mud is formed at locations through remobilization and accumulation of coastal and riverine sediments. Suspended sediments settle to the bed during slack water periods, and this process is accelerated by flocculation (Guo et al., 2017). Such mud layers reduce wave heights efficiently by viscous dissipation. Due to the process of wave-induced streaming (Longuet-Higgins, 1953), fluid mud is pushed in the direction of wave propagation by radiation stresses. Streaming is one of the mechanisms leading to onshore transport of fine sediment (Winterwerp et al., 2020). Over time this onshore pushing of the fluid mud could lead to a build-up of sediment against the coast, which could potentially be colonised and fixated by mangrove species (Borsje, 2019).

2.5. Summary

Mangrove forests are important (sub)tropical intertidal ecosystems providing coastal protection and other ecosystem services. In this research we focus on the dominant transport mechanism of buoyant mangrove propagules: near- and alongshore dispersal. Floating periods of propagules depend on dispersal (tidal flow, freshwater discharge and wind), trapping (retention by vegetation and tidal flats) and seed properties (numbers, size, shape, buoyancy and viability). After dispersal, the propagules need to establish somewhere, successful establishment depends on an inundation free period and root length to withstand wave and current forces.

Possible solutions against erosion of the coastline are implementing hard structures or rehabilitation of mangroves. Hard structures often work counterproductive, as the onshore sediment transport from large waves is reduced by these structures and sometimes they even aggravate the erosion. Mangrove restoration is relatively unsuccessfull at eroding mangrove coasts, plants are washed away into the sea by erosive forces without permeable dams. Fortunately, it is still possible to rehabilitate mangroves following principles that bear in mind the ecology and dynamics of natural mangrove systems.

On mangrove foreshores, alongshore tidal velocities are in general small. The rising tide mainly induces cross-shore tidal velocities, important for the onshore transport of fine sediments. Mangrove coasts are characterized by relative low wave heights, as tidal mudflats dampen the waves. Mangrove development depends on the rate of sea level rise, above a certain rate they fail to keep up with the changes. If rivers are discharging into the coastal waters, estuarine circulation can be important depending on tidal and river influence.

Mangrove coastlines are characterized by sediment mixtures of mud and fine sand, spatial distributions of the mixture are a function of morphology, supply and hydrodynamic conditions. Coastal sedimentation rates mainly depend on the tide, while erosion rates on waves. This balance can be disturbed by too extensive land-use as fish ponds, leading to the start of a positive feedback effect of more and more coastal erosion. Fluid mud layers reduce wave heights and the layers are pushed in the direction of wave propagation. Cheniers are important for stabilising muddy coastlines, as they prevent sediments from being transported offshore.

3

Study Area

This chapter comprehends a study done on the coastal characteristics of the Demak area, from Semarang to the Wulan river.

3.1. Geography

The study area for this research is the Demak area, which is suitable for a idealized model, since it has been a pilot site for coastal protection over the past years. Figure 3.1 shows the location of Demak area on the Java island in Indonesia. Demak is located between $6°43'26'' - 7°09'43''$ S (latitude) and $110°27'58'' - 110°48'47''$ E (longitude), which is the Southern hemisphere (Ismanto et al., 2017). The location between these latitudes close to the equator results in a tropical rain forest climate. The 34.1 km long coastline of the Demak regency is at the Java Sea, enclosed by Kalimantan (North), Java (South) and Sumatra (West). The shallow Java Sea, surrounded by islands, is a protected sea environment with monsoon influence. Because of this environment, there are no large swell waves from the Indian and Pacific Ocean. The area is characterized by a mixed, mainly diurnal tide (Tas et al., 2020).

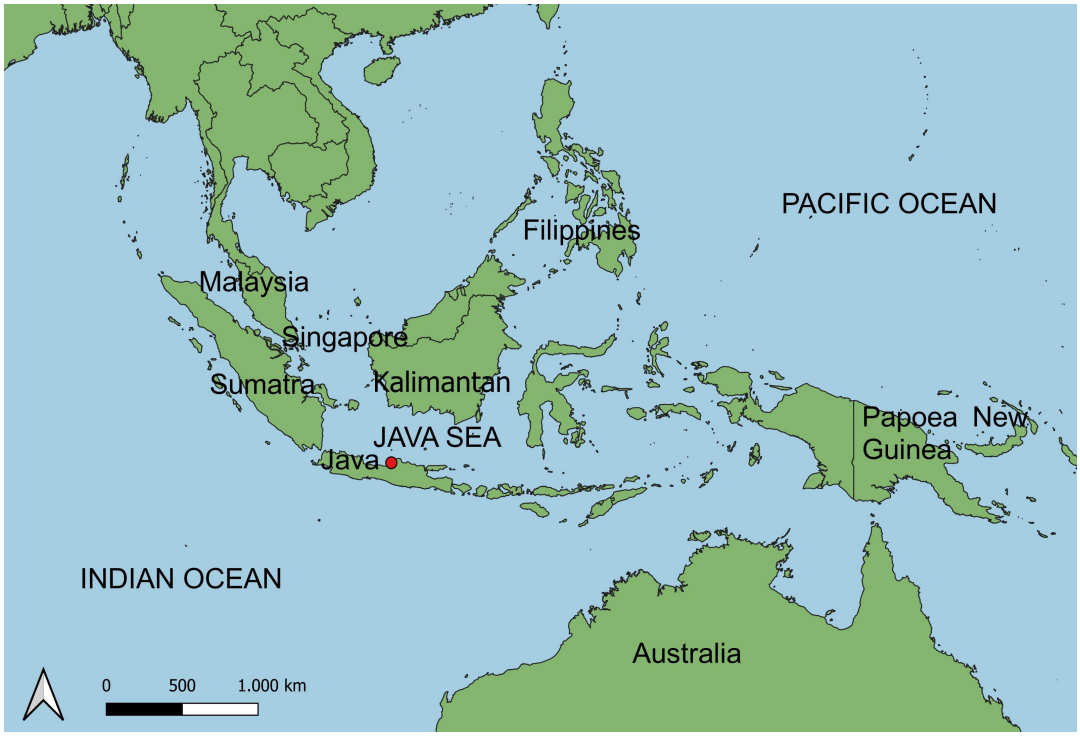

Figure 3.1: Demak (orange dot) is located on the island of Java within the Indonesian archipelago.

3.2. Site Conditions

The model area of Demak stretches from the city of Semarang at the South and the Wulan river at the North boundary, see Figure 3.2. It consists of tidal basins (inundated fishponds), which are subject to tidal infilling. The Demak area has been a pilot site for coastal protection over the past years, therefore already some information is available. At Semarang City a tidal station is located, therefore information is available on the local conditions, such as wave climate and tide. Tidal analysis of water level measurements in Semarang indicate that the tidal range varies between 0.4 and 0.6 m during normal conditions, although the spring range can reach up to 1 m (Tas, 2022). The tide consists of a dominant diurnal component and a smaller semi-diurnal component. Tidal currents close to the coast are mainly perpendicular and not parallel to the coast, since water depths are small (Sugianto et al., 2017; Tas et al., 2017; EcoShape, 2015).

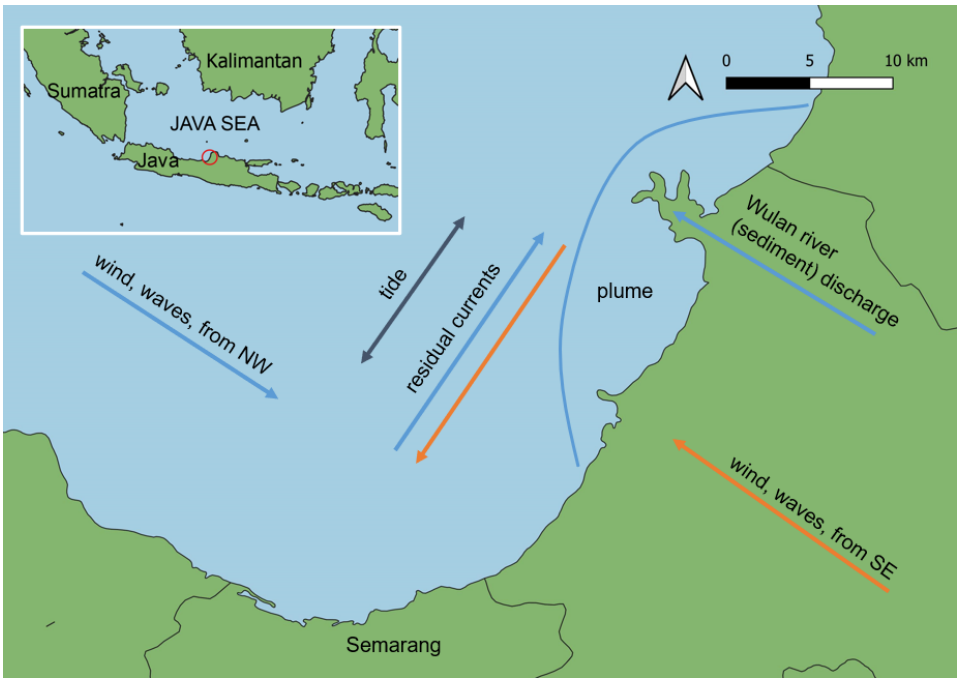

Figure 3.2: Visualization of the important site conditions affecting the Demak coastline during the wet season (blue) and dry season (orange).

The seabed consists of muddy (80%) and sandy (20%) sediments (BioManCO, 2018), however the distribution is spatially heterogeneous as for example areas with cheniers are sandier, though the exact stratigraphy remains unknown (Damastuti et al., 2022; Ismanto et al., 2017). Bed slopes are very mild due to the abundance of fine sediment, close to the coastline around 1:1000 and more offshore around 1:500 (Smits, 2016). Mean wave heights, according to wave data near Semarang, are around 0.46 m and maxima lie around 2.6 to 3 m (Tas, 2022). The salinity in Sayung waters ranged 33-38ppt during the dry season and 27-31ppt during the wet season (Wisha and Ondara, 2017).

In this tropical area there is a monsoon climate with a wet season from November to March and a dry season between May and September with transition seasons in between. During the rainy season, waves and wind come from offshore (NW) and during the calm and dry season from land (SE) (Ervita et al., 2017), see Figure 3.2. The rainfall distribution during the seasons is an indicator for Wulan River discharges. The monsoon influences large-scale currents along the North coast of Java, hence during wet season surface currents are to the East and Westwards in the dry season (Wyrtki, 1961). The long term average residual long-shore current and corresponding sediment transport is towards the East (EcoShape, 2015). As the coastal waters are quite shallow (Sugianto et al., 2017), wind is also likely to affect currents. Wyrtki (1961) derived from observations that during the monsoon in the Java Sea water level set-up builds up. From measurements, set-up was appreciable during the highest waves in a storm, but the rest of the time during the monsoon, the water level seemed to be driven by tides (Alferink, 2022). Current velocities in the area are ranging from 0 to 0.4 m/s (Bariq and Marfai, 2019; Wisha and Ondara, 2017).

months	nov	dec	jan	feb	mar	apr	may	jun	jul	aug	sep	oct
monsoon	wet season					transitional	dry season					transitional
wind	NW (from offshore)						SE (from land)					
waves	NW (from offshore)						SE (from land)					
river discharge	high						low					
longshore currents	eastwards						westwards					

Figure 3.3: Table of the important site conditions affecting the Demak coastline during the wet season (blue) and dry season (orange).

3.3. Relative Sea Level Rise

Relative sea level rise in Demak is dominated by local land subsidence. In and around Semarang large volumes of ground water are withdrawn from deep aquifers to satisfy the needs of the industry sector. But rural villages also have their own deep wells for household use and for aquaculture (EcoShape, 2015). The Demak area is suffering from land subsidence due to groundwater extraction, natural consolidation and added load of constructions (Marfai and King, 2007).

Prasetyo et al. (2019) studied the absolute sea level rise in the Java Sea the from 2011 to 2016, which increased +6.80 mm/yr on average and +5.52 mm/yr close to Semarang. In this period the coastline of Demak retreated 119.08 m. Land subsidence values differ from +2.078 to -8.376 cm/yr depending on the location in the Demak area, near urban ares the subsidence is generally higher (Prasetyo et al., 2019). Since land subsidence values are an order of 10 larger than sea lever rise, they are much more sigificant. The relative sea level rise (land subsidence rates and absolute sea level rise) is far above the maximum rise associated with vertical mangrove development (Saintilan et al., 2020), resulting in a large erosion rates at Demak. Subsidence also produces impacts such as infrastructure damage, problems with drainage and more areas subject tidal inundation (Andreas et al., 2018).

3.4. Coastal Erosion

Demak and Semarang City are facing significant coastal erosion. Semarang is at the south boundary of the study area and is one of the big cities in Indonesia with a population of more than 2 million. The coast of Semarang consists of agriculture, fishery, residential, industrial, public and commercial land uses. Urbanization in combination with subsidence are the major stressors for coastal erosion in Semarang (Marfai, 2011). In Demak there were intensive land use changes of mangrove forests, mid-way the 20th century parts of the coastline were already deforested for rice fields, which were later transformed to fish and aquaculture ponds including larger losses of mangrove forest (EcoShape, 2015). The removal of the mangroves and confinement of the intertidal zone due to construction of earth bunds around the fish ponds caused changes in sediment dynamics. This triggered massive erosion and the related land loss, inundation and saltwater intrusion problems (Winterwerp et al., 2014; Ismanto et al., 2017). Furthermore, an extended port in Semarang including jetties penetrating three kilometer into the sea are affecting residual sediment transports and could have accelerate the erosion in Demak (Maulina, 2010).

As a result of the coastline retreat, around 70,000 people were affected by coastal flooding and erosion in the Demak district. Entire villages have been swallowed by the sea and fish ponds were damaged. Many people experienced a major loss in income, reaching up to 60% to 80% in some villages (Winterwerp et al., 2016). Figure 3.4 shows a retreat of hundreds of meters at part of the Demak coastline from 2003 to 2013. This is likely caused by the high subsidence rates, but also the limitation of sediment input by dammed rivers and the construction of fish ponds at the coastline by local fishermen, which replaced most of the previous mangrove forests (Wilms et al., 2020). Most of the erosion occurs during the wet season when winds are stronger and waves are higher. However, fine sediments from the rivers and foreshore are also expected to be mobilized in this season, which enlarge the supply to the coastal zone available for deposition at the coast (EcoShape, 2015). Summarizing, both the erosion and sedimentation are high during the wet season.

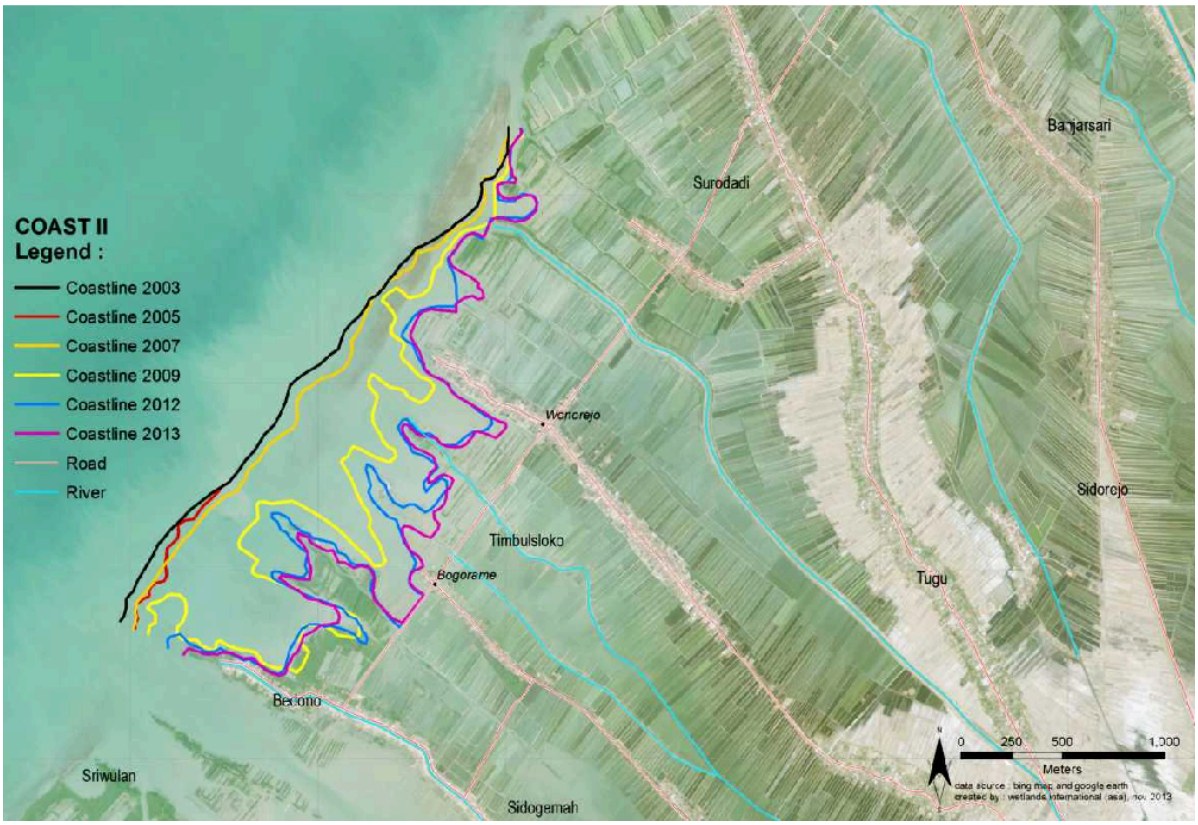

Figure 3.4: Coastal Erosion at Demak from 2003 to 2013 (Winterwerp et al., 2014).

The local government has responded to this erosion by implementing several mitigating measures as dikes, sea walls and breakwaters, but these measures are failing and may become counterproductive (Marfai, 2011; Ismanto et al., 2017). These hard structures were even found to intensify erosion by locally blocking sediment transport towards the coast and enhancing wave effects due to wave reflection (Winterwerp et al., 2013). Furthermore, the community and local government of Demak have planted mangroves along the coast to counteract the erosion (Marfai, 2011). These measures were unsuccessful, because mangrove habitat requirements were not met due to the sediment imbalance.

3.5. Wulan Delta

The Wulan Delta (see Figure 3.5) is a bird-foot shaped delta located in the northern part of Demak and also the northern boundary of the model. The Wulan Delta is shaped by the interaction between the sedimentation of the two bifurcated Old and New Wulan channel and hydrodynamic processes from the sea (Bariq and Marfai, 2019). The delta has a large catchment of 3860 km^2 (Sunarto, 2004). The upper part of this catchment consists of an old weathered volcanos and hills, which are highly susceptible to erosion.

The shallow tidal flat in front of the Wulan Delta causes waves to break, resulting in relatively low wave energy at its coastal margins. As a consequence most of the sediment coming from the Wulan River is transported and deposited at the river mouth. The river mouth prograded till 2011 and the the Wulan Delta area got larger with rates of 4.85% from 1995-2000 (Septiangga and Mutaqin, 2021). The orientation of the river tributaries thus changed, which is likely to largely influenced the outflow direction and hence sediment connectivity with the adjacent coasts. The expansion of land in the delta led to land use change, settlements and fish ponds emerged here. Most settlements were built next to river levees, so they are vulnerable to river and tidal flooding (Marfai et al., 2016).

After 2011, growth rates of the delta area are decreased to values around 0.02 to -0.09% (Septiangga and Mutaqin, 2021). The Wulan Delta can be divided into two parts, the southern and northern area, which experience different changes. The northern shoreline retreats, while the southern one advances due to mangrove planting and sedimentation from the river (Septiangga and Mutaqin, 2021).

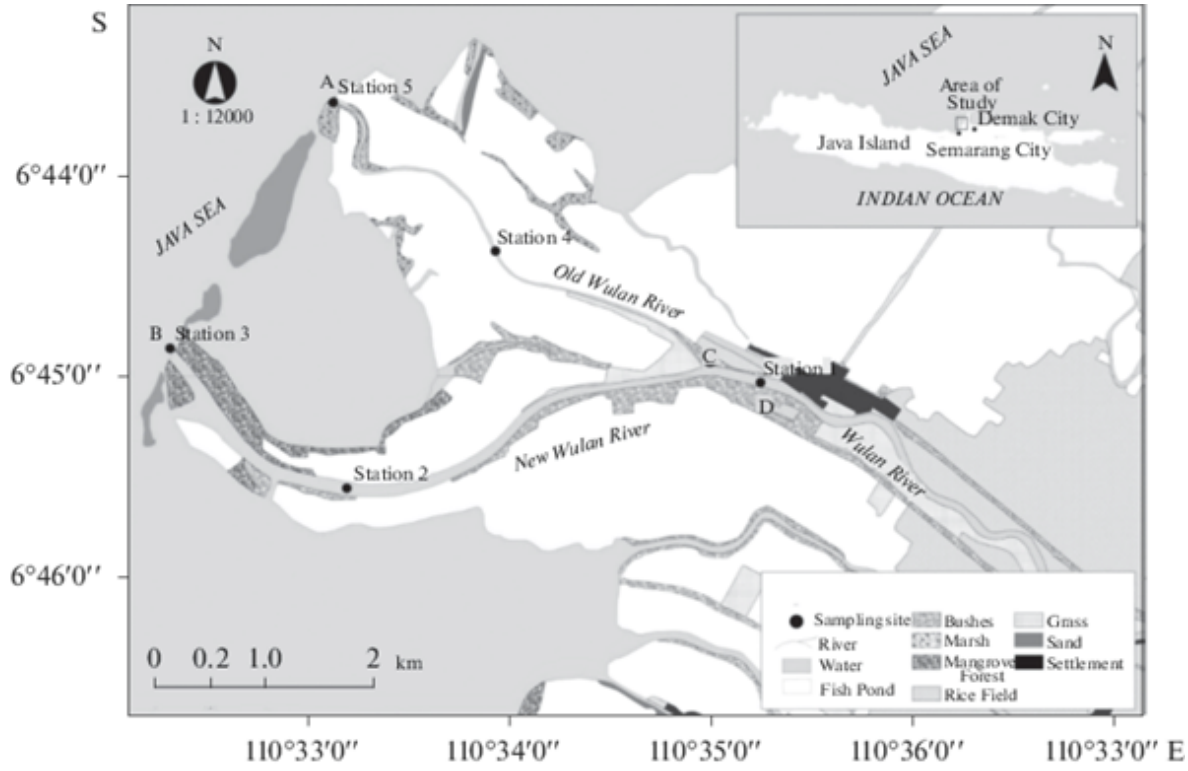

Figure 3.5: The bird-foot shaped Wulan Delta including its new and old tributaries and land uses (Fadlillah et al., 2019).

Based on the information obtained from local communities, river sediment supply and floods are decreasing due to upstream agricultural and urban land use and dam development. The decrease in river floods and sediment supply causes less delta progradation or even coastal erosion (Marfai, 2011). Additionally the sediment supply to the intertidal area is diminished, as fish pond systems disconnect the river from the natural floodplain (EcoShape, 2015).

Coastal erosion is influenced by a lack of riverine sediment supply and at the same time by sea level rise, subsidence and more energetic waves (Marfai et al., 2016). Sediments used to be captured by the mangroves originally present in the coastal zone. However, with the loss of these mangroves, part of those historic deposits have been lost to deeper water. A very rough estimate suggests that about half of those historic deposits have currently been lost, implying that it shall not be possible to restore the eroding Demak coast entirely to its 2003 position (EcoShape, 2015). Although coastal erosion takes place, the Wulan Delta still protrudes into the sea, obstructing prevailing alongshore currents including the sediment load.

As mentioned in section 3.2, the monsoon divides the seasons in a wet and dry period, which has its influence on the Wulan River discharge. The average discharge from Klambu Station during wet season is 138.18 m^3/s, whereas the dry season discharge is 31.6 m^3/s (Fadlillah et al., 2019). This discharge divides itself over the Old and New Wulan River after the bifurcation (Bariq and Marfai, 2019). The sediment load of the Wulan River discharge is a main local source of sediment for tens of kilometers of coastline. Besides the Wulan river, other numerous small rivers supply sediment to the coastal zone. The monsoon climate has the result that there is much more sediment available in the wet season than in the dry season. The deposited sediment at the Wulan River mouth can form cheniers under wave forcing, a sort of sand barriers (Tas, 2022). These cheniers prevent riverine sediments from being transported offshore, resulting in deposition in the shallow areas between the river mouth and chenier. The existence of cheniers in front of the Wulan Delta indicates that sedimentation is no longer controlled by the river, but by current-and wave-induced processes. As a consequence the bird-foot shaped delta will change to a more rounded delta (Marfai et al., 2016).

Estuarine circulation as explained in subsection 2.3.4, is an important process in the Wulan Delta. During the wet season the fresh river water plumes of the Wulan Delta are pushed towards the East following wind direction and residual currents (Fadlillah et al., 2019). Suspended fine sediments stay

close to the coastline in this season, due to weak estuarine circulation. In the dry season the river discharge is lower and blown into the sea, so estuarine circulation mixing is stronger. Therefore, no large scale transport of sediments is expected near the coast, and fine sediments from the foreshore are lost to deeper water in the dry season (EcoShape, 2015). Concluding the river is dominant in the wet season (salt wedge estuary) and the tides in the dry season (well-mixed estuary) (Fadlillah et al., 2019).

3.6. Fish Ponds

In Demak there have been intensive land use changes of the mangrove forests. Around 1950 parts of the coastline had already been deforested for rice fields. The landscape was rearranged to optimize rice cultivation, with a focus on the area at Semarang. Canals for irrigation and drainage were constructed and some mangrove creeks may have been straightened, but the coastal mangrove zone remained intact (EcoShape, 2015). Between 1970 and 1980, the rural population was wealthy, as there was an abundance of rice, shrimp and other fish. In the 1980s, the demand for shrimp increased and world market prices for rice fell. Together with the fish trawling ban in 1984, this pushed the transformation of both rice fields and mangrove forests into shrimp ponds (EcoShape, 2015). The construction of aquaculture ponds along low-lying sedimentary reaches has led to a near-total destruction of mangrove forests since the 1980s (Ismanto et al., 2017). In the 1990s, frequent losses of shrimp harvests, due to diseases, forced farmers to open even more new ponds in mangrove forests. In 2008, 83% of the Wulan Delta area was transformed into fish pond, which expanded to 92% (25 km^2) in 2016 (Fadlillah et al., 2018).

Local communities often turn the shores into artificial fish ponds, because mangrove forests are rich in expensive seafood (Sasekumar et al., 1992). The ponds are used to breed milkfish, shrimp, and crab and in dry season, some fishponds are used as salt ponds. Muddy material is used by the local community in Demak to build fish ponds, which are constructed manually by arranging mud material into a rectangle shape as an embankment. The tidal flow refreshes the water in the fishponds. At many locations fishponds have experienced damages due to the coastal erosion. Damage on the fishponds results in economic losses, since aquaculture is the leading economic sector in the coastal villages in Wulan Delta. (Marfai et al., 2016).

Mangrove patches in between the fish ponds are also damaged by coastal erosion. These patches are a very important ecological buffer for the biological and physical balance in the area (EcoShape, 2015). Mangroves indirectly support the fish ponds by providing food and nursery ground (Walters et al., 2008). Thus conversion of mangrove forests into fish ponds, exacerbated by ongoing coastal erosion, threatens the sustainability of economic activities in the area.

3.7. Summary

The study area for this research is Demak, which is suitable for a idealized model, since it has been a pilot site for coastal protection over the past years. Demak and Semarang City at the southern boundary are facing significant coastal erosion. This is likely caused by the high subsidence rates, but also the limitation of sediment input by dammed rivers, urbanization and the construction of fish ponds. The Wulan Delta in the North is a bird-foot shaped delta, influencing estuarine circulation and supplying seasonally varying sediment to the coastal system, however nowadays the supply is decreasing. The conversion of mangrove forests into fish ponds, exacerbated by ongoing coastal erosion, threatens the sustainability of economic activities in the area.

4

Modelling

This chapter describes SedTRAILS and Delft3D, followed by the set-up of the idealized model and modelling phases.

4.1. Models

This section introduces the SedTRAILS and Delft3D for the development of a idealized model.

4.1.1. SedTRAILS

This research extends the knowledge of the coastal system of Demak, by applying the particle tracking model SedTRAILS to determine the sediment and and propagule pathways from source to sink. Since understanding is essential for predicting the response of coastal systems, such as Demak, to climate change or human interventions.

The framework of connectivity is a structure for analyzing pathways, schematizing the system as a series of nodes and fluxes between those nodes as links (Heckmann et al., 2015). Once structured in this way, the resulting network can be expressed algebraically as a connectivity matrix. This matrix provides the probability that a particle from location *i* came from location *j* (Cowen and Sponaugle, 2008). The conceptual framework of connectivity has the potential to extend sediment pathway understanding. Since coastal and estuarine systems forced by tides, waves, rivers and wind, evolving according to complex non-linear flow and transport processes, can be defined as connected networks of water and sediment flows (Pearson et al., 2020).

Lagrangian approaches are widely used to assess connectivity in the context of oceanography and marine ecology (Cowen and Sponaugle, 2008). Because the models do not only track the start and end points, but the complete pathway of a particle. Lagrangian frameworks are also relatively fast and give a more detailed analysis of connectivity than Eulerian approaches. The Lagrangian approach is based on description of the fluid in a frame of reference that moves with a particle. This framework forms a conceptual visualization of the particle motion (van Sebille et al., 2018), by making use of Eulerian information (e.g. current transport vector fields). Although Lagrangian particle tracking is used in oceanography and marine ecology, it has not a been applied for analysis of coastal or estuarine sediment transport pathways and connectivity, therefore SedTRAILS is developed (Pearson et al., 2021a) (Figure 4.1).

SedTRAILS (Sediment TRAnsport vIsualization & Lagrangian Simulator) is a particle tracking model that uses the conceptual framework of connectivity to map sediment transport pathways in coastal environments, expanding our system understanding and addressing practical coastal management problems (Pearson et al., 2021a). Applications could be determining the planning of a nourishment, potential for sediments to reach a specific location, large-scale sediment transport pathways, impact of human interventions, or sediment sources for dredging in a large range of locations. The approach provides new quantitative and qualitative insights into sediment pathways in complex environments. The effective visualization of complex numerical results improves the understanding of a system even for the local community, decision-makers and stakeholders.

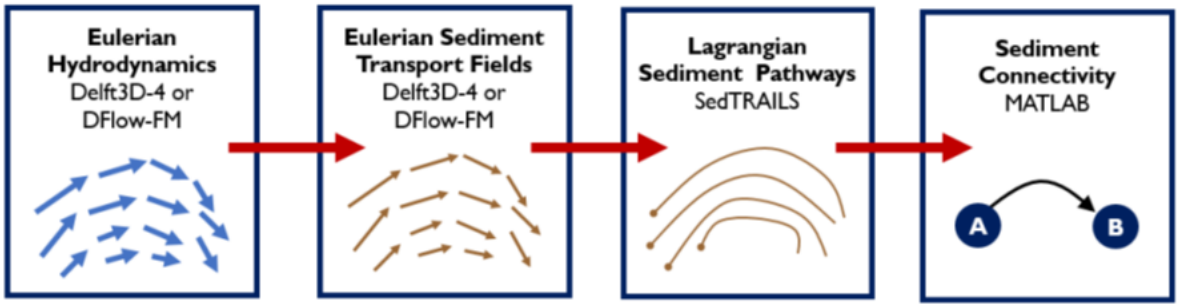

Figure 4.1: Different steps in the SedTRAILS model (Pearson et al., 2021a).

SedTRAILS is specifically developed to simulate sediment pathways accurately and computationally efficient over long time scales. Runtime efficiency is obtained from decoupling the sediment pathway computation from the current transport vector field computation, which are still resolved using an Eulerian model. As a result, sediment pathways can be computed over long enough time scales, so that particle trajectories span the entire morphological system. Therefore, SedTRAILS is suitable for mapping the sediment pathways of the Demak area. Even analysis of propagule pathways can be implemented, which is done before by der Stocken et al. (2019a) on global-scale.

4.1.2. Delft3D

For the approach of estimating Lagrangian sediment transport pathways using SedTRAILS, the hydrodynamics and sediment transport of the Demak area have to be simulated with an Eulerian model first. Eulerian models solve the equations of motion for water and sediment in a reference frame fixed in space, which is the basis for most numerical models (van Sebille et al., 2018). Delft3D is an Eulerian model with a structured mesh suitable for these simulations.

Delft3D is a 2DH or 3D program to model hydrodynamics, sediment transport, morphology, water quality and the interactions between these processes for a river, estuarine or coastal environment. Delft3D consist of different modules, the most important one is the FLOW module. This FLOW module is a hydrodynamic and transport simulation program that calculates non-stationary flow and transport processes resulting from tidal and meteorological forces on spherical coordinates or a curvilinear boundary grid. The vertical grid is defined according to fixed vertical layers or the sigma coordinate approximation in 3D simulations. Furthermore, salinity and temperature differences of flows can be included in this module (Deltares, 2022a; Lesser et al., 2004). Timescales of simulations can vary from days (storm impact) to centuries (system dynamics), any time scale is possible (Deltares, 2022a; Lesser et al., 2004).

Next to the FLOW module, there is the MOR module, which can calculate sediment transport, both suspended and total bed load, and morphological changes for any number of cohesive and non-cohesive fractions. Waves and currents can be both included as forcing and one can choose between multiple different transport formulae. The dynamic feedback between the modules is essential as it allows the flows and waves to adapt to the local geometric and bathymetric characteristics. However, morphological changes and waves are not included in this study in order to keep the computational time reasonable, so fixed bed levels do not change over time. Concluding, a morphostatic model in Delft3D is used to compute the Eulerian hydrodynamics and SedTRAILS for the Lagrangian sediment pathways.To compute these pathways SedTRAILS requires the following parameters as input from Delft3D (Pearson, 2021):

- mean bed shear stress τ_m (currents)
- maximum bed shear stress (waves and currents) τ_{max}
- current velocity U_c
- depth h
- bedload transport q_b

- suspended load transport q_b
- suspended sediment concentration C

4.2. Set-Up

This section discusses the set-up of the idealized hydronamic and sediment transport model of the Demak area using Delft3D-4 and SedTRAILS, including the proccesses and input parameters. The computational grid, bathymetry, sediment and propagule characteristics, boundary conditions as the river inflow and tide, processes as wind, waves and salinity are elaborated below.

4.2.1. Domain & Grid

The model domain of the Demak area stretches from the city of Semarang at the South and the Wulan river at the North boundary (50 x 23 km). A computational grid with cells of 333 by 333 m is chosen to start (Figure 4.2), because such a relative large grid size keeps the computational time reasonably short ($<$ 0.5 hr for a 30 day simulation on an 2.81 GHz laptop). The model resolution can not be improved at areas of interest, such as the river area, where we can mimic the tributaries, the basins and along the coast (shallow areas) in Delft3-4. For the 3D computations the σ-grid is used, consisting of 10 layers in the vertical. Each layer is 10% of the depth, so layers thicknesses are varying of the depth.

Figure 4.2: Model domain from Semarang city to the Wulan river, including the computational grid with cells of 333 by 333 m.

4.2.2. Bathymetry

The bathymetry is obtained from General Bathymetric Chart of the Oceans (GEBCO) in DelftDashboard. The dataset that was used was GEBCO'08, a global bathymetric grid with spacing of about 1 km. In many regions (particularly shallow water areas and semi-enclosed seas) this dataset is extended with additional control contours and sounding point data. It is a continuous digital terrain model for ocean and land, with land elevations derived from the Global Land One-km Base Elevation (GLOBE) database (Smits, 2016).

The GEBCO bathymetry is adapted, because some data was not realistic. For example, in the bathymetry there was an area with a depth of 40 m, which does not correspond with observations in the field. Some slopes of the bathymetry were unrealistically steep for a mangrove-mud system,

which is characterized by mild slopes of 1:1000 and more offshore slopes of 1:500 (Tas et al., 2017). Both Wulan river tributaries were too deep and wide, when comparing it to Google Earth images and the measurements of Fadlillah et al. (2019). In particular, the Old Wulan tributary was not well-represented, as the Old Wulan should be shallower and narrower than the New Wulan tributary. The Serang river is deleted from the bathymetry, because the Wulan is the only river represented in the model. The other small rivers were already absent in the relatively coarse bathymetry. Lastly, GEBCO depth input is relatively inaccurate in the nearshore, the bunds of the old fish ponds are not incllluded. It was thus decided to manually add some of the pond bunds in the intertidal area of Timbulsloko. This was only possible to a certain extent, because the relatively large grid size does not allow for much detail. In the end, the maximum depth is adapted to 20 m, the slope at the North boundary is made a bit milder, the bathymetry of the river tributaries is adapted and some of the pond bunds are added, the resulting bathymetry is shown in Figure 4.3.

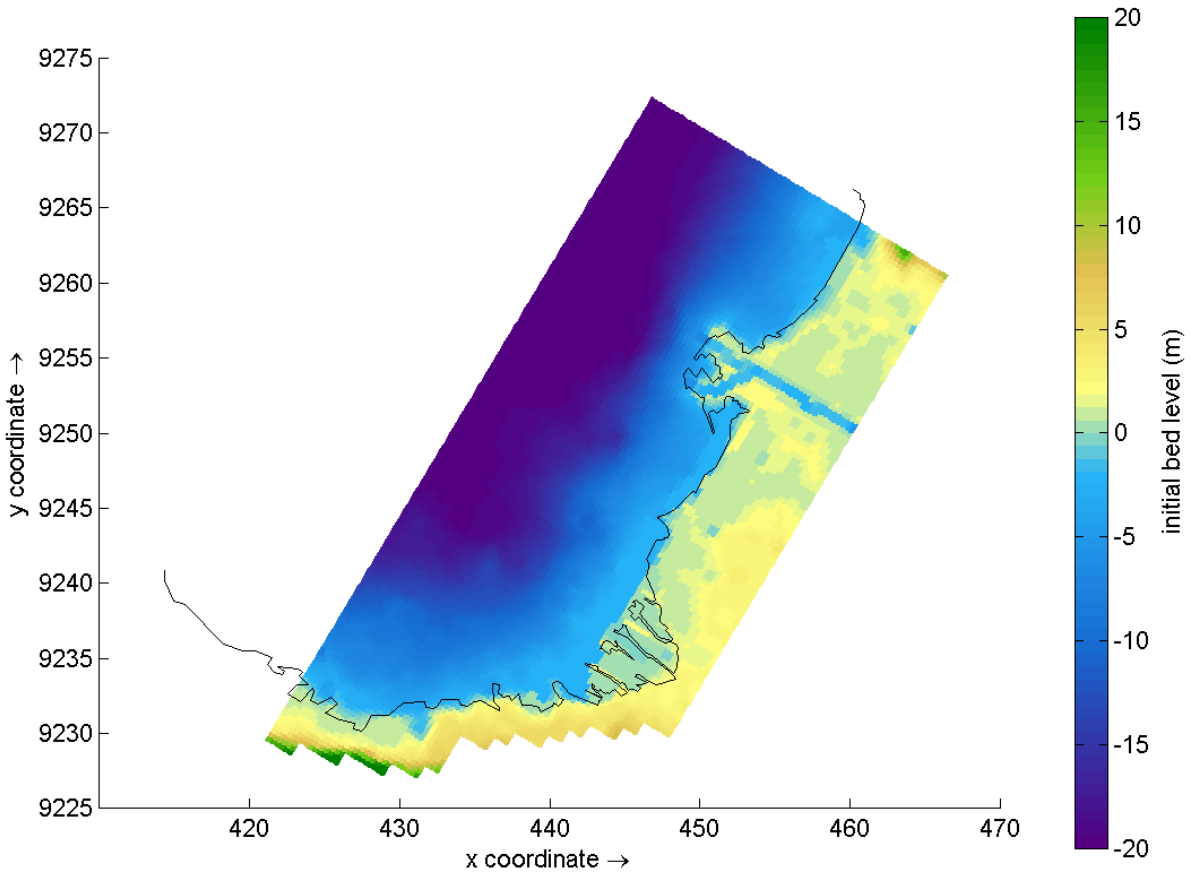

Figure 4.3: Bathymetry map of the model domain from Semarang City in the South to the Wulan river delta in the North. The black line is the 2022 coastline traced out from Google Earth.

4.2.3. Sediment Characteristics

The seabed consists of muddy (80%) and sandy (20%) sediments (BioManCO, 2018), however this composition is spatially heterogeneous. As for example areas with sandy sediments are mainly found at the breaker zone at the cheniers and the rest is more or less consisting of muddy sediments, though the exact stratigraphy remains unknown (Damastuti et al., 2022; Ismanto et al., 2017). To distinguish between sand and mud, we have some data of sediment distribution over transects but not over the scale of the coastline (Van Domburg, 2018; Tas, 2022).

Van Domburg (2018) described the sediment grain sizes along two transects in the Demak area, an accreting transect and an eroding one. The accreting transect is characterised by a chenier and a small vegetation patch in between the chenier and the coastline. The grain sizes along both transects are shown in Table 4.1 and the locations mentioned in this table are visualised in Appendix B. Looking at

the grain sizes with a D_{50} of 18 μm (excluding SED 181 at the chenier), it can be seen that the eroding transect contains coarser sediment (D_{50} = 24 μm) than the accreting transect (D_{50} = 12 μm). This is also supported by the field observations from BioManCO (2018), who experienced that the bed of the accreting transect was much softer. Both transects show smaller grain sizes (5-10 μm) towards the shore, where the bed becomes muddier. The smallest grain sizes are found inside the mangrove forest, except for an old chenier which has been colonised by mangroves (BioManCO, 2018; Van Domburg, 2018). The chenier in the accreting transect is characterised by a more sandy sediment composition (145 μ, BioManCO (2018)), whereas Tas (2022) assumed that the bed is consisting of mostly mud and a small sand fraction with D_{50} of $235\mu m$ at the cheniers.

Altogether, in the main part of the simulations the bed is assumed to be muddy sediment (D_{50} = 18 μm), however for two simulations sand (D_{50} = 145 μm) is assumed. Moreover the model is schematized by looking at the system in a morphostatic way. So sediment transports are computed, but those do not change the fixed bed level over time.

Location	$D_{50}[\mu\mathrm{m}]$	Location	$D_{50}[\mu\mathrm{m}]$
A1 (WL 45)	13.94	A9 (SED 175)	6.42
A2 (SED 180)	12.47	E1 (WL 43)	24.54
A3 (SED 181)	145.22	E2 (WL 44)	32.95
A5 (WL 42)	10.68	E3 (WL 41)	57.61
A6 (SED 178)	27.05	E4 (WL 27)	9.95
A7 (SED 174)	7.35	E5 (SED 176)	7.00
A8 (SED 177)	7.28	E6 (SED 124)	9.59

Table 4.1: Sediment grainsize per location. The instruments are sorted, starting at the accreting transect with A1 in the left column until A9 in the right column. The remainder of the right column represents the eroding transect. For a visualisation of the locations is referred to Appendix B (Van Domburg, 2018).

4.2.4. Propagule Characteristics

The study of Bijsterveldt et al. (2020) indicates that both planting mangroves and natural recruitment can be successful as long as the habitat requirements are met. *Avicennia marina* (grey or white mangroves) and *Rhizophora mucronata* (red mangroves) are the most dominant species in Demak and seedlings are already amply available in the area (EcoShape, 2015). The propagules of both species are shown in Figure 4.4, including their position relative to the water surface while floating. The *Rhizophora mucronata* is mainly located in river/estuarine environments, along riverbanks. *Avicennia marina* colonizes mud flats located at high water level, where it is more dry and saline (Verschure, 2013). However mangroves are highly zoned and a more diverse mangrove ecosystem is required to trap sediment. Mangrove growth and regeneration can be rapid in the area, as naturally recruited *A. marina* grows to a 4 m high tree within 5 years, the same is the case for planted *R. mucronata*. Mangroves were seen growing successfully all along the 4 km of coastal area from the junction of the main road between Demak and Semarang all the way to Timbulsloko (EcoShape, 2015).

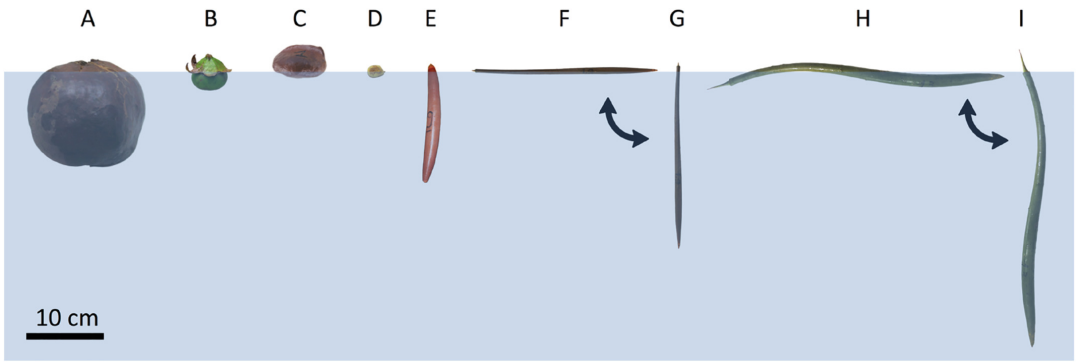

Figure 4.4: Propagules from the following mangrove species: Xylocarpus granatum (fruit) (A); Sonneratia alba (fruit) (B); Heritiera littoralis (C); Avicennia marina (D); Bruguiera gymnorrhiza (E); Ceriops tagal floating horizontally (F) and vertically (G); Rhizophora mucronata floating horizontally (H) and vertically (I) (der Stocken et al., 2019b).

Satellite data showed that in the past, mangrove expansion in pond zone mainly occurred through mangrove planting on pond bunds (van Bijsterveldt et al., 2022). However, there is potential for propagules, as field data revealed that pioneer species propagules were up to 21 times more abundant in pond creeks than near their coastal source. This was especially during wet season with onshore winds, which suggests that propagules can be trapped efficiently in ponds. Furthermore the survival and growth rate of propagules highly varied between species. *Rhizophora mucronata* has a high survival rate (67%), but a lower growth rate. Whereas the pioneer specie *Avicennia marina* has a lower survival rate (21%), but significantly higher growth rates, even resulting in fruiting young trees within 16 months. van Bijsterveldt et al. (2022) concluded that propagule establishment has potential in the coastal pond zones, given that propagules can reach the locations. Therefore this research investigates if propagules can reach these locations from various sources, by simulating their pathways.

Simulating propagule pathways was not implemented in SedTRAILS before this research. As a consequence some rules needed to be included to simulate propagule behaviour, as well as some input parameters as propagule size, lifespan and location need to be known. In the research of Naidoo (2016) propagule sizes of 2.5 ± 0.3 cm for *Avicennia marina* and 36 ± 3 cm for *Rhizophora mucronata* are used. For lifespan, we can use the buoyancy and viability periods of propagules, which der Stocken et al. (2019b) collected. Buoyancy periods of *Avicennia marina* are from 2 to 15 days and a viability of 240 days is reported (Clarke et al., 2001; Clarke, 1993; Clarke and Myerscough, 1991). While buoyancy periods of *Rhizophora mucronata* are from 87 to 150 days and a viability of 150 days is observed (Guppy, 1906; Drexler, 2001). For a complete overview of buoyancy viability and dispersal distances, see Appendix C. Locations of mangrove patches along the Demak coast are at the intertidal area of Timbulsloko (van Bijsterveldt et al., 2022; Irsadi et al., 2022) and at the Wulan Delta (Marfai et al., 2016; Kusumaningrum and Haryono, 2020; Fadlillah et al., 2019).

From the two dominant species in Demak, only *Avicennia marina* is a pioneer specie (Van Domburg, 2018), so the dispersal of this specie is modelled. In order to achieve mangrove re-establishment, their colonisation behaviour, especially the fruiting seasons, is important to understand. Various theories exist about the fruiting seasons of these mangrove species. Kitamura and for Mangrove Ecosystems. (1997) found that *Avicennia marina* has its fruiting season between December and February at Bali (Indonesia), while Latiff and Faridah-Hanum (2014) showed that in Malaysia, the *Avicennia marina* fruits between June and August. Although it could not be investigated in detail, measurements by van Bijsterveldt et al. (2022) suggest that in Demak *Avicennia marina* trees release their propagules just before the NW monsoon start, which is around November. As a consequence, during the simulations propagules released during both the NW and SE monsoon.

4.2.5. River

Since the Demak area has a monsoon climate with a wet season from November to March and dry season from May to September (Ervita et al., 2017). The rainfall distribution during these seasons is a good indicator for Wulan River discharges, see Figure 4.5.

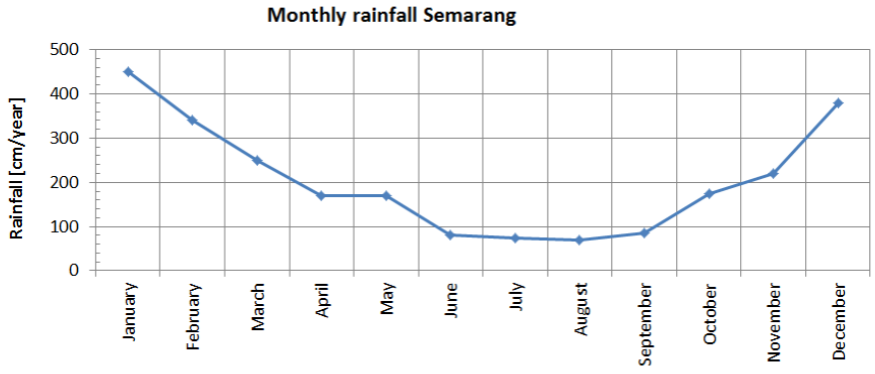

Figure 4.5: Rainfall distribution over the year in Semarang (HK. et al., 2008).

The Klambu Water level and Flow Monitoring Station is located at nearest river dam, however this is more than 30 km from the river mouth. Water flowing from this dam is divided into channels used for irrigation purposes. Therefore using the discharge of the Klambu Station does not provide an very

accurate discharge amount. The average Wulan river discharge measured by the Klambu Station in 2016 during wet season is 138.18 m^3/s, whereas the dry season discharge is 31.6 m^3/s (Fadlillah et al., 2019). As an example of the variation in the river discharge distribution throughout the year, in Figure 4.6 the monthly mean of 2016 is shown. In Station 1 at the coast, shown in Figure 3.5, the average discharge of 2016 in the wet season was 132.95 m^3/s , while in the dry season it was 63.14 m^3/s, these values are used as input for the river boundary condition. This discharge divides itself over the Old and New Wulan River (Figure 3.5) after the bifurcation (Bariq and Marfai, 2019).

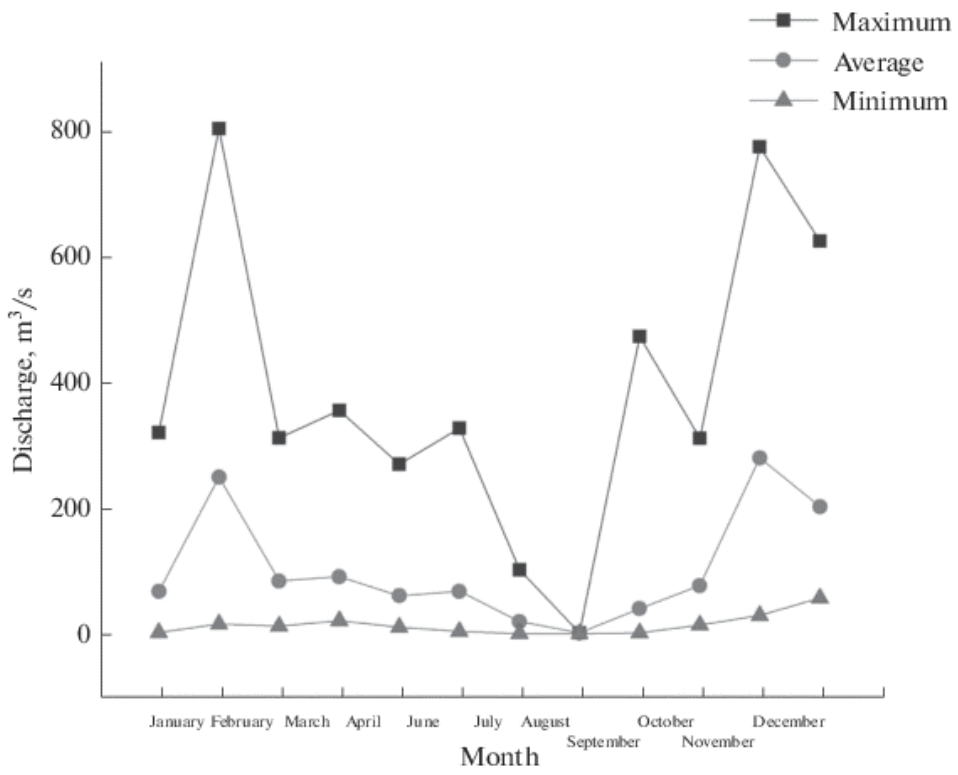

Figure 4.6: Monthly mean Wulan river discharge of Klambu Station in 2016 (Fadlillah et al., 2019).

Since the Wulan Delta protrudes into the sea, it could be an obstruction for the prevailing longshore currents including the sediment load. Furthermore the orientation of the tributaries of the bird-foot river delta changes, which is likely to largely influence the river outflow direction. For example the Old Wulan tributary was more discharging to the North, while the New Wulan tributary is more orientated to the South (Figure 3.5). The sediment load of the Wulan River discharge could be a main local source of sediment for tens of kilometers of coastline. The monsoon climate has the result that there is much more sediment available in the wet season than in the dry season (EcoShape, 2015). Exact sediment concentrations in the Wulan River are not known and they can vary significantly over the year. High concentrations of TSS in the Wulan River happen during high intensity of erosion and land degradation in the upstream area or erosion of the river banks. Fadlillah et al. (2018) did some measurements in the river, in April 2014 TSS concentrations were around 2500 mg/L, while in May and August (2014/2016) values around 50 mg/L were measured in samples. In the sea waters in front of the Wulan Delta, TSS values range from 20 to 200 mg/L (Wisha and Ondara, 2017; Bariq and Marfai, 2019). In the model sediment concentrations of 100 mg/L (0.1 kg/m^3) are assumed in dry season and 1000 mg/L (1 kg/m^3) mg/L in the wet season. TSS concentrations are in general dependent on the water discharge, mostly how higher the water discharge, how higher the TSS (Gray et al., 2014). Not much information is found about the composition (i.e. D_{50} or sand-mud ratio) of the material coming out of the river. In a report of Kerssens (1980) is stated that a diameter of D_{50} = 50 μm representative for the transported sediment in the river.

4.2.6. Tide

The IHO tidal monitoring station is located at the south boundary of the area at the port of Semarang City. Tas (2022) performed a tidal harmonic analysis (Foreman and Henry, 1989) using UTide (Codiga, 2011) on water level data from 2016 to 2018 in the port of Semarang (Flanders Marine Institute (VLIZ) and Intergovernmental Oceanographic Commission (IOC), 2021) to determine the tidal constituents, which are given in Table 4.2.

Constituent	Name	Period [hr]	Amplitude [m]	Phase [deg]
K1	Lunar-solar declinational (diurnal)	23.93	0.226	245
M2	Principal lunar (semidiurnal)	12.42	0.103	55
S2	Principal solar (semidiurnal)	12.00	0.083	308
O1	Principal lunar (diurnal)	25.82	0.079	132
P1	Principal solar (diurnal)	24.07	0.071	247
SSA	Solar (semiannual)	4383	0.047	156
N2	Lunar elliptical (semidiurnal)	12.66	0.042	18
K2	Lunar-solar declinational (semidiurnal)	11.97	0.035	347
S1	Solar (diurnal)	24.00	0.022	64

Table 4.2: Main tidal constituents Semarang (Tas, 2022).

$$F = (\mathrm{K1} + \mathrm{O1})/(\mathrm{M2} + \mathrm{S2}) \tag{4.1}$$

The tidal form factor (see Equation 4.1) resulting from these constituents is 1.72, thus the tide can be classified as mixed, mainly diurnal (Pugh, 1987). Therefore the tide consists of a main diurnal component and a smaller semi-diurnal component. Despite the diurnal character, the spring-neap variation is dominated by semi-diurnal components, due to the large difference in amplitude between O1 and K1 but small difference between S2 and M2 (Tas, 2022). The tidal signal of the IHO monitoring station in Semarang (Figure 4.7) is compared to water levels computed by the Delft3D near Semarang (Figure 4.8). The tidal signal and computed water levels are in close agreement, thus the tidal constituents obtained from the global tidal model in DelftDashboard are well implemented in Delft3D. This is done by dividing the boundaries in small sections with their own tidal constituents to include a tidal phase lag in the model domain, because same tidal boundary in the whole model domain would not be realistic. The tidal constituents are implemented as astronomic open water level boundary along both boundaries, which have a depth larger than 5 m. The months March, April, September and October have much larger semi-diurnal components in their tidal signal, which is approximately during the transition in between the monsoons (Appendix A). Tidal constituents of the month January are therefore applied, as this month has representative constituents for the NW en SE monsoon period. Furthermore, for the reflection parameter alpha a value of 1000 s^2 is chosen, to make the open boundaries less reflective for short wave disturbances that propagate towards the boundary from inside the model. Finally, the currents in Delft3D-4 (this research) and Delft3D-FM (Smits, 2016) are compared to ensure that the boundary conditions provide comparable results and do not induce numerical instabilities, as the main uncertainty will be in the boundary conditions.

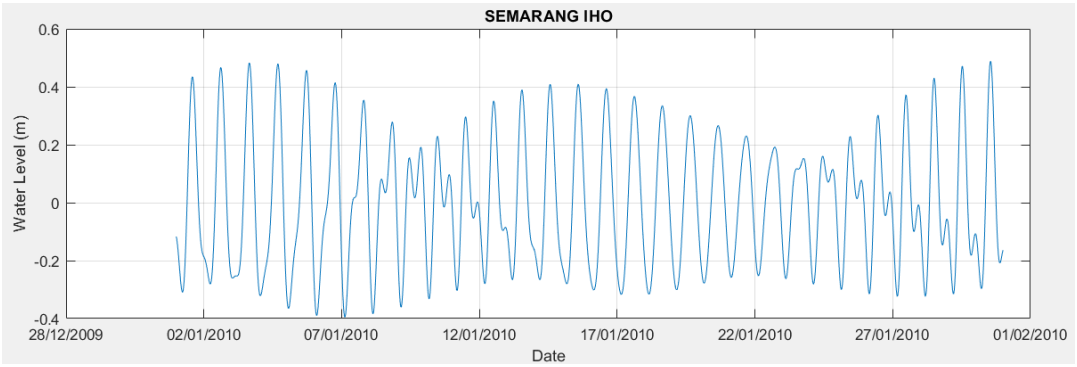

Figure 4.7: Water levels measured in Semarang IHO Station (downloaded from DelftDashboard).

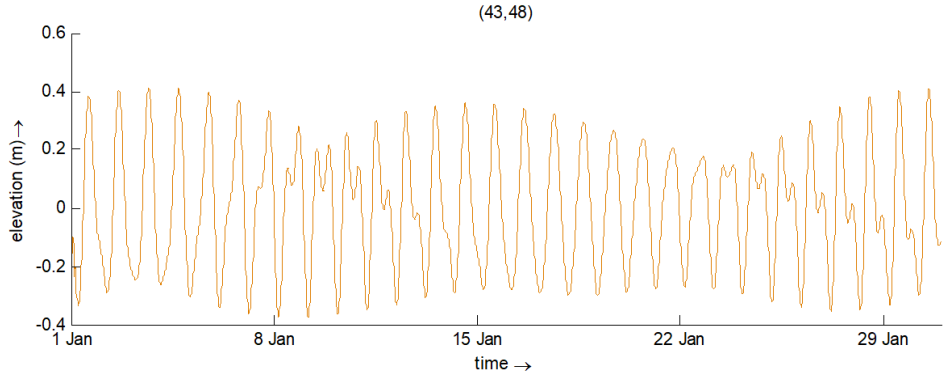

Figure 4.8: Water levels modelled by the Delft3D model near Semarang.

4.2.7. Wind

The Demak area is characterized by a tropical monsoon climate following the Köppen-Geiger climate classification (Peel et al., 2007). This monsoon climate has a wet season from November to March, during this wet season waves and wind come from offshore (WNW) and during the calm and dry season (May-September) from land (ESE) (Ervita et al., 2017).

In addition to the dominant wet and dry season directions, a third peak direction occurs during the dry season, a sea breeze from the North (Tas, 2022). A sea breeze is the result of a local circulation system caused by temperature differences between sea and land, because air above land warms faster during the day than above sea (Haurwitz, 1947). The sea breeze is less frequent than the ESE monsoon wind, however wind speeds are higher. In Demak, the wind direction shifts from ESE (monsoon) to N (sea breeze) between 12:00h and 14:00h, then remains N for about 6 hours before returning to ESE (Tas, 2022). Daily changes in the wind direction may affect sediment and propagule distributions and neglecting those changes could result in a different distributions compared to reality.

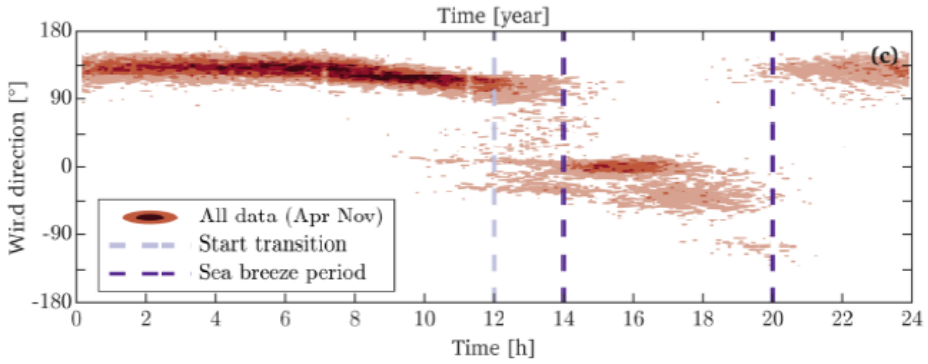

Figure 4.9: Density distribution of the wind directions over the day during the SE monsoon season. All data in this plot is based on measurements between 2015 and 2018 in the port of Semarang (Tas, 2022).

For simplicity a constant wind speed is included in the model, not varying in space. This means during the NW monsoon a constant wind of 4.4 m/s from $292.5°$ is applied (Smits, 2016). In the SE monsoon a wind of 3 m/s from $112.5°$ (Smits, 2016) and between 13.00h and 20:00h the sea breeze from $0°$ (Tas, 2022).

4.2.8. Waves

Demak has a tropical monsoon climate, during the wet season waves of 0.7 m come from WNW and during the calm and dry season waves of 0.4 m from E (Ervita et al., 2017; Smits, 2016). Yearly mean wave heights, according to wave data near Semarang, are around 0.46 m and maxima lie around 2.6 to 3 m (Tas, 2022). Similar to the wind directions, there are three main wave directions, the NE monsoon, the SE monsoon and the sea breeze (N). The wave climate off the coastline of Demak is generally mild, especially during the SE monsoon season. Due to the orientation of Demak's coastline, winds

are directed from land to sea during the SE monsoon, creating calm conditions near the coast. Since the winds are directed towards land during the NW monsoon, they generate higher waves, and storms are frequent during the NW monsoon, resulting in even higher wave conditions. The SE monsoon season pattern shows waves coming from the E for most of the day, except during the afternoon, when waves come from the north due to the sea breeze. Due to the orientation of the coast and higher wind speed, the sea breeze generates significantly higher waves than the prevailing SE monsoon wind. Next, there is the NW monsoon season pattern, with waves coming from the WNW throughout the entire day Tas (2022); Smits (2016).

A SWAN wave model is applied to obtain the wave-induced shear stresses along the coastal system from wave heights and near bottom orbital velocities (see Figure 4.10). Without wave-induced shear stresses, sediment would not be transported in the area. Since computing wave-driven currents is computationally expensive, such currents are neglected in this study.

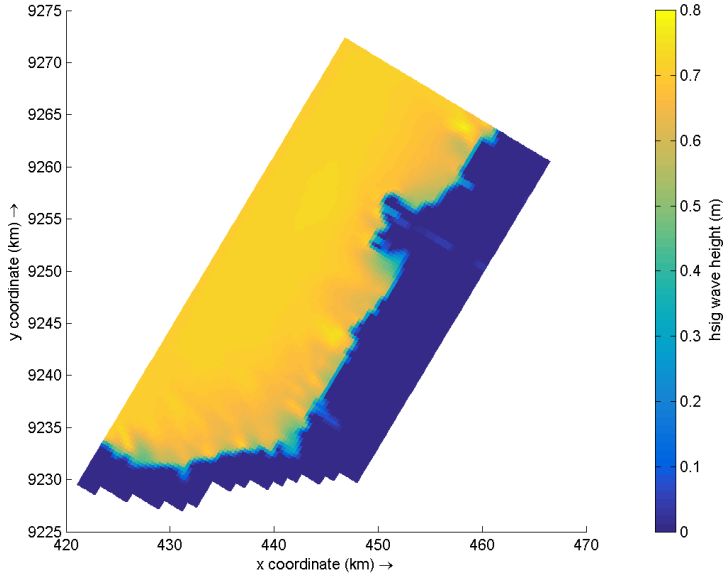

(a) Significant wave height in the NW monsoon.

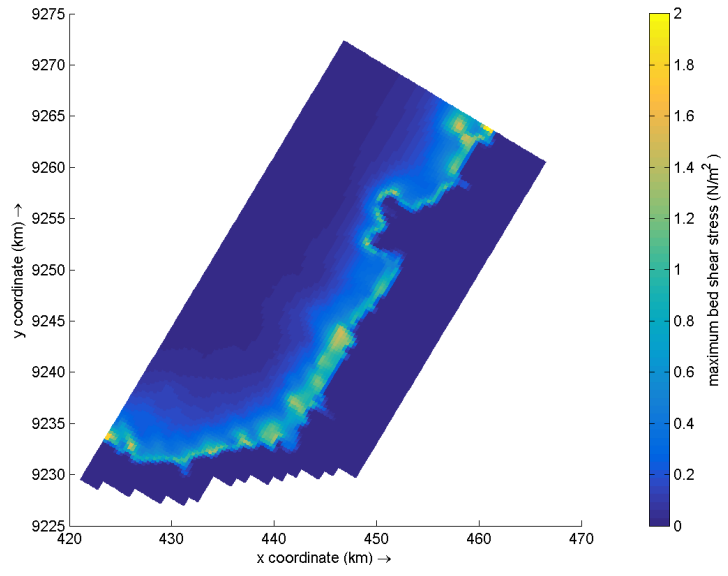

(b) Wave-induced bed shear stress in the NW monsoon.

Figure 4.10: Results of the wave model in SWAN.

4.2.9. Physical Parameters

The salinity in Sayung waters ranged 33-38ppt during the dry season and 27-31ppt during the wet season (Wisha and Ondara, 2017). For simplicity, both in the wet season as in the dry season of an initial condition of 31 ppt is chosen. The water of Wulan river is assumed to be fresh, which means a salinity of 0 ppt. The water density is assumed to be 1025 kg/m^3, which is the standard value for sea water. A Manning roughness value of n = 0.012 is used, representative for smooth mud coasts, and thus lower than typical values around 0.023 for sand coasts (Smits, 2016).

4.3. Modelling Phases

This section elaborates the modelling phases, from computing currents and sediment transport in Delft3D, to pathways in SedTRAILS, eventually modelling other scenarios and finally verifying the model.

4.3.1. Phase A - Currents

The Eulerian currents and sediment transport are computed in the idealized Delft3D-4 model. A first set of simulations includes river, tidal and wind processes, whereas the effect of stratification is included in a second set of model runs. The tide is included by the tidal cycle of the month January, as this month is representative for the tidal constituents. River discharges and wind velocities/directions are dependent on seasonal monsoon patterns. Two seasons are considered: the wet season with high river discharges and winds from the sea and the dry season with lower river discharges winds from land. The system is analyzed with a morphostatic approach, where the bed level is fixed and is not updated over time.

Concluding, initially the model is depth-averaged without density difference effects. This allows us to look into the main barotropic flow patterns and how they interact with topographic features like the protruding delta and basin. When this model is verified, it is adapted to a 3D model to look into baroclinic flow patterns. Thus the model starts simple and layers of complexity are added one by one to understand the processes going on.

4.3.2. Phase B - Sediment Pathways

The results of the simulations done in Delft3D are used as input for SedTRAILS. SedTRAILS computations could be based on a selected representative morphological tide, which is then repeated to simulate longer time scales. However, in this study the tide of one entire month of the Delft3D computation is used, as without a repetitive tide variations in the tidal cycle can be included.

First the output of the Delft3D model is preprocessed by SedTRAILS. As the bed shear stresses from waves are not calculated by the Delft3D flow model, they are computed with a separate Delft3D wave model using SWAN. Implementing bed shear stresses from currents and waves in SedTRAILS is of significant influence, because without stirring by waves there is almost no movement of sediment in the area. Bed shear stresses are not direct output of the Delft3D wave model, but these can be computed from the output parameters. First the particle excursion amplitude close the the bed A is calculated by Equation 4.2 using the amplitude of the velocity near the bed u_{orb} and the peak period T_p (Swart, 1974).

$$A = \frac{u_{orb} \cdot T_p}{2\pi} \tag{4.2}$$

From this the friction factor for waves f_w can be calculated by Equation 4.3 (Swart, 1974), assuming a roughness k_s. The Nikuradse roughness k_s refers by definition to a perfectly flat bottom with a uniform granulometry (Pascolo et al., 2018), for a nominally flat sand bed, $k_s = 2.5d_{50}$ is suggested in literature (Nielsen, 2009). This approach is valid for the flow conditions at the Demak site, because the maximum Shields parameter at the site is below 0.5. Above a Shields parameter of 0.5 to 1.0 sheet flow starts to occur and layers of sand move instead of single grains. During this condition the effective roughness is determined by the thickness of this layer instead of the size of a single grain. The erosion at this condition is dominated by the bulk properties of sand, while at a low Shields parameter erosion is dominated by the behavior of separate grains (Bisschop, 2018).

$$f_w = 0.00251 \cdot \exp\left[5.21\left(\frac{A}{k_s}\right)^{-0.19}\right] \quad \text{for } \left(\frac{A}{k_s}\right) > \frac{\pi}{2}$$
$$f_w = 0.30 \quad \text{for } \left(\frac{A}{k_s}\right) < \frac{\pi}{2} \tag{4.3}$$

Next the maximum bottom shear stress due to waves is computed in Equation 4.4, with ρ is 1025 kg/m^3 as assumed before.

$$\tau_{waves} = \frac{1}{2} \cdot \rho \cdot f_w \cdot u_{orb}^2 \tag{4.4}$$

The current-driven bed shear stress τ_c (Equation 4.5) in Delft3D is determined by the current velocity U and the Manning roughness value n. The formulations of the mean bed shear stress τ_m and maximum bed shear stress τ_{max} are simplified. The mean bed shear stress τ_m is assumed to be equal to bed shear stress due to currents, as the time averaged bed shear stress by waves is zero (Equation 4.6). While the maximum bed shear stress τ_{max} is assumed to be equal to $\tau_c + \tau_w$, so non-linear interactions between the bed shear stresses are not taken into account (Equation 4.7).

$$\tau_c = \frac{\rho g U|U|}{C^2} \text{ with } C = \frac{\sqrt[6]{H}}{n} \tag{4.5}$$

$$\tau_{\text{mean}} = \tau_{\text{c}} \tag{4.6}$$

$$\tau_{\text{max}} = \tau_{\text{c}} + \tau_{\text{w}} \tag{4.7}$$

After preprocessing the data, the model domain is splitted into clusters and from each cluster a sediment particle is released (Figure 4.11). Finally the Lagrangian sediment pathways can be computed using Equation 4.8 (Soulsby et al., 2011). In this formula U_{gr} the speed of a grain. F is a freedom factor, for these simulations is assumed F = 1. This means that interactions within the bed are not taken into account, approximating a concrete bed where deposited grains are always free to move. P is the probability that grain is moving as bed or suspended load. R is speed reduction factor and lastly U_c is the current speed averaged over the lowest 1 m of the water column, however in SedTRAILS this is simplified by using the depth-averaged velocity. This formula differs from other sediment transport formulas as it represents the movement of individual grains, instead of the bulk movement.

$$\mathrm{U_{gr}} = \mathrm{F} \cdot \mathrm{P} \cdot \mathrm{R} \cdot \mathrm{U_c} \tag{4.8}$$

It is important to understand that SedTRAILS does not compute the movement of an individual particle. SedTRAILS visualizes how a particle would move through an already computed transport field by Delft3D and which path it follows. Interaction with the bottom is not included, which is in reality an important factor for the movement of sediment. The underlying equations in Soulsby et al. (2011) are intended for non-cohesive sand sized (63-1000 μm) particles and do not account for flocculation, hindered settling and consolidation effects.

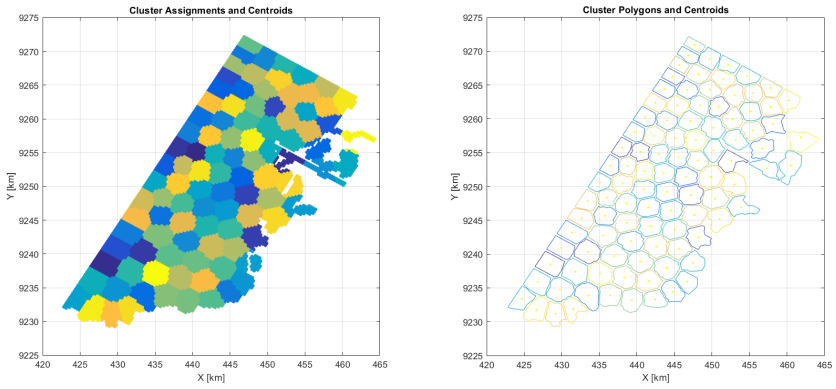

Figure 4.11: SedTRAILS splits the model modain into clusters, from each cluster a sediment particle is released.

4.3.3. Phase C - Propagule Pathways

Adjustments to the SedTRAILS code are developed to compute mangrove propagule pathways. This propagule module is based on several assumptions.

Because mangrove propagules float, it is assumed that they move with the horizontal velocity of the surface layer in Delft3D. This surface layer has a strong wind influence, given the importance of this influence for dispersal (subsection 2.1.3). It is decided to skip an extra windage factor as observations of propagules confirm that they are floating below the water surface (Figure 4.12). So wind does not force the propagules directly, only indirectly by wind-driven currents in the surface layer.

Figure 4.12: Observation by A. Gijon Mancheno of a propagule floating nearby Timbulsloko.

Moreover, some assumptions need to be included to simulate the conditions in which the propagules settle. For settlement the ”sticky depth” in SedTRAILS can be used, defined as the depth that enables particles to flow without ”sticking” on the seabed. In this case the sticky depth is set to 0.2 m. The maximum depth at the sticking location of a propagule must thus not exceed 0.2 m in the simulated month, if the maximum depth is lower than this value the propagule ”sticks” on the sea bottom. As maximum tidal water levels in a month are +0.4, propagules ”stick” above bed levels of approximately +0.2m. Maximum depths are only computed per grid cell, therefore the algorithm interpolates between the grid cells to determine the depth along the pathway of the propagule. After settlement, refloating of propagules is not allowed in the model, since it is not possible to decide if a partly-rooted propagule is still viable for resettlement elsewhere if it is destabilized. Hence the objective is to analyze whether and where propagules can initially settle, because the subsequent processes are too complex and beyond the scope of this project. Another input parameter is the sticky time, defined as a period in which particles cannot stick. For this sticky time, the obligate dispersal period (ODP) of propagules is chosen, which is the period after abscission when a propagule is not yet able to initiate root growth or to germinate (Rabinowitz, 1978). *Avicennia marina* propagules have ODP’s of about 4 to 7 days. In our model there is no ODP assumed for simplicity.

In SedTRAILS it is possible to give particles a lifespan, as the underlying model was developed for coral larvae Storlazzi et al. (2017), for which the lifespan is important. Mangrove propagule of *Avicennia marina* may no longer be viable after 240 days (Clarke, 1993). Since this model simulates one month, the viability period should not be a limiting factor in most places. Buoyancy periods are around 2 to 15 days (Clarke et al., 2001; Clarke, 1993; Clarke and Myerscough, 1991), however after this period they can become buoyant again. Therefore the buoyancy period is assumed to be non-limiting and it is not necessary to give propagules a lifespan in the simulated month.

An additional algorithm is added to the propagule module to determine the survival of the sticking propagules. After stranding propagules need to survive the windows of opportunity propagules to successfully establish (Figure 2.3, subsection 2.1.3). The first phase is an inundation-free period for the propagules, in which the propagules must not be floating away while growing its roots, and this is considered as an period with water depths below 0.05 m. Van Domburg (2018) mentioned that this period is around 5 days based on the paper of Balke et al. (2011). During the second phase roots

need to become long enough to to withstand dislodgement by hydrodynamic forces from waves and current, for this research the maximum bed shear stress is considered as the bed shear stress induced by waves with maximum tidal levels (MSL + 0.4 m). According to Balke et al. (2011), the maximum shear stress to prevent dislodgement for *Avicennia alba* increases linearly from 0.17 N/m^2 to 0.52 N/m^2 in approximately 3 days. The next phase, where even longer roots are needed to survive sheet erosion, is too complicated to include in survival part of the propagule module. To include this, the model would have to be changed from morphostatic to morphodynamic, and thereby set a threshold for a maximum bed level change in a grid cell. Altogether, the algorithm determines at every sticky location of the propagules the inundation-free period (phase 1) and maximum bed shear stress (phase 2) by interpolation.

5 Results

This chapter comprehends the results of current simulations in Delft3D and pathway simulations in SedTRAILS, after that the sediment and propagule pathways are compared.

5.1. Currents

This section shows the results of the currents in the Demak area modelled in Delft3D.

5.1.1. Barotropic Forcing (2D)

This subsection shows the resulting currents influenced by the interaction of barotropic forcings (tidal flows, river discharge and wind) and topograhpic features (protruding delta and basins).

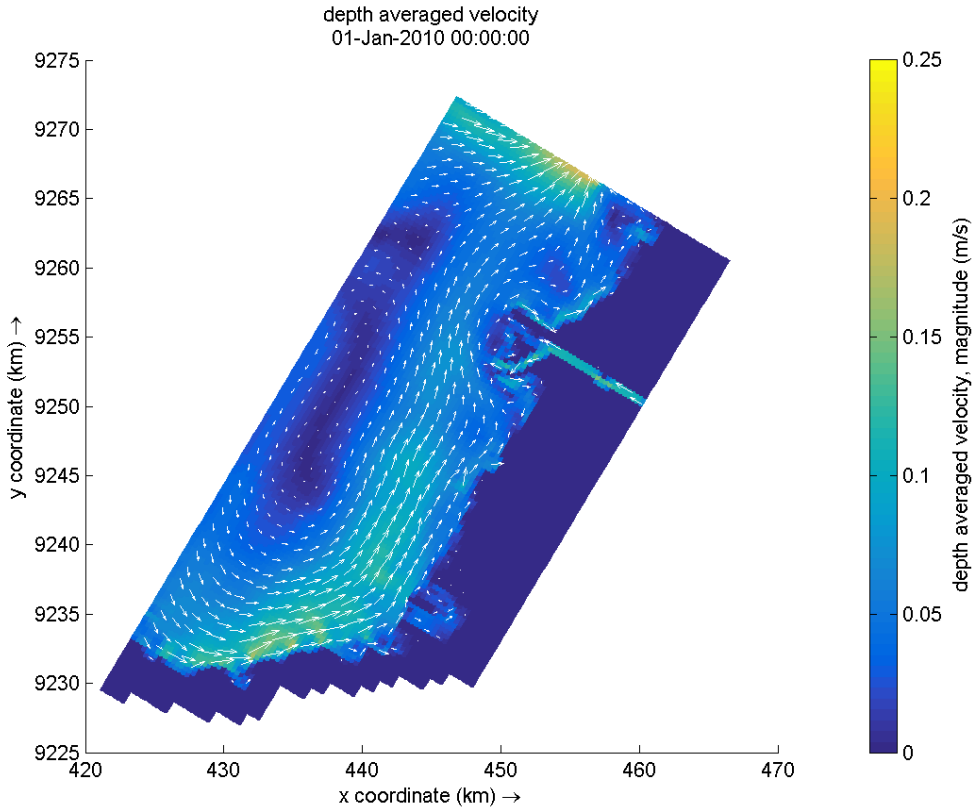

Figure 5.1: Average current patterns for a month in the NW monsoon (wet season), only including barotropic forcing.

The average currents over a month during the NW monsoon are directed from SW to NE along the coast (Figure 5.1). Although the tidal current direction varies during a tidal cycle from flood (to NE) to ebb (to SW) with small flow velocities in between, these variations in currents are not visible in a monthly average. In contrary to the tidal cycle, the wind is constant and the alongshore currents resulting from the WNW wind are pushed along the coast from South to North. The Wulan river delta is protruding, therefore currents are pushed to more offshore water passing the delta. At the intertidal area of Timbulsloko, currents are inducing cross-shore tidal filling. Since water depth are small in this area, currents are mainly perpendicular and not parallel to the coast. Although the average current velocities are low, the actual ebb and flood velocities (filling and emptying the intertidal area) are reaching up to 0.35 m/s.

5.1.2. Baroclinic Forcing (3D)

This subsection shows the resulting currents influenced by the interaction of barotropic forcings (tidal flows, river discharge and wind), topograhpic features (protruding delta and basins) and baroclinic forcing (salinity). Note that for this model run, the freshwater plume was developing, as the initial condition was 31 ppt for all sea water and the fresh river water (0 ppt) was flowing in during the model run.

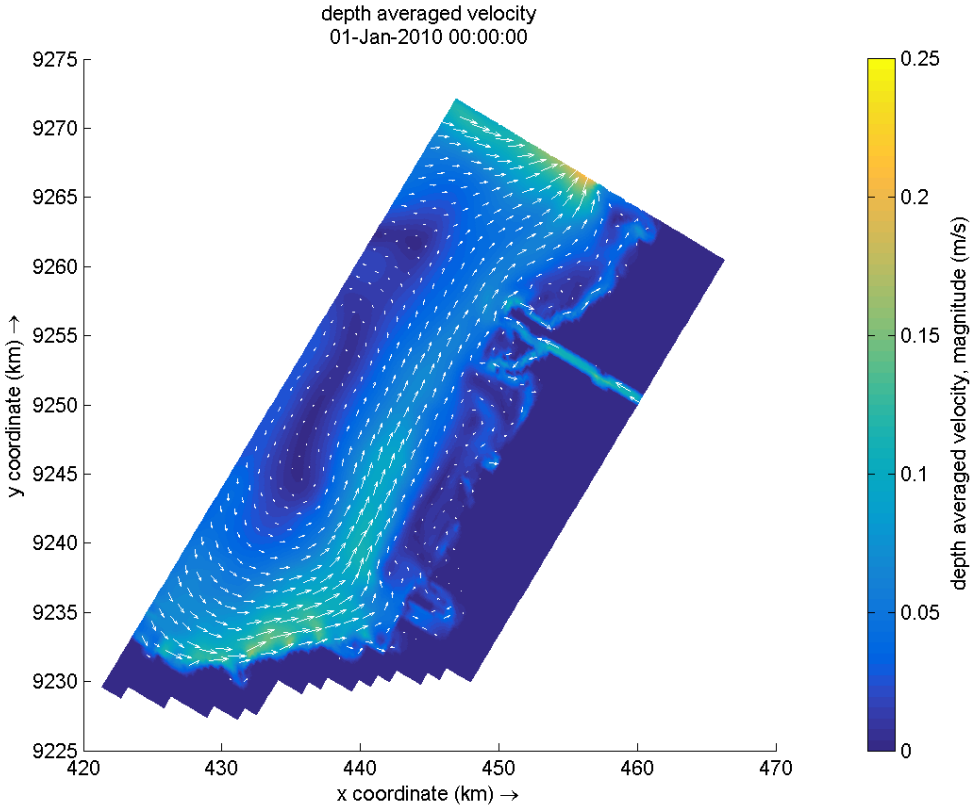

Figure 5.2: Average current patterns for a month in the NW monsoon (wet season), including baroclinic forcing.

When baroclinic effects are included in the flow model, the alongshore currents in the NW monsoon are shifted to a more offshore location (Figure 5.2), compared to the barotropic current pattern of Figure 5.1. When comparing the currents of Figure 5.2 to the surface layer salinity of Figure 5.3, it seems that the alongshore currents are flowing around the fresh water plume, creating a region of low flow velocities (mainly below 0.05 m/s) South and North of the delta. The reason for this is that stratification prevents mixing of the sea and river water.

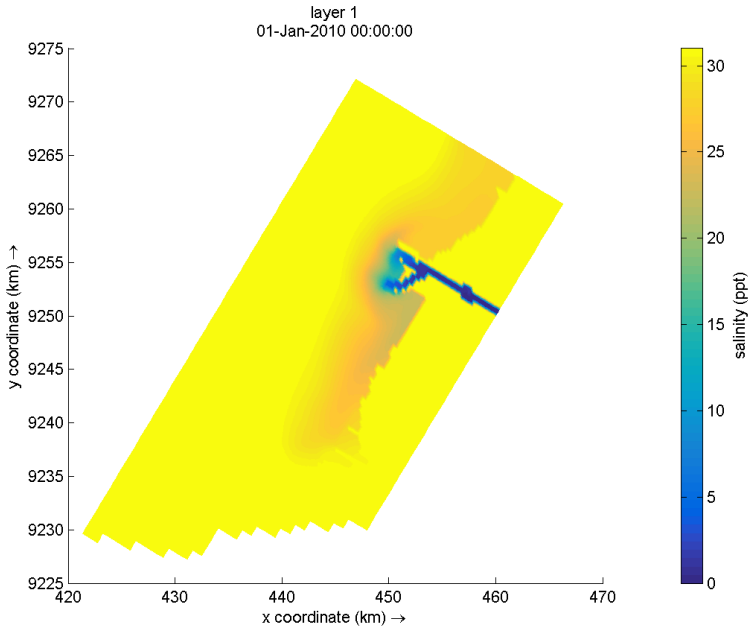

Figure 5.3: Average surface salinity pattern for a month in the NW monsoon (wet season), including baroclinic forcing.

As the computations are in 3D, it is also possible to look into the processes per layer instead of depth-averaged. When the Wulan river meets the sea, the lighter fresh river water flows over the denser salt sea water (Figure 5.4). A layer of sea water slightly intrudes into the river beneath the outflowing layer of river water, pushing its way upstream along the bottom. The currents of the surface layer are shown in Figure 5.5, in which the Wulan river is flowing out into the sea. The water of the left tributary (New Wulan) flows out to the south and is barely mixed, because the plume is trapped along the coast to the southwest. Conversely, the water of the right tributary (Old Wulan) flows out to the North and is mixed by the alongshore currents. Thus, the orientation of the tributaries plays an important role in the deflection of the river plume. The currents of the bottom layer (Figure 5.6) are offshore directed at the Wulan Delta, while there are alongshore currents in the surface layer. These offshore currents at the bottom layer could be a return current caused by the onshore winds. Concluding, significant differences are modelled between current magnitudes and directions over the various depth layers. As a consequence, the modelled pathways of sediment largely depend on the velocity layer or depth-averaged velocity they are based on.

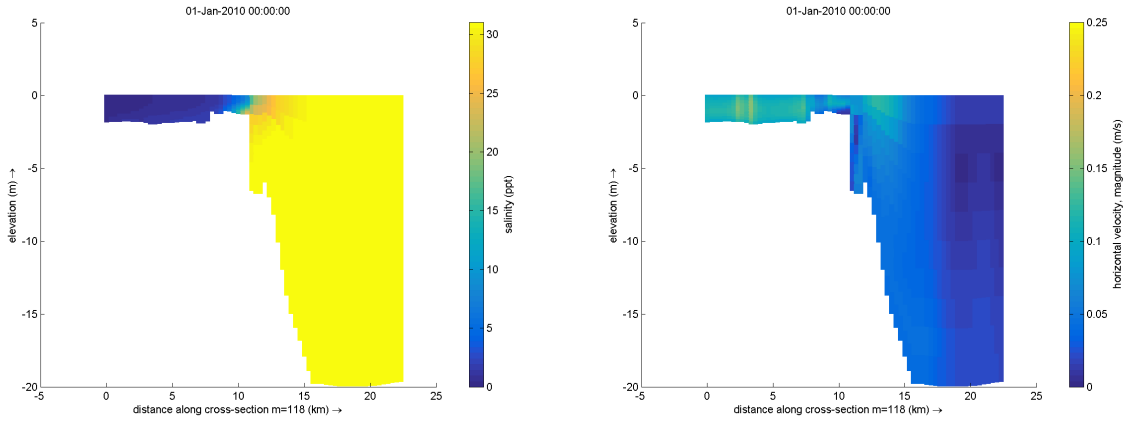

(a) Average horizontal velocity.

(b) Average salinity.

Figure 5.4: Cross-section of the river outflow in the NW monsoon (wet season), including baroclinic forcing.

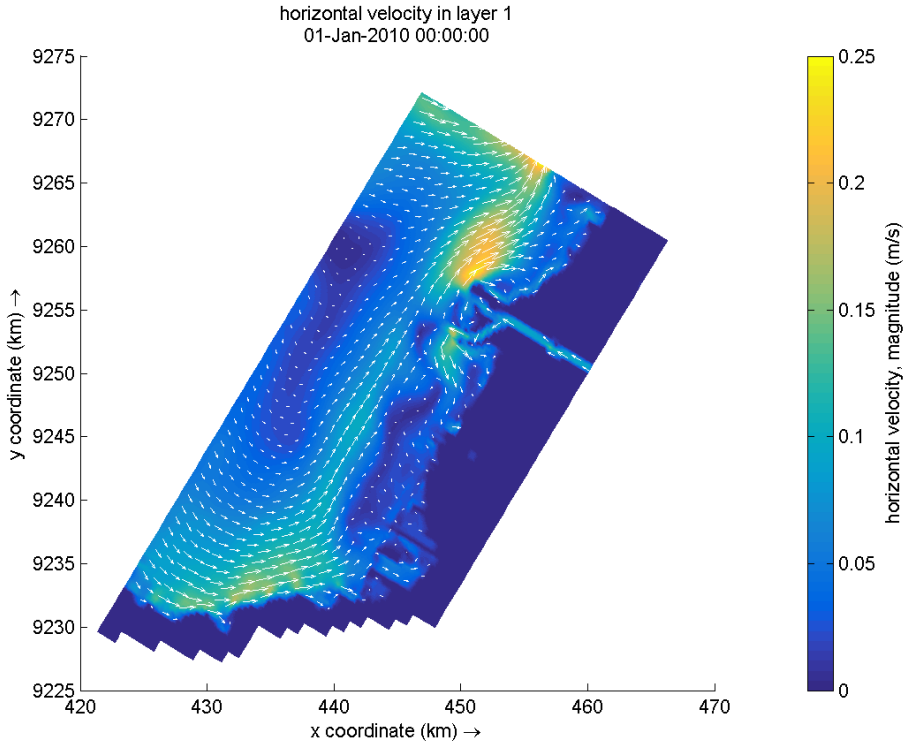

Figure 5.5: Average current pattern of the surface layer for a month in the NW monsoon (wet season).

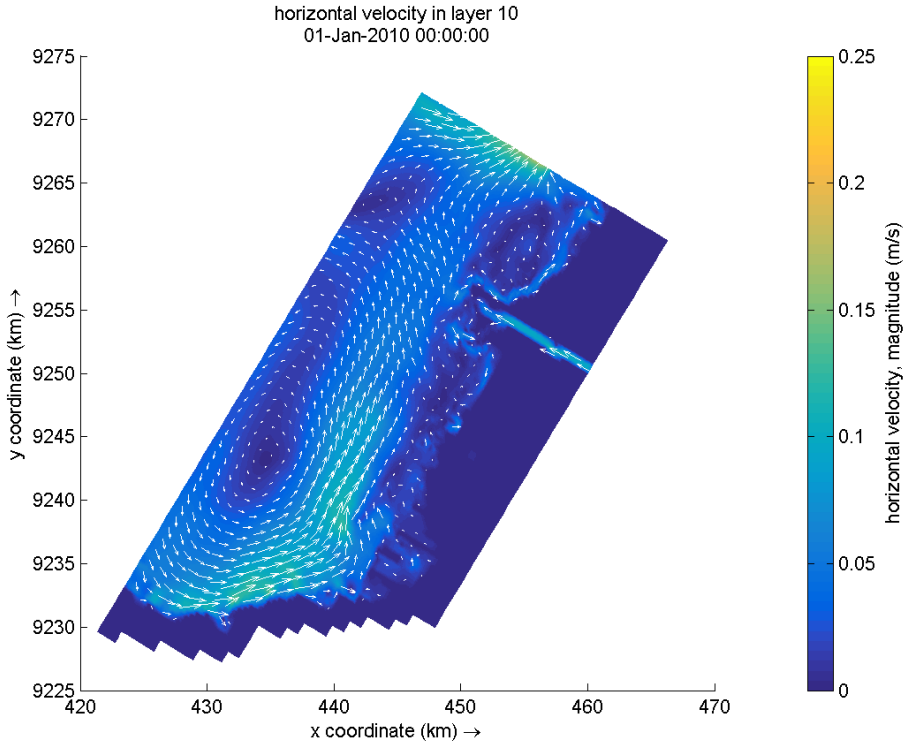

Figure 5.6: Average current pattern of the bottom layer for a month in the NW monsoon (wet season).

In the SE monsoon, alongshore currents are in the opposite direction as the NW monsoon, from NE to SW (see Appendix D). Furthermore, there is hardly any fresh water plume, due to a much smaller Wulan river discharge. Because there there is no plume obstructing currents, alongshore currents stay closer to the coast in the SE than NW monsoon.

5.1.3. Validation

This subsection comprehends a validation of the hydrodynamics computed by model in Delft3D. Validation of the model is mainly done by comparisons to existing models of the area (Smits, 2016; KOICA, 2012; MMAF, 2012; Deltares, 2020), expert judgement, underlying physical principles and literature. Because it is an idealized model rather than an actual representation of Demak, it can not be directly validated by comparison with field data.

First the modelled current pattern in the Demak area is compared to the large-scale current pattern in the Java Sea (Wyrtki, 1961), which is showed in Figure 5.7. The large-scale current in the NW monsoon is from West to East, which corresponds to the alongshore current from SW to NE in our specific modelling area. Besides the modelled alongshore current pattern in the SE monsoon has been validated with the large scale current pattern from East to West in that monsoon.

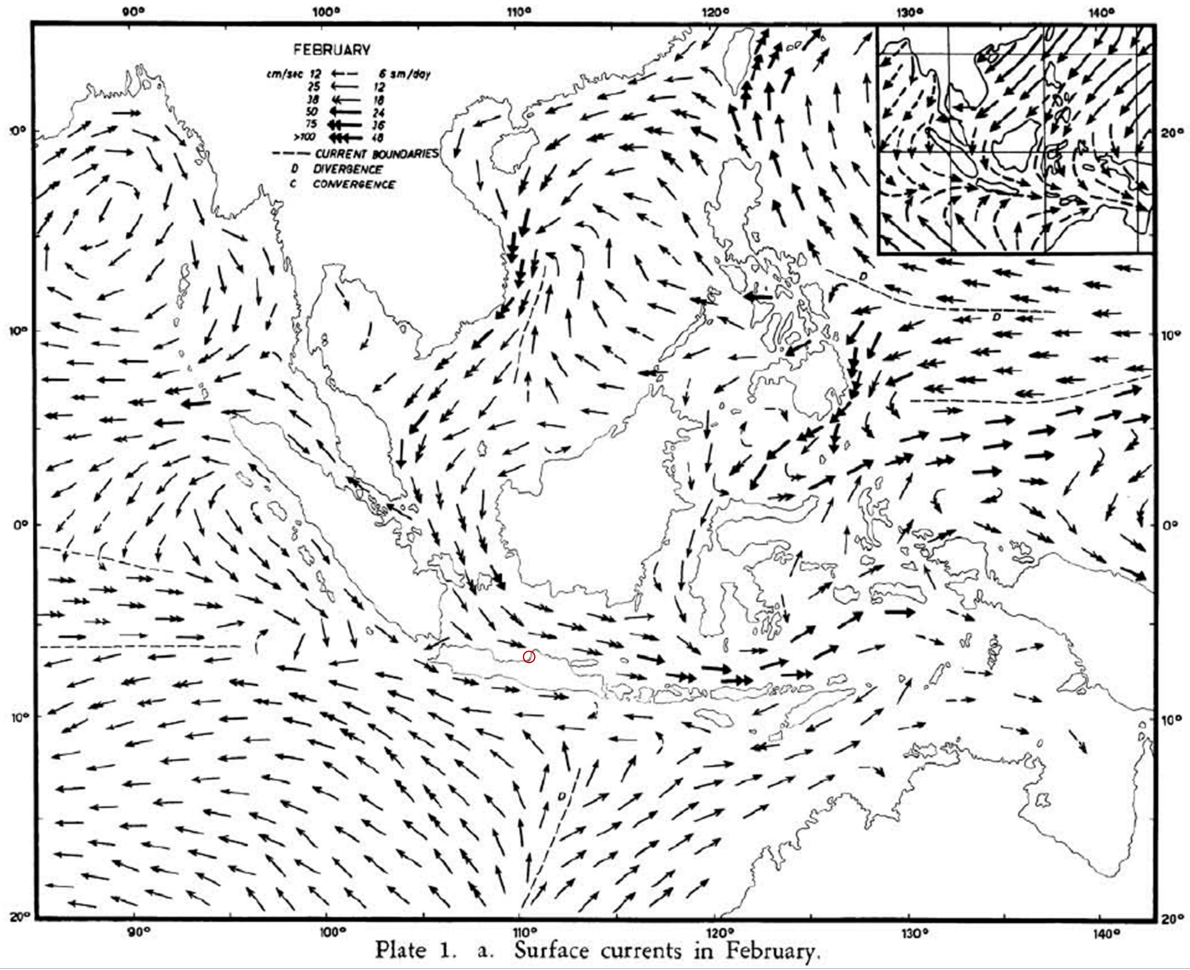

Plate 1. a. Surface currents in February.

Figure 5.7: Large-scale surface currents in the NW monsoon, Demak is highlighted by a small red circle (Wyrtki, 1961).

The general pattern of the tidal flood (to NE) and ebb (to SW) currents in the area can be validated by the reports of KOICA (2012) and MMAF (2012). Furthermore, Deltares (2020) did a modelling study of the area and found the monthly averaged current pattern Figure 5.8. Although our model is more simple and conceptual than the model of Deltares (2020) and our domain is less expanded to offshore, the general current pattern seems to be similar.

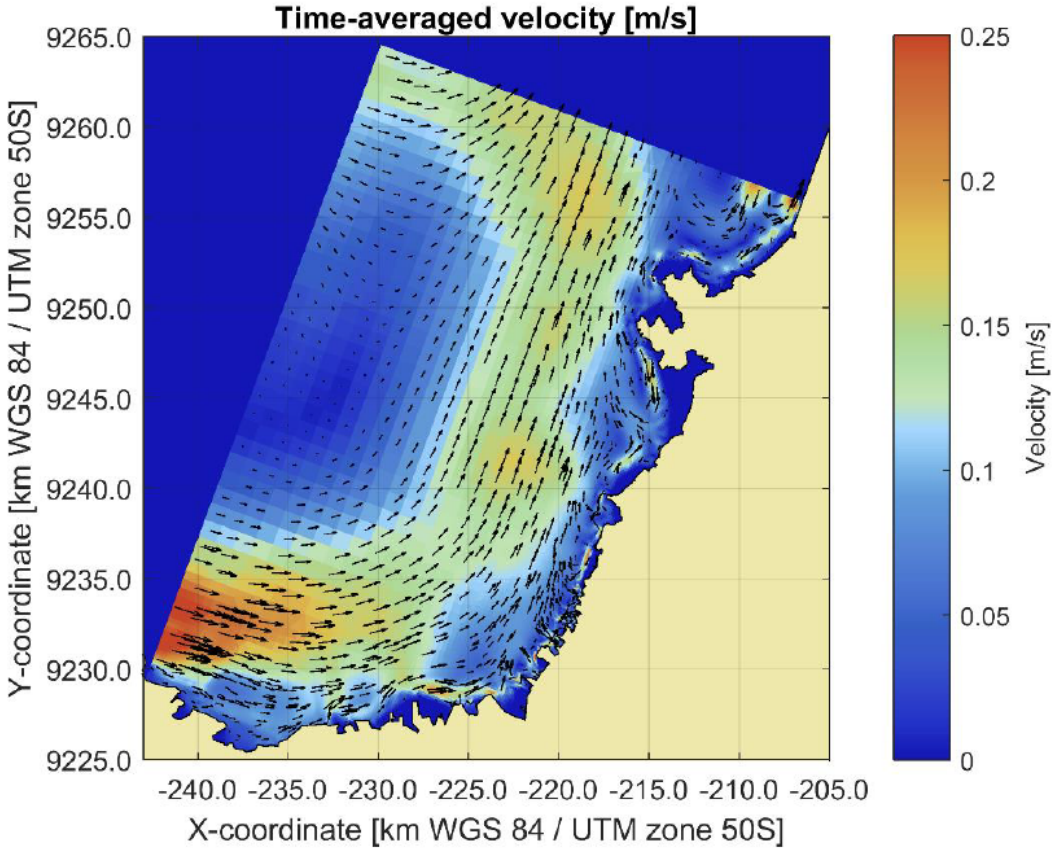

Figure 5.8: Monthly averaged current pattern in the NW monsoon (Deltares, 2020).

5.2. Sediment Pathways

This section includes the results of the sediment pathways in the Demak area modelled by SedTRAILS. Although the the results of the currents where shown as a monthly averaged pattern, the pathways computed by SedTRAILS are not based on the monthly average, but on the full time series over a month. Sediment pathways are only computed for the NW monsoon (wet season), because in the SE monsoon (dry season) there is barely any sediment transport, as wave heights are much lower during this monsoon. The results are only an indication for what the possible muddy sediment pathways could be, since the underlying equations in Soulsby et al. (2011) are intended for non-cohesive sand sized (63-1000 μm) particles and do not account for flocculation, hindered settling and consolidation effects.

5.2.1. Barotropic Forcing (2D)

The pathways of fine sediment (Figure 5.9) show the same alongshore SW to NE motion as that was observed in the monthly averaged current pattern (Figure 5.1). The Wulan Delta confines the area for alongshore sediment pathways. Although the Wulan delta is an obstruction for sediment, most sediment pathways follow the dominant currents and part of them is able to pass the protruding Wulan delta. In some sediment pathways the variation in tidal current direction is seen as a sort of spiralling motion, while other pathways are less influenced by the tide and therefore more straight. South from the Wulan Delta an eddy of circulating sediment is found. At the intertidal basins of Timbulsloko the length of the sediment pathways is much shorter, however, sediments seems to be imported in these tidal basins. In subsection 5.2.4, the intertidal basins are analyzed in more detail. Shorter pathway lengths inside the tidal basins mean that sediment particles are moving slower or having lower mobility, comparing to the long alongshore sediment pathways with thus particles that are moving faster or having higher mobility. From these results can be concluded, it can that the Wulan river is not the only source of sediment for the Demak coastline, as alongshore transport of sediment from the southwest is significant.

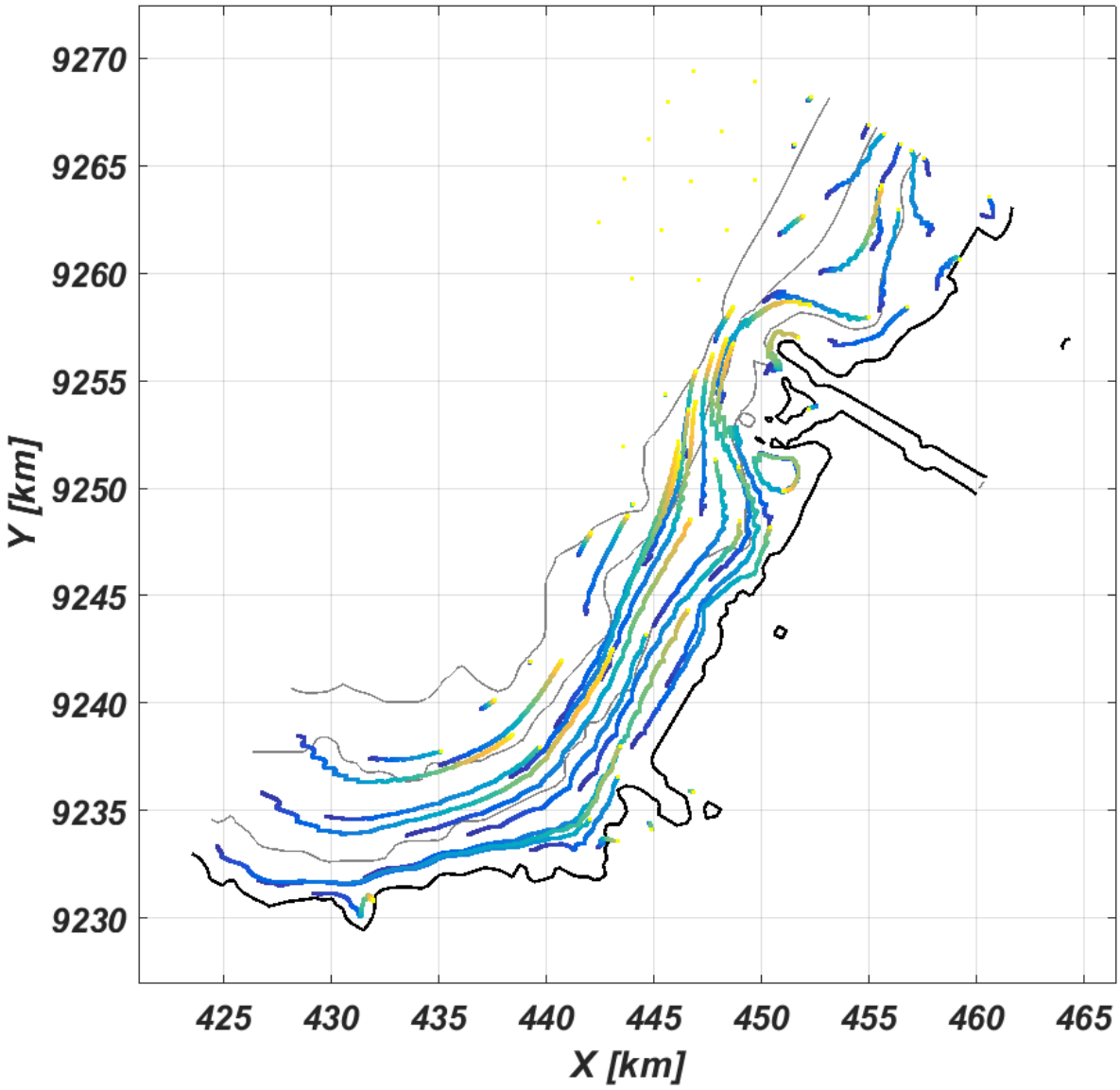

Figure 5.9: Sediment pathways of fine sediment (D_{50} = 18 μm) based on the depth-averaged velocity for a month in the NW monsoon (wet season).

5.2.2. Baroclinic Forcing (3D)

Next, baroclinic effects (salinity/density and 3D effects) are included, however pathways are still computed based on the depth-averaged velocity. The river plume created by the salinity effects confines the area for alongshore sediment pathways even more than the protruding Wulan Delta itself. The result is that alongshore pathways are shifted to a more offshore location and sediment transport decreased significantly in the fresh river water plume (Figure 5.11), compared to the barotropic pathways of Figure 5.9. Not only pathways are shifted to offshore, also some pathways stop offshore along passing the river plume in the baroclinic situation, instead of being transported further by the current along the delta in the barotropic situation. This stopping of the pathways, means that sediment velocities decrease, enabling sediments to settle offshore before and do not pass the plume and protruding delta. Furthermore, sediments from alongshore currents are not able to enter the plume and serve as source for the coastline behind the plume. This highlights the influence of the freshwater plume as an barrier for sediment transport. The decreased amount of sediment able to pass the plume and delta is confirmed by the connectivity analysis in Figure 5.10, as the degree value in the upper circle at the delta is lower in the baroclinic than barotropic simulation, so this node at the delta is connected a smaller number of nodes.

In addition, there is much less transport of sediment inside the river plume, than in the barotropic situation. The trapped sediments in the plume are not moving in the direction of the dominant alongshore sediment transport. The decreased amount of sediment transport in the river plume is confirmed by the connectivity analysis in Figure 5.10, as the degree values in the lower circle at the plume are lower in the baroclinic than barotropic simulation, so these nodes in the plume are connected to a smaller number of nodes. Wolanski (1992) confirmed that particulates, sediments and dissolved nutrients outwelled from mangrove forests into coastal waters can be retained in a coastal boundary layer formed by estuarine circulation. Moreover, at the southern boundary of the plume where currents shift to offshore waters, sediment velocities decrease to zero, which enables sediment to settle. Lastly, flocculation of fine sediment could affect the pathways at the plume in several ways (Eisma, 1986), but this process has not been modelled. So on the one hand, the river plume is a barrier for alongshore sediment transport, but on the other hand, coastal sediments are trapped inside the plume.

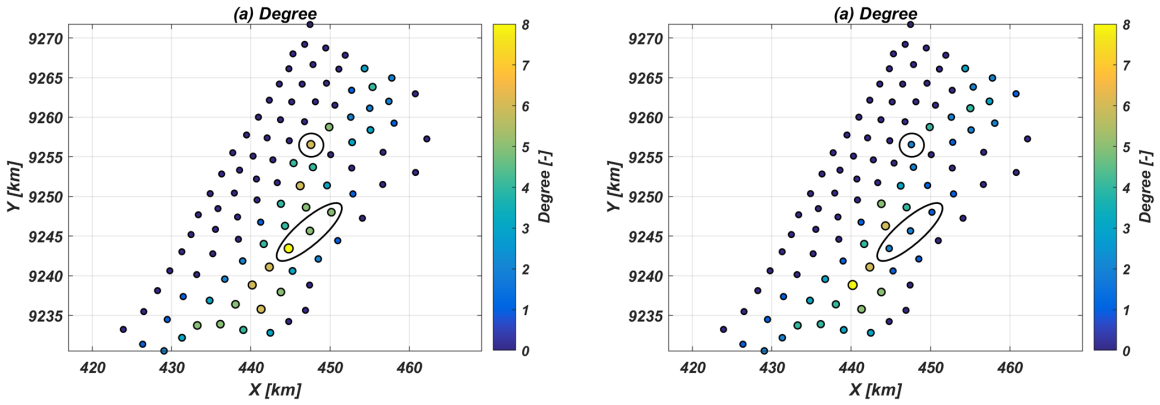

(a) Barotropic forcing (2D).

(b) Baroclinic forcing (3D).

Figure 5.10: Comparing the sediment connectivity of the barotropic (2D) and baroclinic (3D) simulation. High degree values mean that the node is connected to a large number of nodes. The circles show the differences at the river plume and at the Wulan delta.

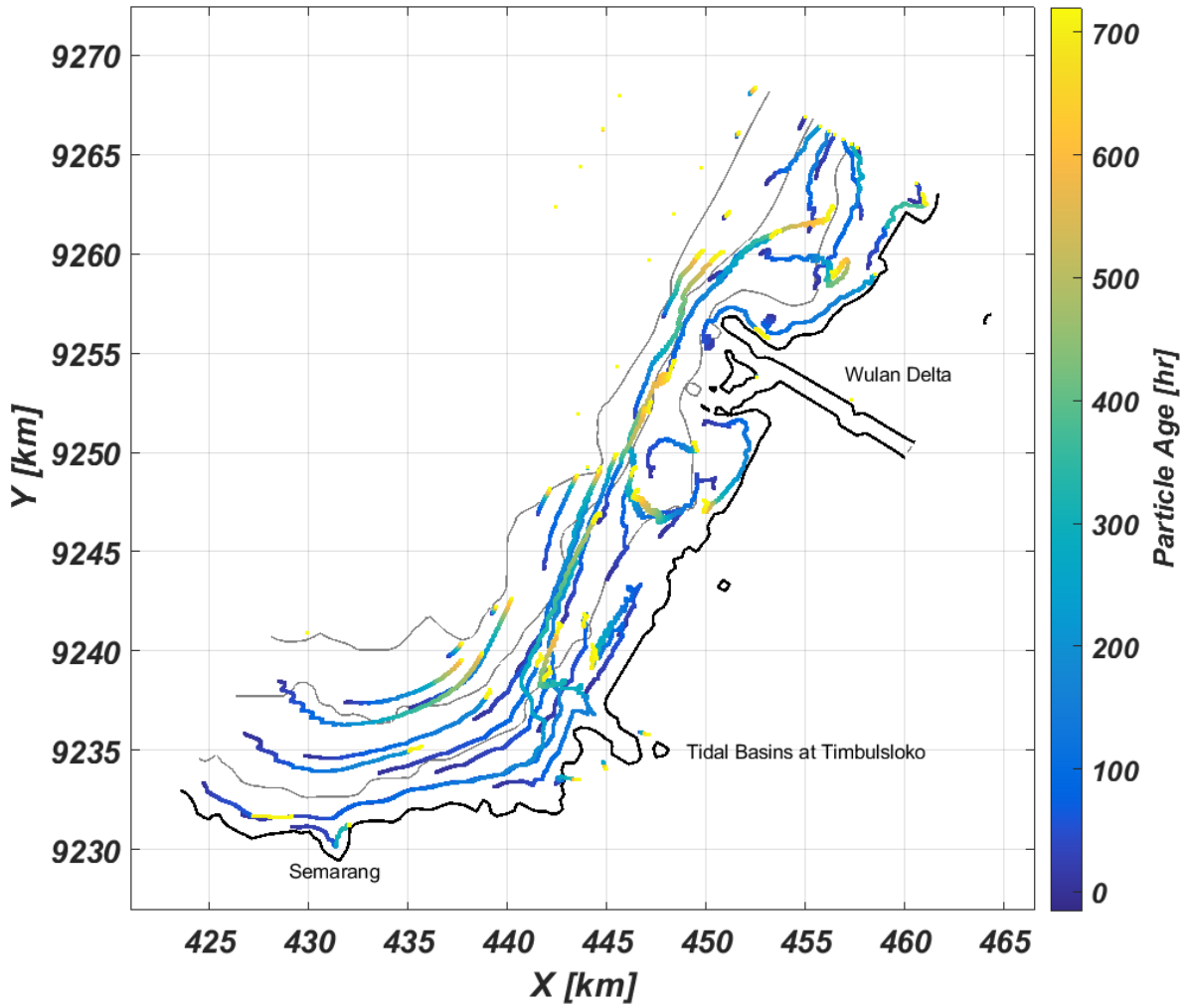

Figure 5.11: Sediment pathways of fine sediment (D_{50} = 18 μm) based on the depth-averaged velocity for a month in the NW monsoon (wet season), including baroclinic forcing (3D).

5.2.3. Bed Velocity (3D)

SedTRAILS was developed to compute sediment pathways based on the depth-averaged velocity for 2D models. However, the underlying sediment equation of Soulsby et al. (2011) is actually intended for the velocity of the lowest 1 meter of the water column. As 3D computations are done (sigma layering), it is possible to have a better approximation of the equation of Soulsby et al. (2011), by using the horizontal velocity of the lowest 10% of the water column (bottom layer). Most sediments are suspended relatively close to the bed, for these sediment this approximation is better. Although fine sediments can be suspended higher up in the water column, thus for these sediments the depth-averaged may be more representative.

Sediment pathways based on the velocity near the bed (Figure 5.12) are less obstructed by the river plume, than the sediment pathways based on depth-averaged velocities (Figure 5.11). Near-bed suspended sediments are intruding underneath the river plume towards the coast. At the south part of the area near Semarang sediment both pathways (Figure 5.11 and Figure 5.12) are similar.

Concluding, there may be differences in pathways for sediments suspended at various heights in the water column at the same location. Pathways of sediment suspended close to the bed may be offshore directed, further from the bed may be alongshore directed and near the water surface may be onshore directed. Furthermore, it needs to be taken into account that suspended sediments are not evenly distributed over the water column, but sediment concentrations in general increase towards the bed (Figure 2.4).

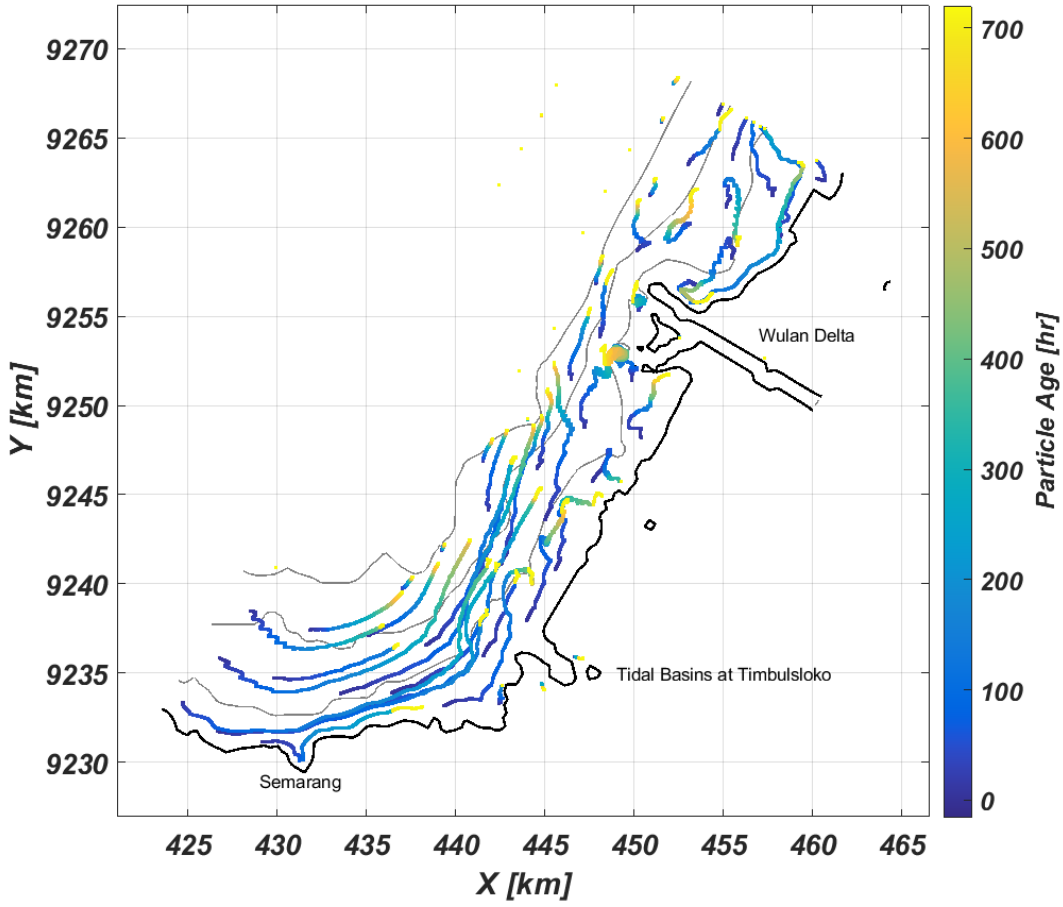

Figure 5.12: Sediment pathways of fine sediment (D_{50} = 18 μm) based on the near-bed velocity for a month in the NW monsoon (wet season), including baroclinic forcing (3D).

5.2.4. Intertidal Basins (3D)

At the intertidal basins of Timbulsloko, currents induce cross-shore tidal filling, as shown in Figure 5.13. Although the average current velocity seems to be low, the actual ebb and flood velocities (filling and emptying the intertidal basins) are reaching up to 0.35 m/s, especially in the deeper part. Therefore, it is interesting to look in more detail at the sediment pathways in this area. Including some of the old pond bunds in the intertidal area barely changes the sediment pathways. In the deeper part (below mean sea level) in the middle of the area, sediments are exported to a sort of ebb tidal delta and further alongshore. The sediment dispersed further alongshore is clearly transported around the obstructing river plume and thus not entering the plume. This export of sediment through the northern part of the area is confirmed by the high degree values in the North (Figure 5.14b). In the more shallow part (above mean sea level) sediment are imported towards the coastline, which can be seen in Figure 5.14a by slightly higher strength values.

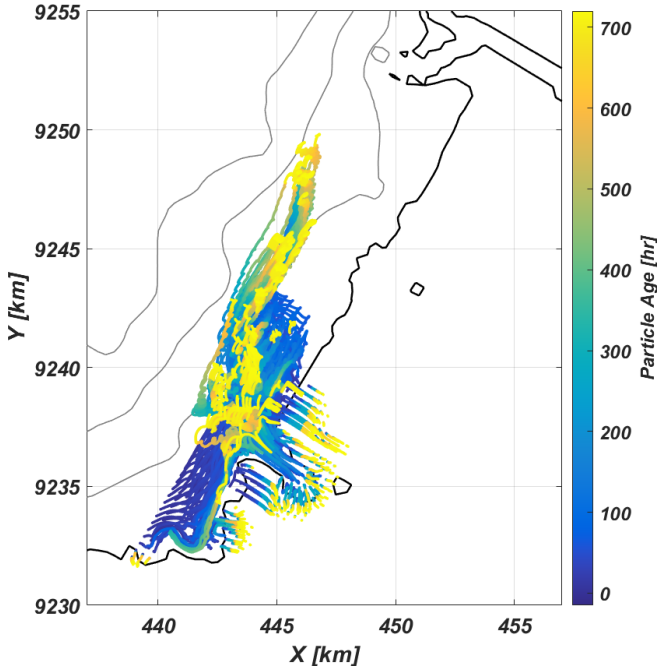

Figure 5.13: Sediment pathways of fine sediment (D_{50} = 18 μm) based on the depth-averaged velocity at the intertidal basins of Timbulsloko for a month in the NW monsoon (wet season), including baroclinic forcing.

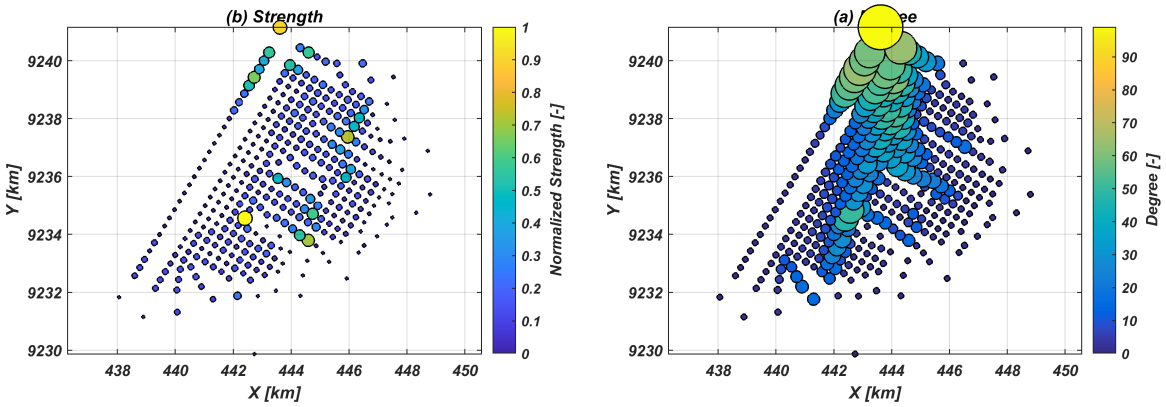

(a) Strength.

(b) Degree.

Figure 5.14: Sediment connectivity in the intertidal basins of Timbulsloko. High degree values mean that the node is connected to a large number of nodes and high strength values mean that the total transport of propagules in and out of a node is large.

The ebb velocities in the basins are slightly higher than the flood velocities, which is a sign of ebb dominance (Figure 5.15). While in the more shallow area sediments are imported during a few events, and not during the entire month. During these events flood velocities reach values up to 0.25 m/s. Ebb velocities are in general below 0.1 m/s and not inducing any sediment export (Figure 5.16). Since flood velocities are higher than ebb velocities on the flats, this part could be flood dominated.

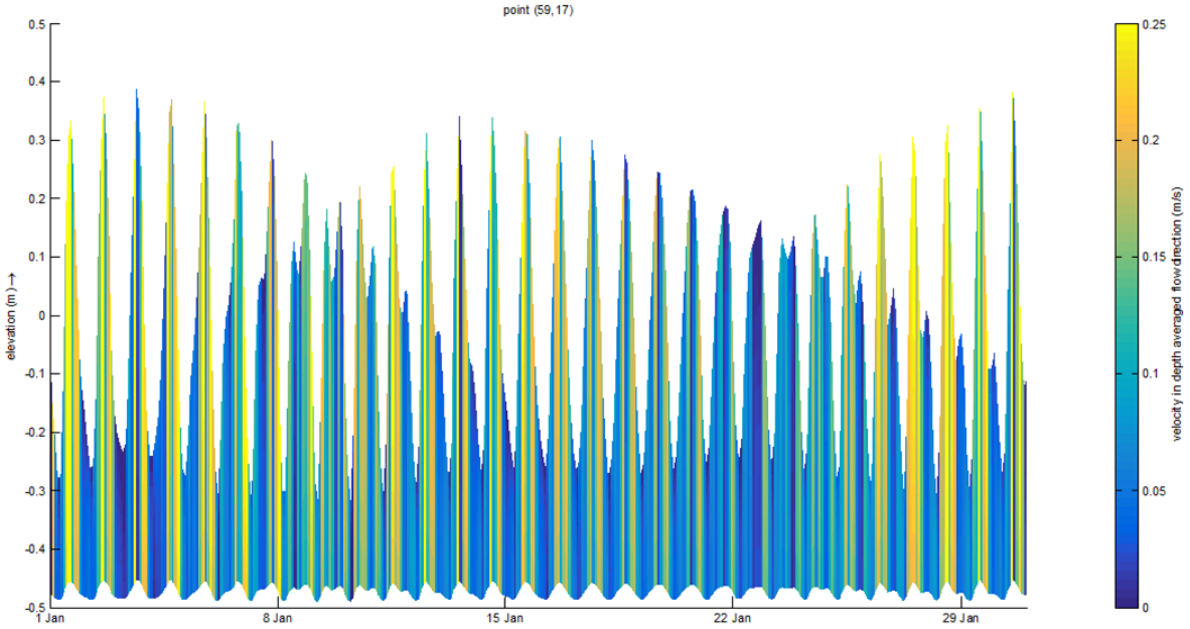

Figure 5.15: Water levels and velocities in a deep part at the intertidal basins at Timbulsloko.

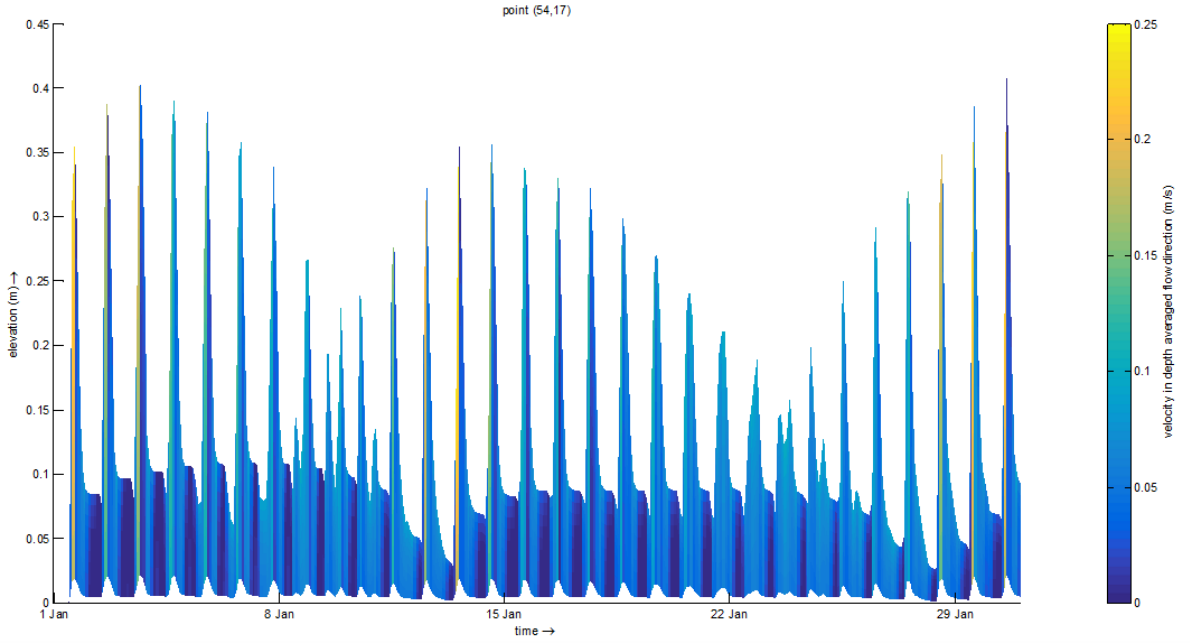

Figure 5.16: Water levels and velocities in a shallow part at the intertidal basins at Timbulsloko.

5.2.5. Wulan Delta (3D)

The Wulan Delta could be a source of sediment for the adjacent coastline (Tas, 2022), therefore these pathways are visualized in more detail. As sediment concentrations in the river and total sediment amounts are much larger during high river discharge events (Q = 800 m^3/s), it may be that during these all the delta building happens. In Figure 5.4 and Figure 5.5, it was already shown that the river flows out into sea in the surface layer, whereas seawater is flowing under the river water, slightly intruding the river mouth. As a consequence, velocities of the river surface layer are seawards and velocities of the sea bottom layer are landwards at the mouth. For the small area near the mouth the surface layer is representative for the riverine sediment pathways. However, the further away from the mouth, the larger the mixing between the river and sea water, and the more representative the depth-averaged velocity is for the sediment pathways.

Sediment pathways based on the depth-averaged velocity show that riverine sediment out of the Wulan river is a source for the adjacent coastline Figure 5.17. Part of the sediments is trapped inside the river water plume along the coast, while the remainder is more mixed by the alongshore currents. Most of the sediments out of both tributaries remain in the coastal zone and are not lost to offshore waters, which means that they are a potential source for the adjacent coastline. Furthermore, the New Wulan (Northern tributary) is deeper and wider than the Old Wulan (Southern tributary) and thus has higher discharge and more potential as sediment source. As a consequence, most of the sediments seem to be trapped in the river water plume to the south and have potential to be a source for this part of the coastline. This corresponds to the observations of Septiangga and Mutaqin (2021), who concluded that the northern shoreline of the delta retreats and the southern one advances due to sedimentation from the river and the mangroves.

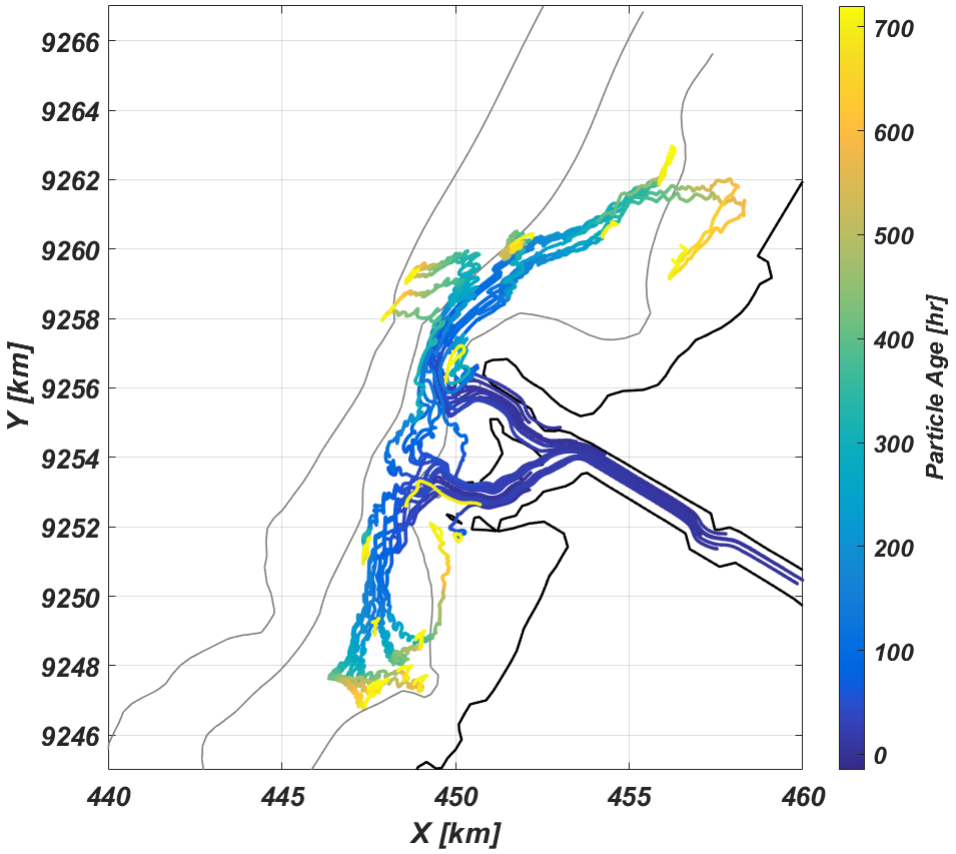

Figure 5.17: Sediment pathways of fine sediment (D_{50} = 18 μm) at the Wulan Delta during maximum river discharges (Q = 800 m^3/s) based on the depth-averaged velocity, including baroclinic forcing (3D).

5.2.6. Mud & Sand (3D)

This section shows the similarities and differences between the muddy and sandy sediment pathways. Although the largest part of the sediment in the area is mud, there is some fine sand present in between these mud particles. Therefore, it is modelled what the small portion of sand particles in between the mud particles could take as pathway, without accounting for interactions between the sandy and muddy particles in the bed or water column. A difference between mud and sand transport, is that sand is transported closer to the bed and mud is more suspended over the water column. Due to this difference, this simulation is based on the near-bed velocity instead of depth-averaged velocity.

The pathway length of sandy sediment (Figure 5.18) is shorter of mud (Figure 5.9), indicating that sand particles are moving slower or having less mobility. Not only pathways are shorter, also much less sand than mud is in movement. For sand only the particles really close to the coast are in movement, whereas for mud also particles slightly further offshore are in movement. The sand particles close to the coast, which are in movement, are transported towards land by sea water intruding under the river plume and feeding the coastal zone, this estuarine circulation is explained in Figure 2.4.

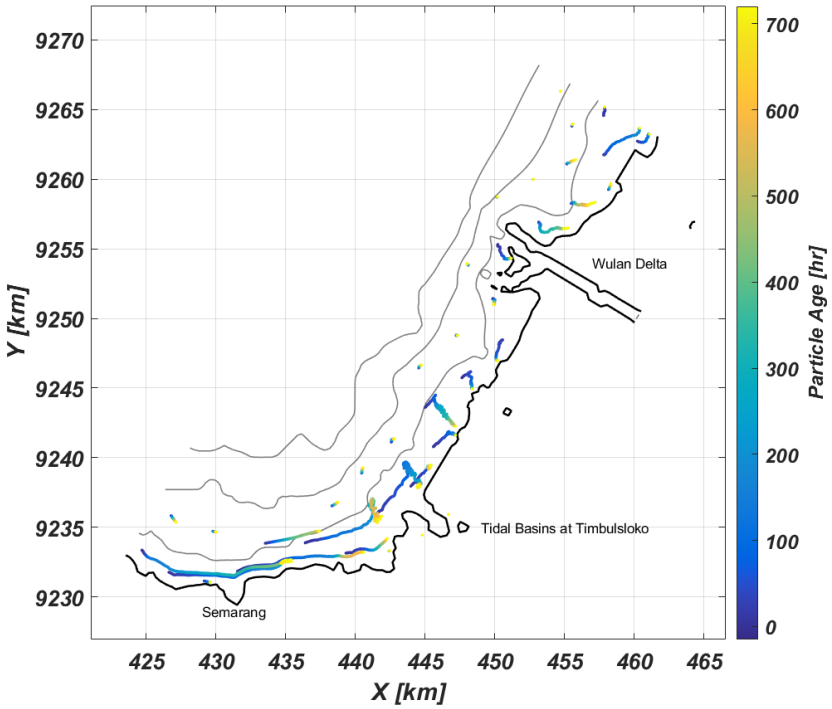

Figure 5.18: Sediment pathways of sand (D_{50} = 145 μm) based on the near-bed velocity for a month in the NW monsoon (wet season).

The proportion of sand is especially relatively high at the cheniers. Nevertheless, it is not exactly known where all the sand from the cheniers is coming from (Tas, 2022). Since the Wulan river is a possible source of that sand, the pathways of the riverine sand are modelled during a high discharge event. Figure 5.19 shows that sand transported by the river is less mobile than mud (see Figure 5.17). Sand accumulates at the river mouth, because flow velocities decrease there. These sands in front of the delta can be transported by waves and deposited around the delta forming a chenier (Marfai et al., 2016). In this way, some of the sands out of the Old Wulan may be reaching the cheniers on the North side of the delta (see Figure 5.20). Altogether, it may be possible that cheniers are formed by the riverine sands.

Lastly, a computation is done based on the near-bed velocities instead of the depth-averaged velocities, as sands may be more suspended towards the bed. Sand particles are released in the river, however, there is almost no movement of these sands. The litte amount transport may be due to the river flowing more in the upper layers and the sea intruding slightly at the bottom layer (Figure 5.4). In this way the sea is inhibiting riverine near-bed sand transport.

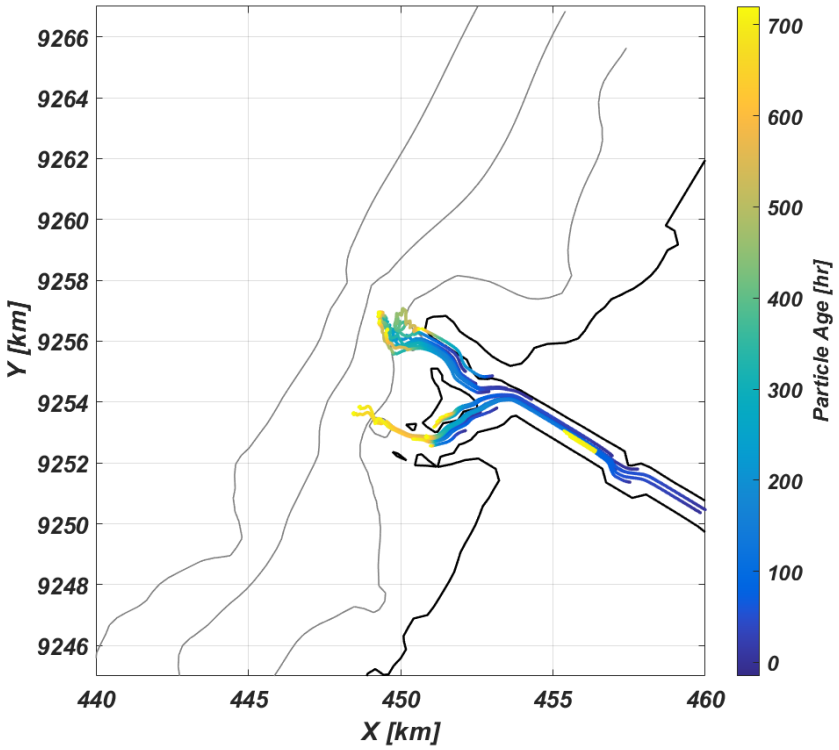

Figure 5.19: Sediment pathways of sand (D_{50} = 145 μm) at the Wulan Delta during maximum river discharges the depth-averaged velocity, including baroclinic forcing (3D).

Figure 5.20: Satelite image of the Wulan Delta from Google Earth.

5.3. Other Scenarios

This section comprehends the results of three other scenarios: relative sea level rise, construction of a jetty and former pathways.

5.3.1. Relative Sea Level Rise (3D)

Relative sea level rise in Demak is dominated by large rates of local land subsidence (section 3.3). Therefore, it is important to know what the influence is of relative sea level rise on the sediment pathways. To understand this, the mean offshore water level boundary condition is raised by 1 m to approximate relative sea level rise, whether due to local subsidence or eustatic sea level rise. Thus, the adjustment of the bathymetry to the increase of relative sea level rise is not taken into account, as the water level change is imposed instantaneously over the existing bathymetry. For instance, a part of the intertidal basins was importing sediments (Figure 5.13), which would increase the bed level in the meantime.

Including relative sea level rise increases the area that is flooded. Timbulsloko, which consisted of intertidal basins, is now permanently flooded. Moreover, a lot of new intertidal basins arise between Timbulsloko and the Wulan Delta. To analyze the difference in pathways in these intertidal basins, sediment particles are released specifically in these areas. When comparing the scenario with sea level rise (Figure 5.21) to the present scenario (Figure 5.13), the larger tidal basin area is exporting sediment instead of importing sediment. Water depths are larger now in these basins, which could change them from flood to ebb dominant. However the new tidal basins with smaller water depths are actually importing sediment. This highlights the importance of depth on sediment transport in tidal basins.

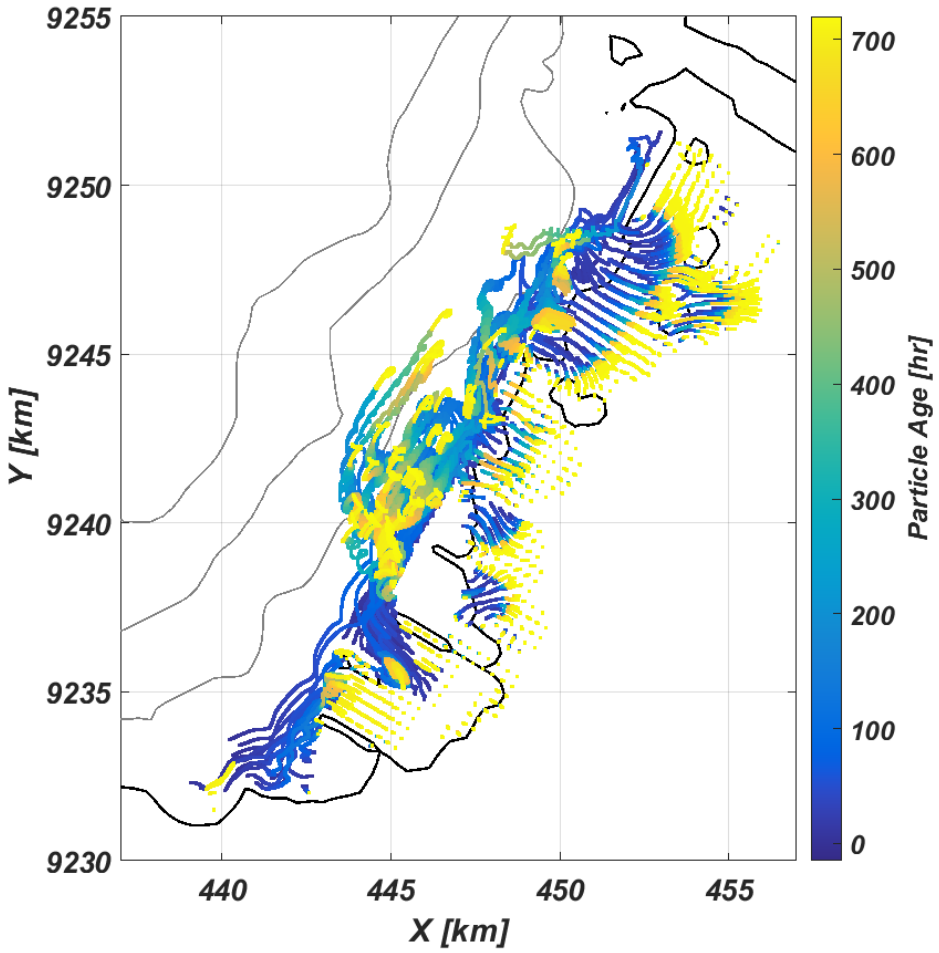

Figure 5.21: Sediment pathways of mud (D_{50} = 18 μm) in the intertidal basins of Timbulsloko for a month in the NW monsoon (wet season) the depth-averaged velocity, including baroclinic forcing (3D) and 1 m of relative sea level rise.

5.3.2. Construction of a Jetty (3D)

At the port in Semarang a jetty is constructed, which penetrates 3 km into the sea. Maulina (2010) stated that this jetty could affect residual sediment transports and could have accelerate the erosion in Demak. Although the exact design of the construction is not known, the jetty implemented as thin dam and the possible influence on the sediment pathways is modelled with a baroclinic (3D) model of the area.

Alongshore sediment transport seems to be slightly decreased due to the construction of the jetty (Figure 5.22). Without jetty the sediment particles ends up within a mean distance of 11.0 km from their release point, when a jetty is constructed the mean distance is 10.1 km. Furthermore, less sediment pathways are reaching less close the the coast at the tidal basins of Timbulsloko, which could lead to a decrease of sediment input for this area. As described insubsection 2.4.1, in and outgoing sediment fluxes are large in general at mangrove mud coast, whereas the between the two fluxes is small. Thus, when a jetty is causing a small difference in one of the fluxes, it can change a coastline from prograding to degrading.

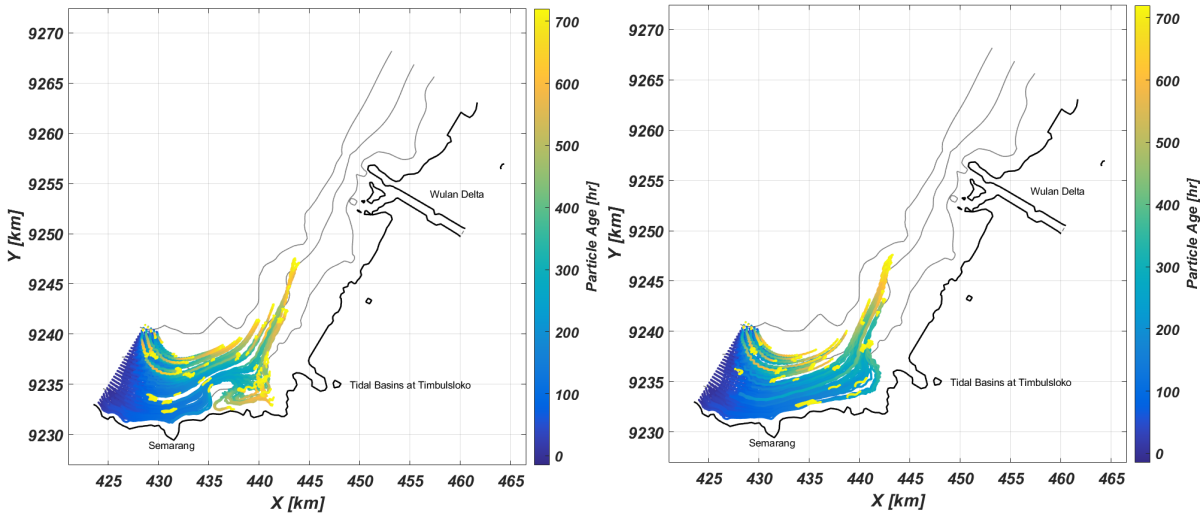

(a) With jetty.

(b) Without jetty.

Figure 5.22: Comparison between the alongshore transport of sediment with and without jetty at Semarang.

5.4. Propagule Pathways

This section includes the results of the propagule pathways in the Demak area modelled by SedTRAILS. The white dots represent the release point, the green dots the sticky point and the crosses represent the end point of propagules that did not stick.

5.4.1. Local Mangrove Propagule Sources (3D)

Local mangrove propagule sources could be the intertidal basins at Timbulsloko and further Northwards along to the coast to the Wulan Delta. The city of Semarang in the south is not considered as source, as it barely has any mangrove vegetation. The propagule release locations differ in elevation and access to tidal water and thus in depth, duration, and frequency of flooding. Although it could not be investigated in detail, measurements by van Bijsterveldt et al. (2022) suggest that in Demak *Avicennia marina* trees release their propagules just before the NW monsoon start, which is around November. As a consequence and to investigate the differences, simulations are done with propagules released during both the NW and SE monsoon.

In the NW monsoon, all propagules inside the intertidal basins remain there (Figure 5.23). Most of those propagules end up at the landward side of the basins, as winds from offshore push them to the coast, and a smaller part sticks at the old pond bunds. At the Wulan Delta almost all propagules float away to the nearby coastline southwards and northwards, as the protruding delta is more exposed to currents. Moreover, propagules at the straight coastline (in between the basins and delta) only float a short distance of about a few km and strand at a nearby location. The different mangrove communities along the coast are disconnected to each other, as propagules are not exchanged between them. In total, 95% of all propagules strand within a distance shorter than 4.3 km from their release location (Figure 5.24a). This corresponds to multiple observations found in literature (Appendix C), which report dispersal of *Avicennia marina* within a few kilometers.

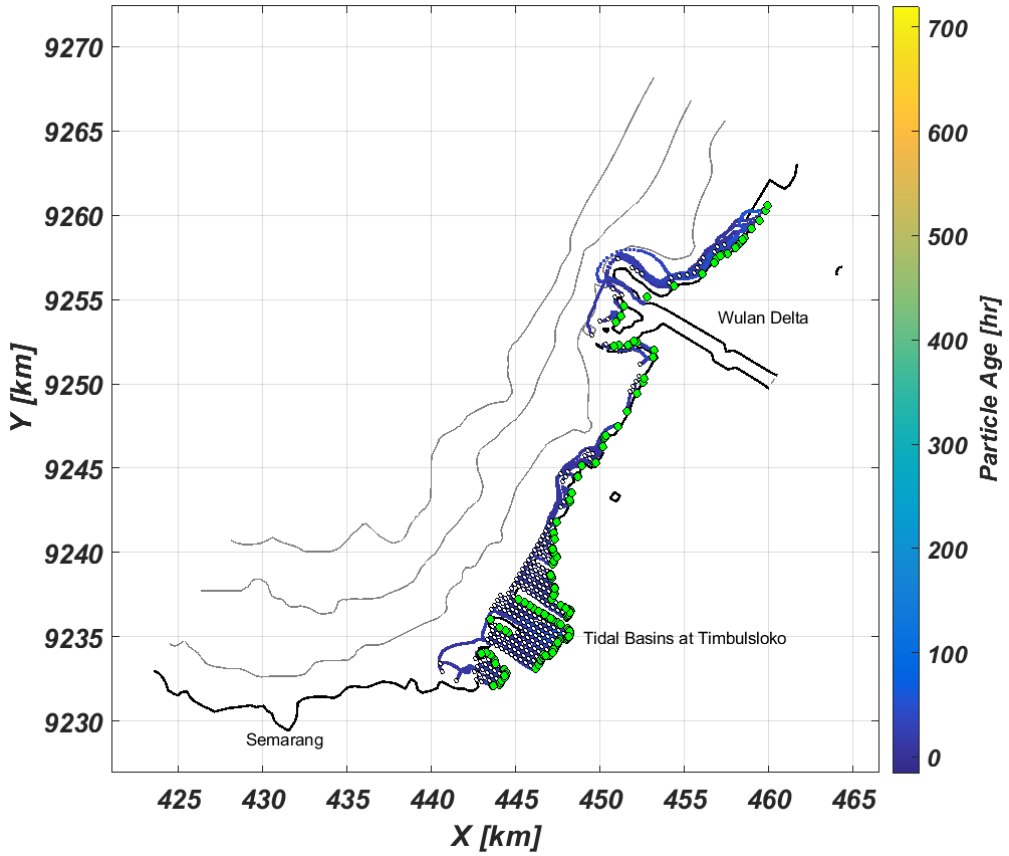

Figure 5.23: Mangrove propagule pathways of local sources for a month in the NW monsoon (wet season), including baroclinic forcing (3D). The white dots represent the release point, the green dots the sticky point and the crosses represent the end point of propagules that did not stick.

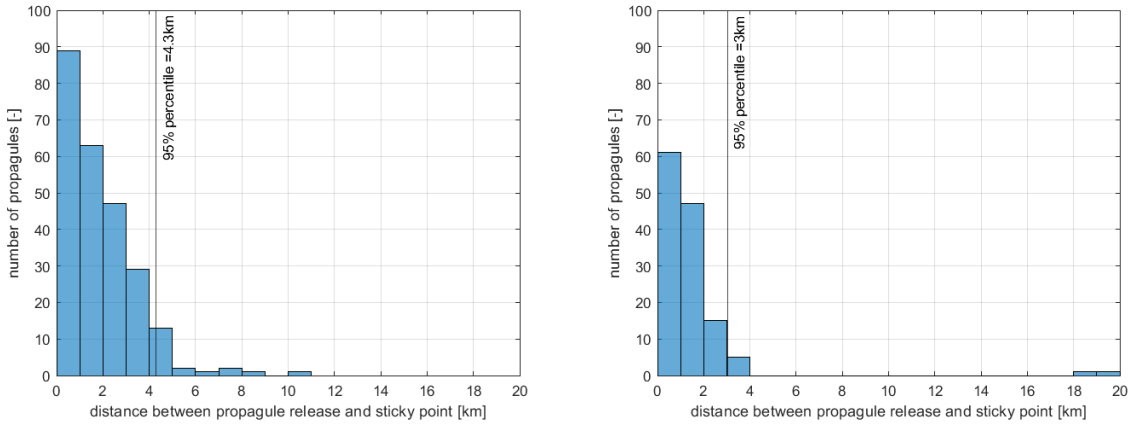

(a) NW monsoon.

(b) SE monsoon.

Figure 5.24: Histograms of distance between propagule release and sticky location.

In the SE monsoon a smaller part (52%) of the propagules is able to stick at the coast and in the intertidal basins, and those stick closer (within 3 km) to their release point than in the NW monsoon (Figure 5.24b). While in the NW monsoon most of the propagules stick at the landward side of the intertidal basins, in the SE monsoon most of the propagules stick at the old pond bunds (Figure 5.25a). This is confirmed by Figure 5.26, degree and strength values are especially high at the landward side in the NW monsoon, whereas the higher values are more diffused over the area in the SE monsoon. High degree values mean that the node is connected to a large number of nodes and high strength values mean that the total transport of propagules in and out of a node is large. In the SE monsoon, most of the propagules that are not able to stick in the basins seem to leave the basins at the southwest side, where degree values are high (Figure 5.26d).

The propagules floating out of the basins follow the alongshore current along Semarang. However, most of them do not stick at Semarang, as there is not much intertidal space in the city, where they can strand. Almost all propagules at the coastline and Wulan Delta float away to offshore waters, because the winds are mainly coming from land in the SE monsoon. The long distance dispersal of propagules lost to offshore waters outside the model domain is not known, but the chance increases that they are lost during transit or arrive at a site unsuitable for establishment (der Stocken et al., 2019a).

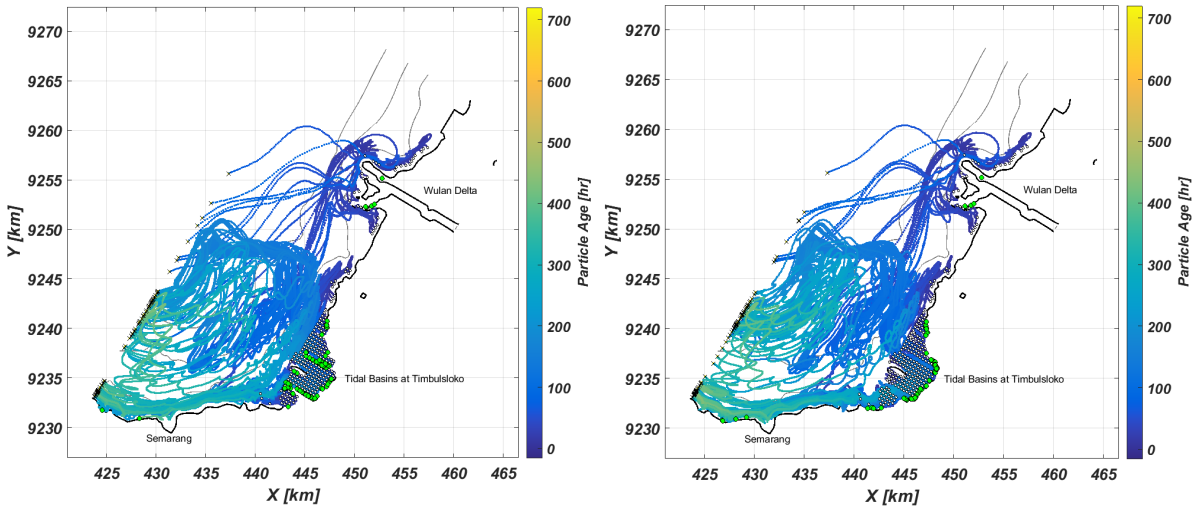

(a) With pond bunds.

(b) Without pond bunds.

Figure 5.25: Mangrove propagule pathways of local sources for a month in the SE monsoon (dry season), including baroclinic forcing (3D). The white dots represent the release point, the green dots the sticky point and the crosses represent the end point of propagules that did not stick.

Without the old pond bunds (Figure 5.25b) in the intertidal basins only 45% of the basin propagules sticks against 59% including bunds, so the bunds can prevent the propagules from floating offshore in a certain extent. In the situation without bunds, only the propagules released close to the coastline are able stick on land.

Another important factor for propagule dispersal is the fresh river water plume. During the NW monsoon there is a large river plume in front of the coast, which prevents mixing of the coastal waters with offshore water. Inside this plume the propagules are trapped along the coast. However during the SE monsoon, the river discharge is much smaller, there is almost no plume and coastal waters are mixed. Hence propagules are not trapped in a plume, which favors picking up by currents and going offshore.

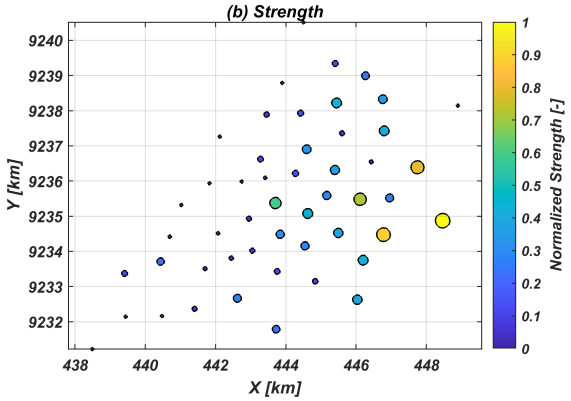

(a) Strength in NW monsoon.

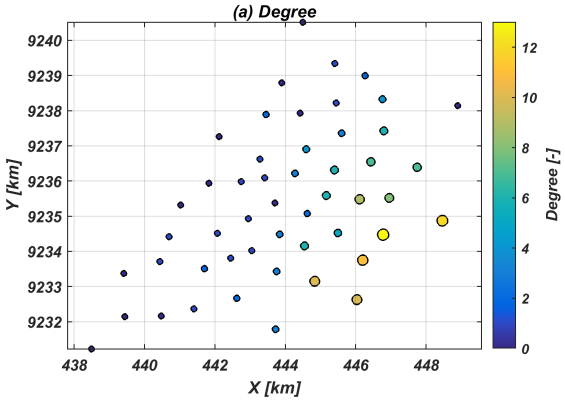

(b) Degree in NW monsoon.

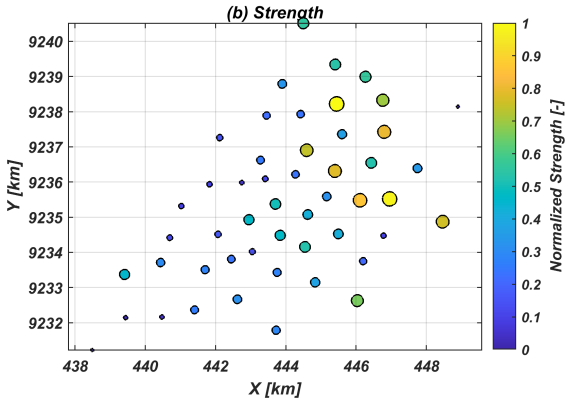

(c) Strength in SE monsoon.

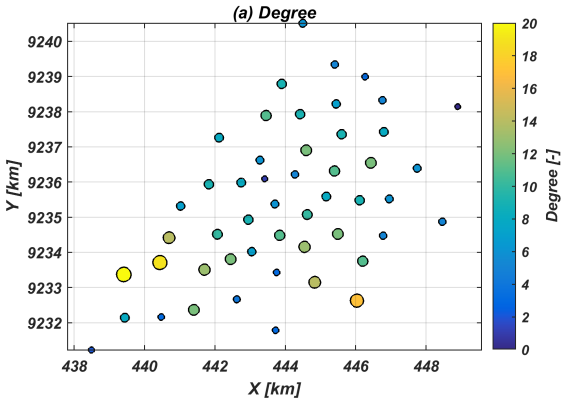

(d) Degree in SE monsoon.

Figure 5.26: Mangrove propagule connectivity in the intertidal basins of Timbulsloko. High degree values mean that the node is connected to a large number of nodes and high strength values mean that the total transport of propagules in and out of a node is large.

5.4.2. Alongshore Current as Mangrove Propagule Source (3D)

When looking at larger scale dispersal, another possible mangrove propagule source is the alongshore current during NW monsoon. Propagule sources further westward at Java could be picked up and dispersed by the alongshore current in Northeastern direction along the coast (Figure 5.27). Winds from offshore seem to be favourable for the propagules to reach the land and stick there. A significant part (84%) of the propagules carried by the alongshore current finds its way towards the coast and intertidal basins. A part of the propagules seems to be trapped in the fresh river water plume, then floating in opposite direction of alongshore currents, and sticking at the Northern side of the tidal basins. The remaining part of the propagules (16%) carried by the alongshore current is dispersed further, and is not reaching the coast as the plume is acting as a barrier for them. The plume may be even more a barrier for propagule then for sediments as, the fresh water plume is less dense and thus more present in the upper layers of the water column. No propagules are thus reaching the delta or the area north and south of it, Triest et al. (2018) confirmed that rivers are physical barriers affecting connectivity. So on the one hand, the river plume is a barrier for propagule transport, but on the other hand, propagules are trapped inside the plume.

At the same time, the plume is thus obstructing as well as trapping sediment and propagules.

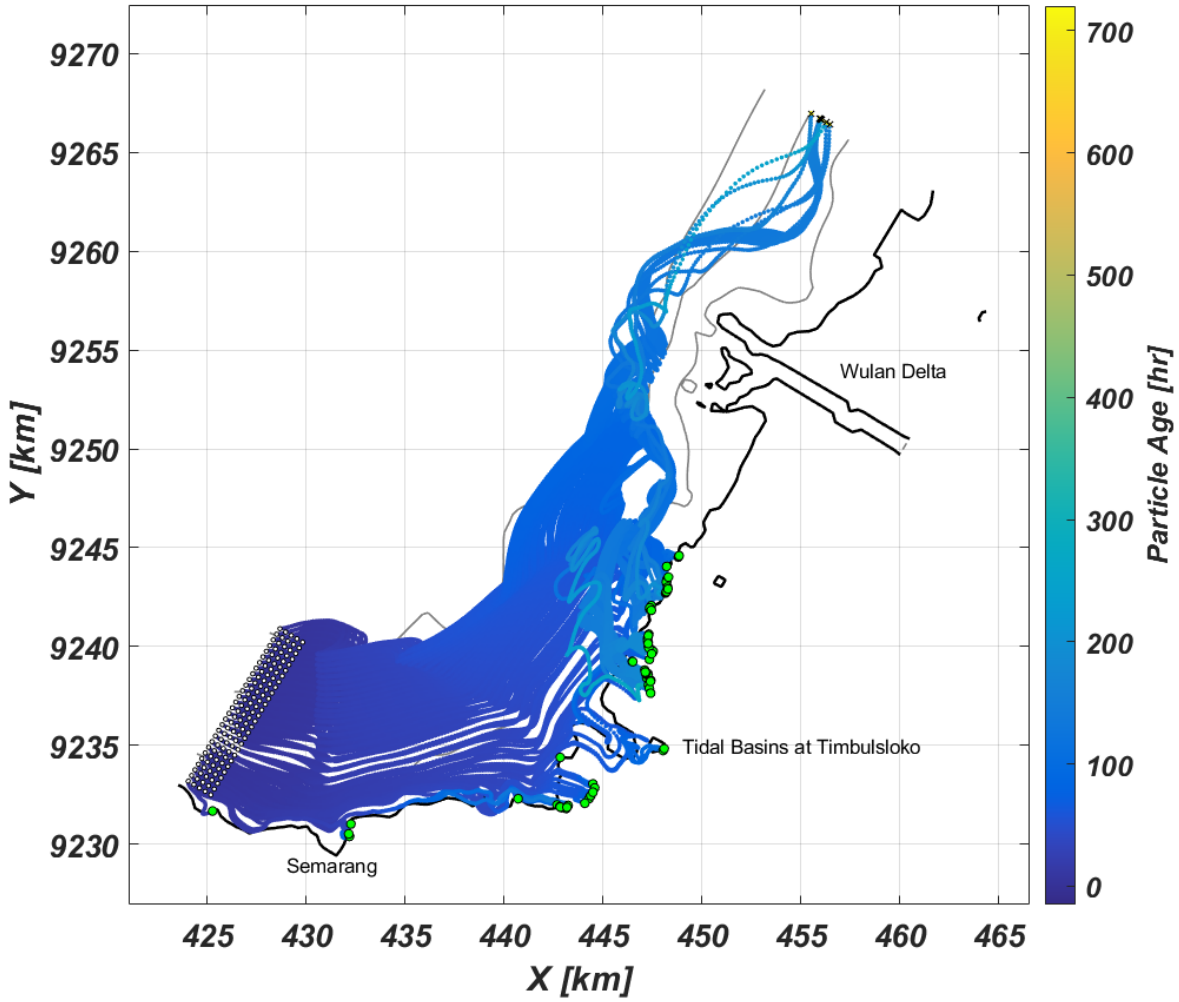

Figure 5.27: Mangrove propagule pathways of alongshore current sources for a month in the NW monsoon (wet season), including baroclinic forcing (3D). The white dots represent the release point, the green dots the sticky point and the crosses represent the end point of propagules that did not stick.

5.4.3. Validation of Propagule Pathways

Figure 5.28 shows that during the NW monsoon (wet season) more propagules are found in the pond zone, while during the SE monsoon (dry season) more propagules are found in the coastal zone at the intertidal basins of Timbulsloko (van Bijsterveldt et al., 2022). This is likely to be largely influenced by the wind direction, as winds are from offshore in the NW monsoon and from land in the SE monsoon. In total the largest amount of propagules is found in the pond zone during the NW monsoon.

The observations of the propagule pathways by van Bijsterveldt et al. (2022) show the same behaviour as our results, with propagules in the NW monsoon mostly ending up in the landward end of the basins, which is the pond zone. While during the simulation of the SE monsoon propagules stick on average slightly closer to the coastal zone, or float offshore. The differences between the observations and our model results may be due to propagules small scale processes such as trapping by mangrove roots, because these details are not captured by our relatively coarse idealized model (subsection 6.3.4).

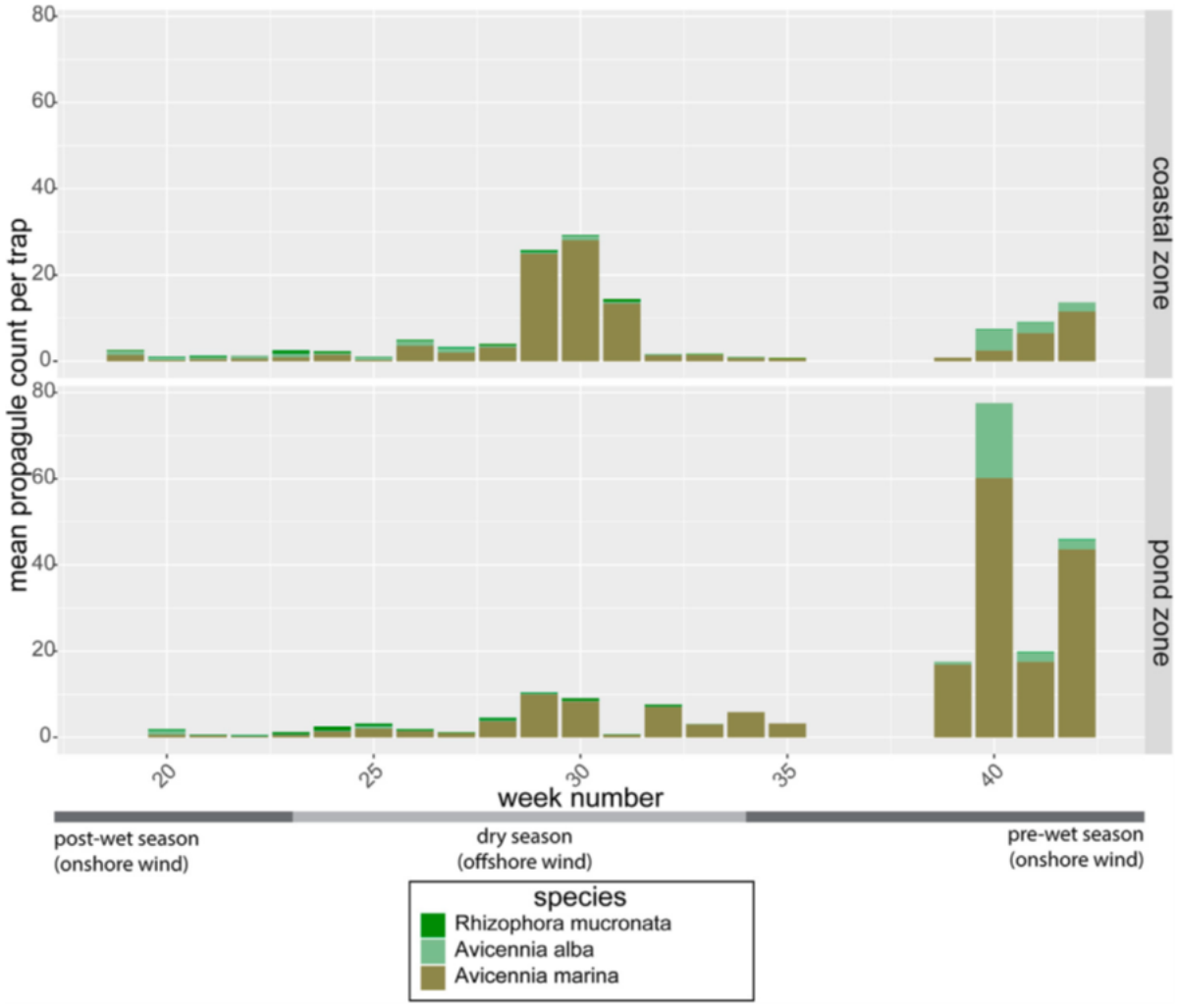

Figure 5.28: Average weekly propagule counts of the three most abundant mangrove species per trap in the coastal zone and in the pond zone at the intertidal basins of Timbulsloko (van Bijsterveldt et al., 2022).

5.5. Propagule Survival

This section discusses the survival of mangrove propagules at the establishment area influenced by the 'Windows of Opportunity' (Figure 2.3, subsection 2.1.3), for this a propagule module is developed to determine the survival based on the inundation-free period and maximum bed shear stress.

5.5.1. Phase 1 Inundation Free Period

There are five windows of opportunity (phase 0 to 4, see Figure 2.3) that propagules should survive (or thresholds of establishment) before they can colonize a site (van Bijsterveldt et al., 2022; Balke et al., 2011). The first criterium is an inundation-free period for the propagules, in which the propagules must not be floating away while growing its roots (phase 1). Van Domburg (2018) mentioned that this period is around 5 days based on the paper of Balke et al. (2011). An inundation-free period is considered as an period with water depths below 0.05 m. For all locations where propagules stick in Figure 5.23 during the NW monsoon en SE monsoon the inundation free period is interpolated (Figure 5.29), but is has to be taken into account that for our grid size the interpolation is not very accurate (subsection 6.3.1). The result that all propagules sticking in our model satisfy the five day period threshold may not be entirely correct. The straight coastline behind the river plume between the tidal basins and Wulan delta may be an area with large inundation free periods, whereas these periods may be smaller at the intertidal basins.

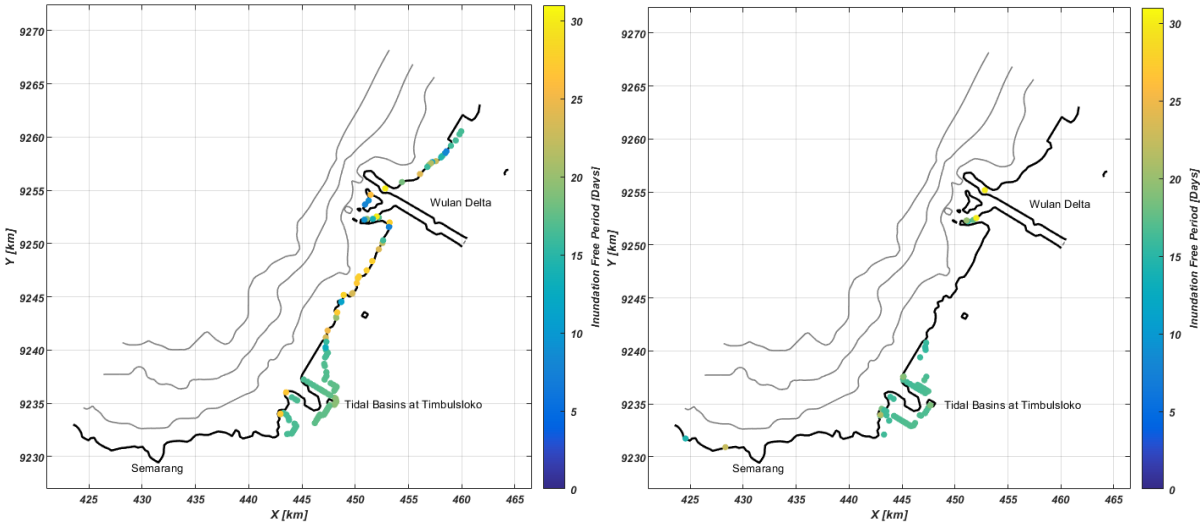

(a) NW monsoon.

(b) SE monsoon.

Figure 5.29: Inundation-free periods at all propagule sticky locations from local sources.

5.5.2. Phase 2 Maximum Bed Shear Stress

After this inundation-free period, roots need to become long enough to to withstand dislodgement by hydrodynamic forces from waves and current (phase 2). According to Balke et al. (2011), the maximum shear stress to prevent dislodgement for *Avicennia alba* increases linearly from 0.17 N/m^2 to 0.52 N/m^2 in approximately 3 days, it should be taken into account that is another specie than our *Avicennia marina* propagules. For all locations where propagules stick in Figure 5.23 during the NW monsoon the maximum bed shear stress is interpolated. The maximum bed shear stress is considered as the bed shear stress induced by waves during the NW monsoon with maximum tidal water levels (MSL + 0.4 m), because the wave model is stationary. Areas with low bed shear stresses are the landward ends of the tidal basins and the straight coastline (between the tidal basins and Wulan delta) behind the river plume. Areas with relatively higher bed shear stresses are the seaward side of the Wulan delta, North of the Wulan Delta and at the seaward end of the tidal basins. Although in the relatively high bed shear stress area most of the values are still below the 0.17 N/m^2 limit, during storms waves can be higher than the modelled mean wave height of 0.7 m. In the situation of storms during the NW monsoon the survival limits would thus be exceeded in these areas. In the SE monsoon the bed shear stresses are even lower as the hydrodynamic conditions are calmer. Although the availability of propagules is much larger in the NW monsoon, survival of propagules during the stormy NW monsoon may be slightly lower due to higher bed shear stresses than in the calm SE monsoon. Permeable dam structures may be a solution for survival problems during storms, because they can reduce bed shear stresses. van Bijsterveldt et al. (2022) observed that the dams significantly increased the survival of already established mangrove seedlings compared to sites more exposed to waves. Furthermore,

these dams can prevent propagules in the SE monsoon from floating offshore by trapping them and thereby increase the increase the establishment of propagules in the SE monsoon.

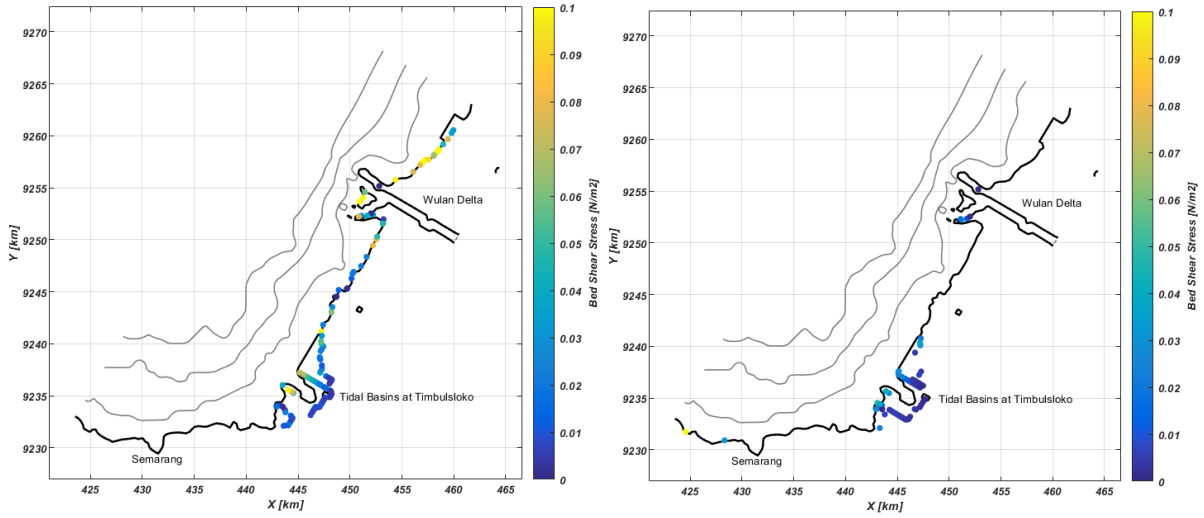

(a) NW monsoon.

(b) SE monsoon.

Figure 5.30: Maximum wave-induced bed shear stress during maximum tidal levels at all propagule sticky locations from local sources.

5.6. Comparison

This section evaluates the similarities and differences between the sediment and propagule pathways in the Demak area modelled by SedTRAILS.

In Figure 5.31 the sediment and propagule pathways of an alongshore source are compared. Both the sediments as well as the propagules are following the alongshore current, until they settle or stick somewhere to the bed. Since sediment velocities are lower and sediments are not in motion during the entire simulation (only if flow velocities are high enough), sediment pathway lengths are shorter than propagule pathway lengths. The larger part of propagules are floating into the freshwater plume, whereas none of the sediments are transported into the plume. Although for a smaller part of the propagules the freshwater plume is a barrier similarly as for the sediment. The landward wind is influencing the propagules more than the sediment particles, because propagules are floating just below the water surface and sediment are suspended in the water column closer to the bed. Hence propagules are more likely to reach the coastal zone.

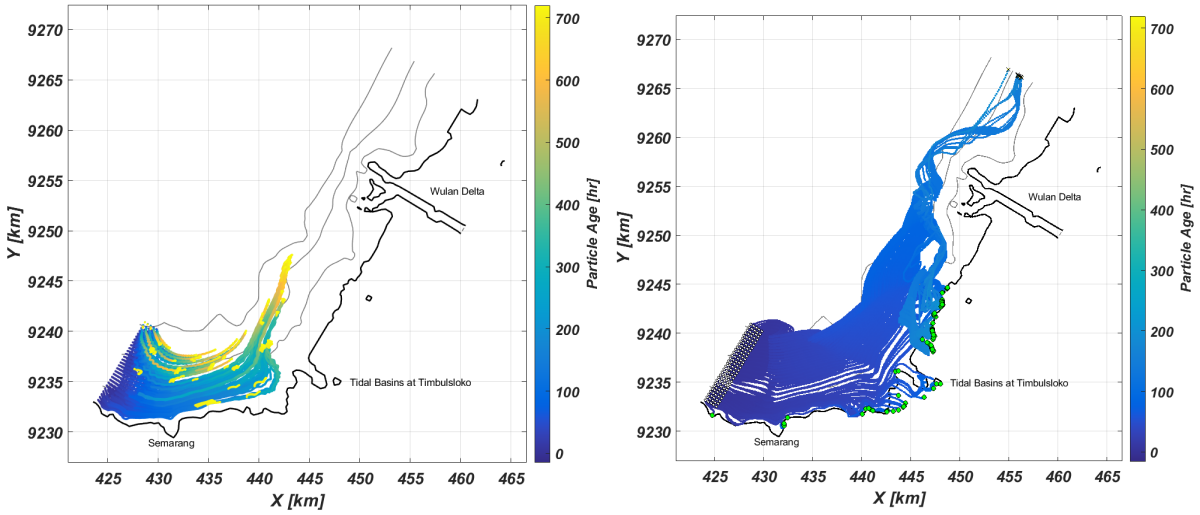

(a) Sediment. (b) Propagules.

Figure 5.31: Comparison between the sediment and propagule pathways of an alongshore source.

In Figure 5.32 the sediment and propagule pathways of an coastal source are compared. At the shallow part of the tidal basins both sediments and propagules are transported towards the coastline. However, at the deeper part of the tidal basins sediments are transported to offshore and propagules are still floating towards land. Since, sediments are less influenced by wind and more influenced by the actual flood and ebb velocities than the propagules. Both propagules and part of the sediments around the Wulan Delta seem to stick or settle at the coast.

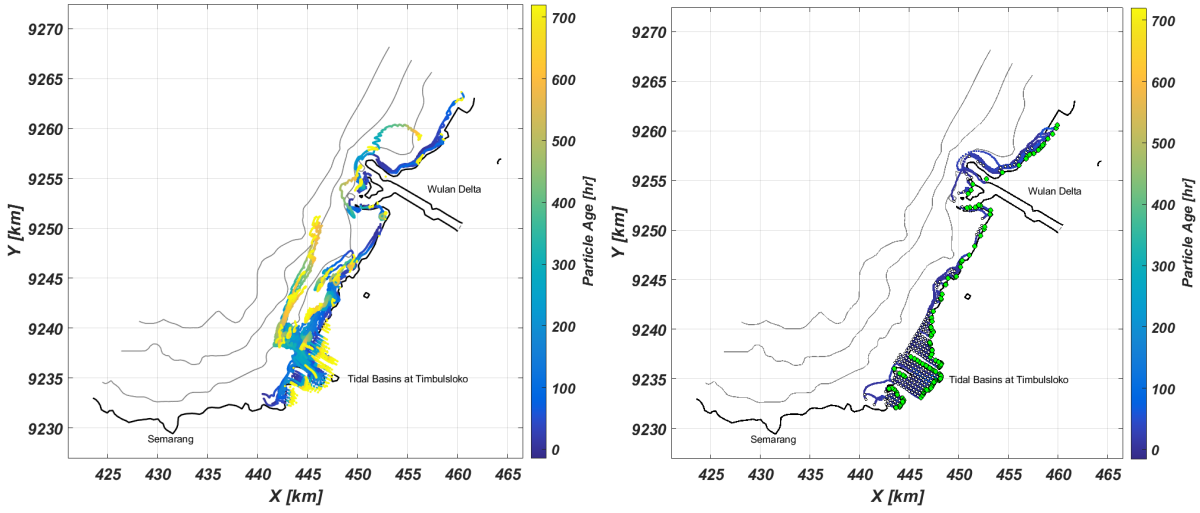

(a) Sediment. (b) Propagules.

Figure 5.32: Comparison between the sediment and propagule pathways of a coastal source.

6

Discussion

This chapter discusses the results of the model simulations, starting with the hydrodynamics, followed by the sediment and finally the application of this research to other areas.

6.1. Hydrodynamics

This section discusses the flow pattern, river and grid size in the hydrodynamic model.

6.1.1. Flow Patterns

Waves are neglected in the hydrodynamic model in Delft3D-4 and thus the wave-driven currents are not reproduced by the model. However, Smits (2016) concluded from his simulations that the large-scale flow pattern in Demak is hardly affected by waves, but waves may still have localized influence on for example cheniers, as onshore transport for cheniers is mostly due to wave asymmetry (Tas et al., 2022). The waves are so small that wave-driven currents are an order of magnitude smaller than tidal currents. The large-scale flow pattern computed by our model with alongshore currents from southwest to northeast corresponds to the model of Smits (2016). The large-scale monsoon wind pattern dominates the flow pattern, because changing the wind direction can change the direction of the residual alongshore currents.

6.1.2. River

The riverine input was highly simplified due to the lack of field measurements. Wulan river discharges are based on only one year of measurements, and the long-term variability is thus unknown. Despite that the exact discharge distribution is unknown, the discharge of the New Wulan tributary (westerly branch) is larger than the Old Wulan tributary (easterly branch), which is also modelled this way. Furthermore, the river was not well represented in the GEBCO depth input compared to values measured by Fadlillah et al. (2019), therefore both tributaries were narrowed and river depths are decreased. According to Fadlillah et al. (2019), the Wulan river plume is pushed towards the East by winds and residual currents in the NW monsoon, whereas the model predicts lower salinity values at the West side of the river. This disagreement between observations and predictions may be due to the reduced size of the domain, which is not sufficient for the plume to fully develop. A larger domain is thus recommended for a quantitative comparison of plume development.

The orientation of the tributaries is likely to largely influence the outflow direction and hence sediment connectivity to the adjacent coasts. Since the orientation and discharge distribution of the tributaries changed in 1972 by constructing the New Wulan canal, pathways before this could be significantly different than the modelled pathways in this study. Due to upstream land use and dam development (Marfai, 2011), river discharges and sediment loads decreased over the past decades. The river mouth prograded till 2011, and after that the growth decreased. Currently the northern shoreline retreats, whereas the southern one still advances slightly (Septiangga and Mutaqin, 2021).

6.1.3. Grid Size

The grid size is relatively large (333 x 333 m) in our model in order to reduce the computational time and thus be able to run a larger number of scenarios. These computational times allow us to learn about the physical processes in the coastal system in a relatively simple way, as input can be changed easily in a short time. In offshore waters this relatively large grid size would not have much influence on the accuracy. However, in more nearshore water and the river the model is not accurate enough to simulate all small-scale processes at the coast. At the intertidal basins of Timbulsloko not all pond bunds could be included as grid cells are too large for these details. Pond bunds and other non-included subgrid features such as mangrove roots have a direct influence on the hydrodynamics, which likely means that there is reduced trapping of propagules and sediment in our model. Another factor to consider is that the bathymetry of the intertidal zone has an extremely mild slope in this area, so small variations in water level can mean that a much larger area is flooded or not.

As a consequence, the results of this modelling research are more qualitative than quantitative. The loss of detail is considered acceptable as the aim of this project was to qualitatively study the area of Demak with a simplified model. The research thus focuses more on the large-scale processes than on for instance the exact magnitude of erosion or accretion.

6.2. Sediments

This section discusses the implications of the morphostatic model, sea breeze wind, waves and transport formulation and mud vs. sand transport.

6.2.1. Morphostatic Model

Our model in Delft3D-4 only simulates the hydrodynamics, to keep computational times reasonable. Although the model is capable of computing bed level changes, it is set up in a morphostatic manner. However, cheniers have been observed to migrate at speeds between 0.5 and 8 m/day in Demak, even during relatively calm conditions (Tas et al., 2020). These cheniers are important for stabilizing muddy coastlines, as they keep the sediments near the coastline, instead of being transported to offshore (subsection 2.4.3). Cheniers may be thus influencing the large-scale sediment transport patterns, but this effect is not included in the morphostatic model.

6.2.2. Sea Breeze Wind

During the SE monsoon a wind is persistently blowing from land to sea. Due to the limited fetch length, the waves generated by the offshore directed monsoon wind are very short and only marginally stir up sediment (Tas, 2022). Sediment pathways are therefore only modelled during the NW monsoon, in the SE monsoon there is barely any sediment transport by the short waves. Nevertheless, during this SE monsoon a persistent sea breeze develops in the afternoon. The wind waves generated by this onshore sea breeze are typically much larger than the waves generated by the offshore directed monsoon wind. These larger sea breeze waves could create larger bed shear stresses and thus stir up more sediment. Although these bed shear stresses by the sea breeze are not included in the model, they could significantly affect sediment transport in the area.

6.2.3. Waves

Breaking waves induce mass transport in the direction of wave propagation above wave trough level and a return current (undertow) under wave trough level, which is not included in the present model. This mass transport towards the coast is also called the Stokes drift. Although above wave trough level there may not be much suspended sediment, for propagule transport the Stokes drift may be of significant influence. The propagules are already pushed towards the coast by the winds during the NW monsoon, the Stokes drift may enhance this effect. The undertow is important for seaward sediment transport, because of the relatively high offshore-directed velocity in the lower and middle part of the water column. The undertow is especially large during storms, due to higher waves and high sediment concentrations in the breaker zone. Wave attenuation due to breaking dominates over frictional effects in stormy conditions. However, the wave conditions at Demak are in general relatively calm, even during the wet season. Due to these calm conditions, undertow currents remain small. Borsje (2019) furthermore proved it is necessary to compute viscous wave dissipation by fluid mud layers in Demak, but this complex process is excluded from our modelling approach.

Although large-scale currents in the area are hardly affected by waves (Smits, 2016), waves are still of significant influence for sediment transport. Waves transport sediment directly due to wave skewness, generating higher orbital flow velocities in landward than seaward direction (Tas et al., 2022). This mechanism of sediment transport is excluded of our modelling approach. Waves also induce transport indirectly by wave orbital motion inducing bed shear stresses stirring up sediment, which may subsequently be transported by currents. Without implementing these wave-induced bed shear stresses in SedTRAILS, sediments are not moving at all. A separate stationary wave model is therefore set up in Delft3D-4 to compute the wave-induced bed shear stresses, which are added up to the current-induced bed shear stresses in SedTRAILS. Non-linear interaction of both bed shear stresses are not taken into account and it is assumed that the mean wave-induced bed stresses is zero. Since our model is idealized, focusing on the processes, the simplifications of the bed shear stresses should be reasonable. The most uncertain factor in the wave-induced bed shear stress is the wave friction factor f_w. For sands there is an formulation validated to compute this friction factor (Swart, 1974). This factor is also used for mud, however, the equation was not intended for this type of sediment.

Furthermore, there is a coupling between resuspension and erosion of sediment by waves and the subsequent sediment transport by tidal currents. Sediment is transported landward or seaward, depending on the tidal phase. The drawback of our stationary wave model is that the computed waves are based on a stationary water level. Since no tidal water level variations are included in the wave model, waves do not penetrate into intertidal areas and this coupling is not well-simulated. This means that sediment pathways in intertidal area are driven by bed shear stresses due to currents and not waves. Whereas, in all area below mean sea level pathways are driven by both bed shear stresses. In reality when tidal levels are above mean sea level, waves would intrude into the intertidal area inducing sediment stirring and transport. This implies that sediment in intertidal area would be more mobile, so pathways are longer and thus there is more sediment import towards the coast. This explains why in our current model, pathways above mean sea level are much shorter than below. Lastly, in the seperate stationary wave model wave heights are mainly determined by the depth-induced wave breaking and bottom friction. Although depth-induced breaking is included, waves are not breaking over the cheniers as these small-scale features are not present in the bathymetry input.

6.2.4. Transport Formulation

SedTRAILS is based on the Lagrangian particle tracking model of Soulsby et al. (2011), which uses the following equation to calculate the sediment transport velocities:

$$\mathrm{U_{gr}} = \mathrm{F} \cdot \mathrm{P} \cdot \mathrm{R} \cdot \mathrm{U_c} \tag{6.1}$$

Within this equation it is only possible for sediment to move in the same direction as the depth-averaged velocity (2D or 3D) or the velocity of a horizontal layer (3D). Most of the sediment pathway simulations are based on the depth-averaged velocity, additionally, a simulation is done for pathways based on the near-bed velocity. Originally the equation of Soulsby et al. (2011) was developed for fine non-cohesive sands, where U_c was considered equal to the near-bed velocity. The mobility of a particle (Equation 6.1) with dimensionless grain size of D_* is determined by the critical Shields number θ_{cr} (Soulsby, 1997; Soulsby and Whitehouse, 1997):

$$\theta_{cr} = \frac{0.3}{1 + 1.2D_*} + 0.055\left(1 - \exp\left(-0.020D_*\right)\right) \tag{6.2}$$

Equation 6.2 was derived for predicting the threshold of motion of non-cohesive sands and gravels ($D_{50} > 63\mu m$) in coastal environments influenced by waves and current on beds of any slope. However, in this research it is applied for fine cohesive sediment ($D_{50} < 63\mu m$) at a muddy coast, knowing that the erosion behavior of sand and mud is fundamentally different. This has some implications for the results as muddy processes are not taken into account. For instance flocculation, hindered settling and consolidation effects influence the undrained strength of mud, and hence the erodibility. A recommendation is thus to compute transport of cohesive sediment in SedTRAILS with the conventional Partheniades-Krone equation, which includes flocculation and hindered settling (Partheniades, 1965):

$$E = \begin{cases} M\left(\frac{\tau_{b,\max}}{\tau_{cr,e}} - 1\right), & \text{when } \tau_{b,\max} > \tau_{cr,e} \\ 0, & \text{when } \tau_{b,\max} \leq \tau_{cr,e} \end{cases}$$
$$D = \begin{cases} w_s c\left(1 - \frac{\tau_{b,\max}}{\tau_{cr,d}}\right), & \text{when } \tau_{b,\max} < \tau_{cr,d} \\ 0, & \text{when } \tau_{b,\max} \geq \tau_{cr,d} \end{cases} \tag{6.3}$$

In Equation 6.3 the erosion E is determined by parameter M and deposition by the settling velocity w_s and the sediment concentration c. For the method of Partheniades (1965) a constant critical shear stress τ_{cr} determines the mobility of a particle, whereas Soulsby (1997) applies a critical Shields number θ_{cr} varying depending on the grain size. This means that if the equation of Partheniades (1965) was included in SedTRAILS, the mobility of fine sediments could be different. Another difference is that the Partheniades (1965) equation includes a deposition term, such that with high concentrations there will be hindered settling of sediment. Sediment concentrations are not taken into account by Soulsby (1997), so sediment pathways in SedTRAILS will therefore not be influenced at locations with high sediment concentrations. In addition, Partheniades (1965) includes flocculation of cohesive sediment in the settling velocity, because sediment tend to form flocs depending on the salinity of water. These sediment flocs are much larger than the individual sediment particles and thus settle faster. Although this means that the size of the sediment particles is not constant, in our model this is assumed constant. In reality sediments in the fresh water plume will therefore be less able to form flocs than sediments in the salt sea water. When sediments in the plume reach the front, salinity values increase and sediments would form flocs and deposit at the interface (Eisma, 1986). In our model flocculation is excluded, but if that would be implemented, our results would slightly change with some deposition of sediment at the river plume front.

Concluding, it is important to understand that SedTRAILS is better in determining how an already eroded particle would move through a computed transport field and which path it follows, than determining the erosion and settling proccesses of that particle.

6.2.5. Sand vs. Mud Transport

In the Equation 6.1 of Soulsby et al. (2011) the depth-averaged velocity or the near-bed velocity can be used as input for U_c, depending on the local situation. While sand can be transported both as bed load and suspended load, in general most of the sand is transport relatively close to the bed (Figure 6.1a). Conversely, mud is more equally distributed over the water column than sand, and the larger part is suspended load (Figure 6.1a). BioManCO (2018) found that 80% of the sediment in the area is mud and 20% is sand. Tas et al. (2022) confirmed that sand and mud are mainly transported as suspended load in Demak. It was therefore chosen to approximate the muddy sediment transport as suspended load driven by the depth-averaged velocity, and the sand transport by the near-bed velocity as considered in by Soulsby et al. (2011). The fluid mud layers above the bed are not modelled and would lead to onshore transport of fine sediment (Winterwerp et al., 2020).

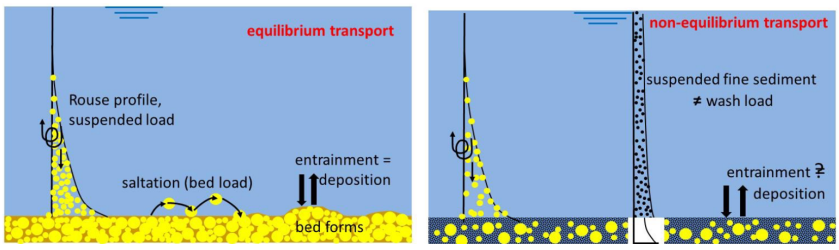

(a) Sand bed.

(b) Consolidated muddy bed with some sand.

Figure 6.1: Sandy vs. muddy transport (van Prooijen, 2021).

Another limitation of the modelling approach is the absence of sand-mud interactions, in the computations the fractions were considered to behave independently. However, a study by van Ledden et al. (2004) on erosion behaviour indicates that a sand-mud mixture exhibits cohesive mixture when the mud contents above 30% (subsection 2.4.2). A sand-mud mixture typically has a higher critical bed shear stress for erosion (van Rijn, 2020), thus sand particles may be less mobile and the model may overestimate the pathway length.

6.3. Propagules

This section discusses the computed propagule pathways.

6.3.1. Windows of Opportunity

There are five windows of opportunity (phase 0 to 4, see Figure 2.3) that propagules should survive (or thresholds of establishment) before they can colonize a site (van Bijsterveldt et al., 2022; Balke et al., 2011). This research mainly focuses on the availability of propagules (phase 0), by assessing propagule pathways, sources of propagules and which locations are connected to these sources. Nevertheless, it does not mean that if a propagule is available somewhere, that it will be successfull, since it needs to meet the other criteria too. Therefore, a survival part of the propagule module is developed during this research, which determines the inundation-free period (phase 1) and maximum bed shear stress (phase 2) by interpolation. Water depths in areas where propagules stick (maximum water depth < 0.2 m) are checked for an inundation-free period (Figure 6.2 and Figure 6.3). Although during neap tide there is a period of more than 5 days when water depths are only a few centimeters and flow velocities are zero, there is no inundation-free period. This may be due to the flooding and drying algorithm in Delft3D, hence we consider the inundation-free period as a period with water depths below 0.05 m.

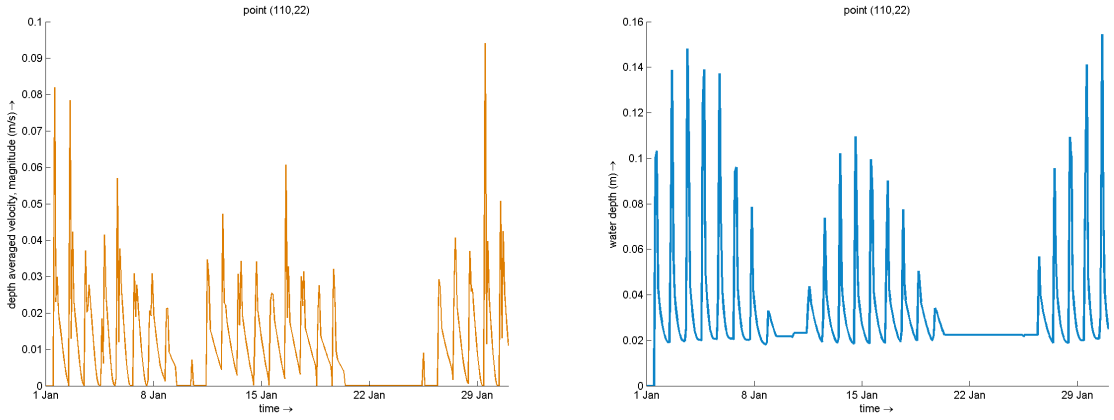

(a) Flow velocity.

(b) Water level.

Figure 6.2: Inundation-free period check for a grid cell at the Delta (110, 22), where propagules stick (max. water depth $< 0.2m$).

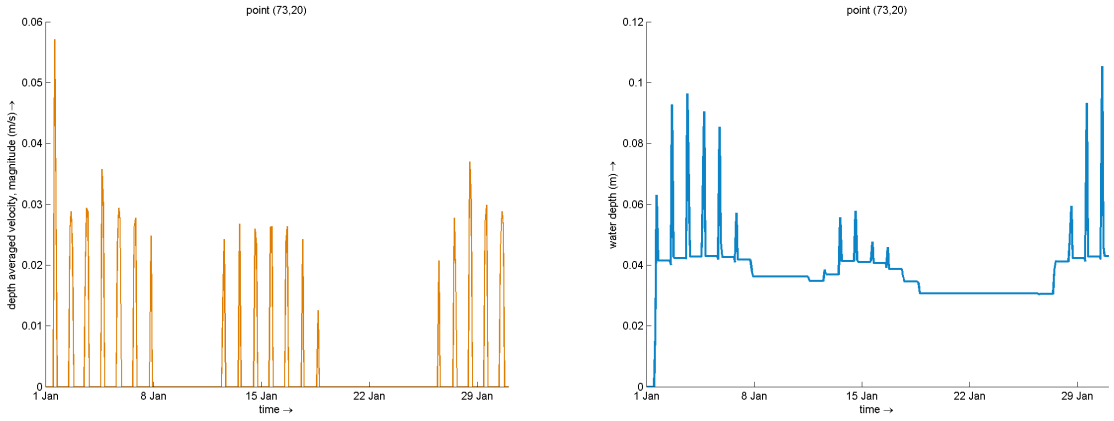

(a) Flow velocity.

(b) Water level.

Figure 6.3: Inundation-free period check for a grid cell in the basins (73, 20), where propagules stick (max. water depth $< 0.2m$).

For each grid cell the maximum inundation-free period is computed during the month of simulation time (Figure 6.4). At the sticky locations of the propagules the threshold is checked by interpolating the inundation-free period between the grid cells. The limitation of our model is the relatively large grid size at the coastline, hereby the inundation-free period of the locations where the propagules are sticking is inaccurate. A lot of propagules are sticking in between a wet cell (around 0 to 1 day inundation-free) and a fully dry cell (31 days inundation-free), which is for instance interpolated as 20 days inundation-free fulfilling the threshold.

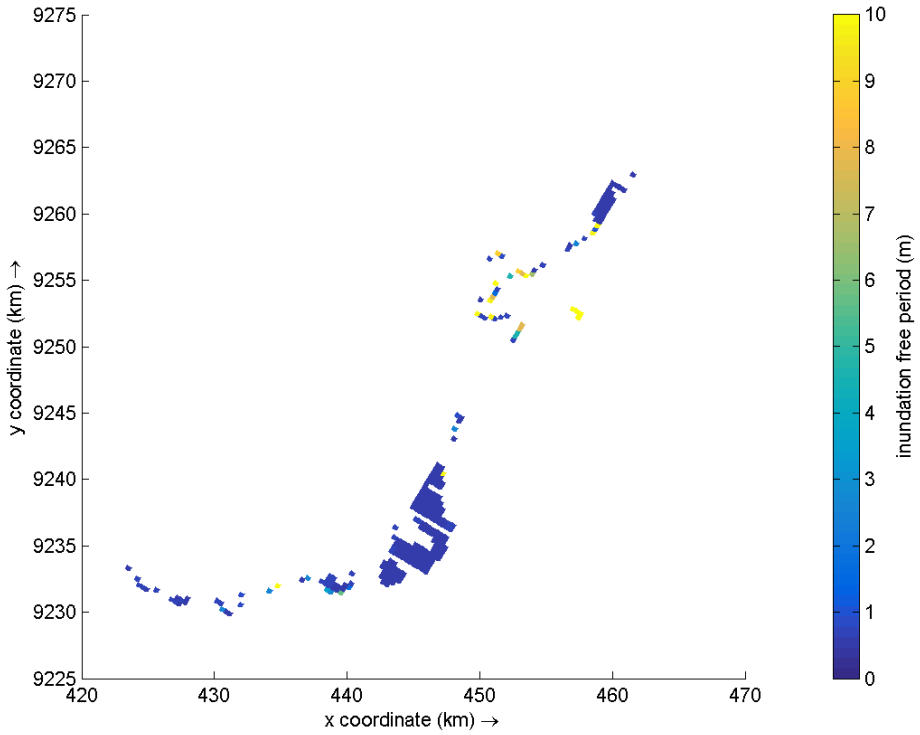

Figure 6.4: Inundation free period per grid cell, cells that are fully wet (0 days) or fully dry (31 days) are already removed.

The limitation of a stationary wave computation (see subsection 6.2.3) is that waves are not penetrating into intertidal area, and this exactly where the propagules are sticking. Therefore, we did an extra stationary wave computation during maximum tidal levels (MSL +0.4 m), when waves can penetrate in this intertidal area. For this research the maximum bed shear stress is thus considered as the bed shear stress induced by waves during the NW monsoon with maximum tidal levels. Although taking into account maximum tidal level which only occur once in a month may be slightly conservative, it can be determined if a location is suitable for propagules to establish. On the other hand, a stationary wave model is not conservative, because some of the waves will be higher than the significant wave height, so there is a sort underestimation.

It is not possible to include the maximum bed erosion (phase 3 of the windows of opportunity) in the survival part of our propagule module. For this the model would have to be changed from morphostatic to morphodynamic, and thereby set a threshold for a maximum bed level change in a grid cell. The maximum bed erosion may be the determining factor for a propagule to survive in this specific area, since a sediment imbalance may prevent establishment of propagules at intertidal areas and the early growth of planted mangroves.

Concluding, a propagule that can stick to the bed at a certain location may not survive and grow into a mature mangrove tree. van Bijsterveldt et al. (2022) observed survival rates of planted *Avicennia marina* in the Demak area of 21% and the ones that survive can be fruiting young trees within 16 months. The survival part of the propagule module therefore gives the following results: sticking location, inundation-free period and bed shear stress to compute survival rates taking into account the thresholds. Our model is not optimal to compute accurate survival rates, because of the large grid size and stationary waves input.

6.3.2. Sticky Depth

Implementing a sticky depth is a reasonable first step to determine where propagules strand, however there are also some limitations of this method. Although time-varying depths are important to include in our system, the sticky depth method was originally developed for the deep ocean where water level variations were relatively unimportant for coral larvae dispersal. As a consequence, the criterion if a particle sticks to the bed is not based on the actual time-varying water depth, but on the maximum depth at a certain location across the entire simulation.

Determining if a particles sticks based on the maximum depth of a grid cell has some implications. A particle will have an higher chance to stick or strand at spring tide, because during neap tide the waterline is more seawards and the maximum depth in this area allows less propagules to stick (Figure 6.5b). The implication that on average less propagules stick during neap tide than during spring tide is confirmed by Figure 6.5a (in our model simulations propagules are released around spring tide). During neap tide there is less variation in the amount of sticking propagules than during spring tide, this may be due to the lower ebb and flood velocities. If sticking of propagules would be based on actual time-varying water depths, propagules would strand both at spring as at neap tide. Although the model does allow less propagules to strand at neap tide, it is assumed that this simplification is reasonable. Firstly, survival rates of propagules stranding at neap tide are assumed to be low as in this region the inundation-free period is not long enough (phase 1). Secondly, the probability is high that propagules stranded at neap tide would be carried away by the currents during spring tide and finally strand then.

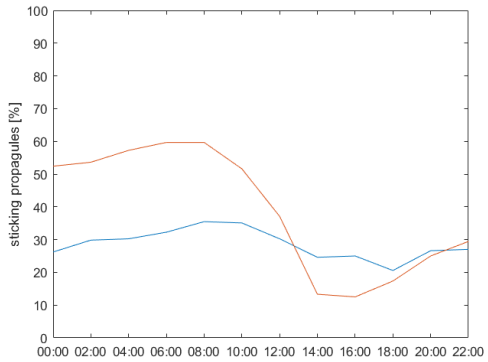

(a) Comparison of amount of sticking propagules released every two hours during spring tide (orange line) and neap tide (blue line) during one tidal cycle (one day).

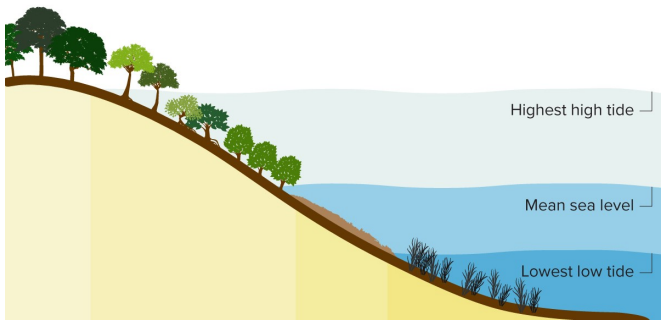

(b) A propagules will have an higher chance to stick or strand at spring tide, because during neap tide the waterline is more seawards and the maximum depth in this area allows less propagules to stick.

Figure 6.5: Sticky Depth.

In this research the value of the sticky depth parameter is set to 0.2 m for the *Avicennia marina* propagules. However, the value of the parameter can be changed and adapted per specific location and specie. For instance, the *Avicennia marina* specie colonizes mud flats located at high tidal water levels, where it is more dry and saline (Verschure, 2013). Whereas the *Rhizophora mucronata* specie is mainly located in river/estuarine environments, along riverbanks. A larger value than 0.2 m for the sticky depth may be more appropriate for the *Rhizophora mucronata* specie, since they are sticking at location lower in the tidal zone.

During the model simulation some of the propagules are not sticking and floating out of the model domain. These propagules may still stick via long distance dispersal (LDD) enhancing genetic diversity in other areas, but chances of loss during dispersal or arriving at a site unsuitable for establishment increase (der Stocken et al., 2019a). This LDD is beyond the scope of this research.

6.3.3. Windage

Windage is the influence of wind in deflecting the course of an object, but in this research it was decided to not take into account this windage as observations of propagules confirm that they are floating below the water surface (Figure 4.12). However, the studies of (Stocken et al., 2013, 2015a) illustrated that different propagule types have a different likelihood of reaching offshore waters depending on prevailing wind and hydrodynamics. As a consequence, propagules in another life stage or of other mangrove species, may actually be partly floating above the water surface, as was seen in Figure 4.12. In the case (Figure 6.6) that the wind does not only force the propagules indirectly by wind-driven currents in the surface layer ($F_{current}$), but is also directly forcing on the part of propagule being above the water surface (F_{wind}). Although the windage factor is not used, it is already implemented in the propagule module. This windage factor is based on the formulation of Kuitenbrouwer et al. (2018) (Equation 6.4), which was originally developed for the pathways of oil spills.

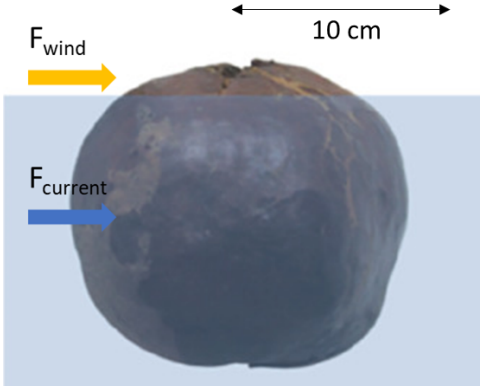

Figure 6.6: Wind (F_{wind}) and current (F_{wind}) forces acting on a *Xylocarpus granatum* propagule (from Figure 4.4).

$$\frac{\partial x}{\partial t} = u_{D3D}(x,t) + u_w P \tag{6.4}$$

Because mangrove propagules float, it is assumed, that they move with $u_{D3D}(x,t)$, the horizontal velocity of the surface layer in Delft3D. In case of winds, propagules drift downwind with a velocity of the windage factor P times the wind speed u_w. For oil spills this windage factor was determined 1-3%, and for propagules this factor still needs to determined depending on the amount of propagule floating above the water surface.

6.3.4. Small-scale Processes

The tidal basins are a potential establishment area for propagules, as field data revealed that pioneer species propagules were up to 21 times more abundant in pond creeks than near their coastal source (van Bijsterveldt et al., 2022). This was especially during wet season with onshore winds, which suggests that propagules can be trapped efficiently in ponds. In our model many propagules float towards the landward end of the basins, which implies not all propagule behaviour is mimicked. The small-scale is actually very important, for trapping of propagules in intertidal areas. There are large differences between the small-scale geographical features of the modelled tidal basins and the real situation (Figure 6.7). These differences are partly caused by the inaccuracy of the GEBCO depth input, which is not including the abandoned pond bunds and detailed nearshore bathymetry. Moreover, the grid size of the model is relatively large, so manually adding pond bunds and other features to the basins is only possible to a certain extent. Adding more detail to this area requires locally decreased grid sizes. However, Delft3D-FM would be more suitable for decreased grid sizes in certain areas of interest than Delft3D-4 (this model).

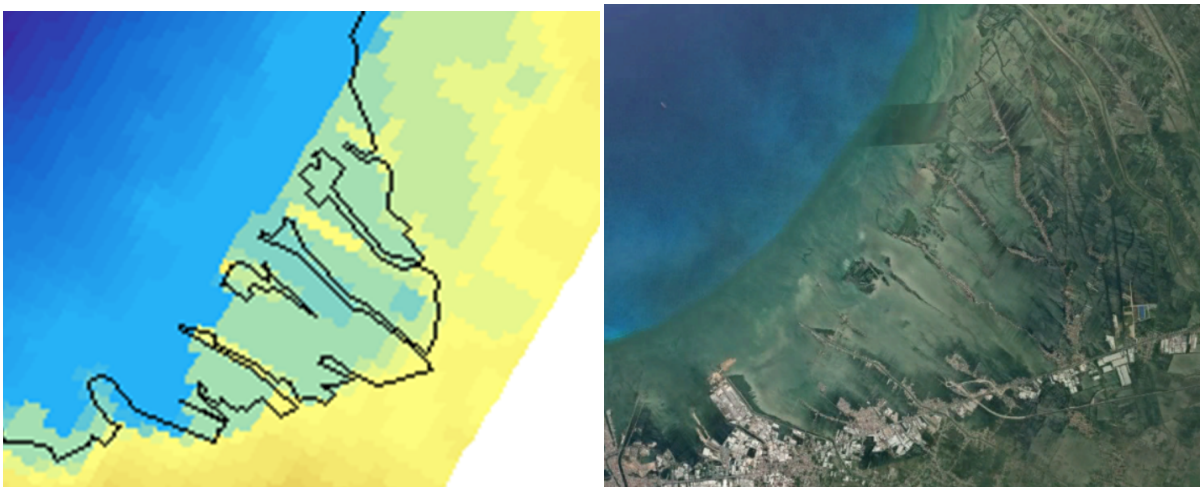

(a) Model (black line is the coastline obtained from Google Earth). (b) Google Earth.

Figure 6.7: Comparison of tidal basins in the model and Google Earth.

Although it is not possible to include trapping within a mangrove stand in a Delft3D model, this is a limitation of the propagule module. Retention processes within a mangrove stand are too detailed and small-scale to model, thus only mangrove propagules successfully exported out of a mangrove stand are modelled (der Stocken et al., 2019a). For example, the complicated branched root system of mangrove trees can affect dispersal by constraining propagule movements and the number of propagules reaching open water. Propagules from trees near the edge of the stand or near channels are typically exported over longer distances, facing fewer physical barriers (Nitto et al., 2013). Whereas, propagules in the inner forest may face a dense physical barrier of mangrove trees, in which they can become stuck during transport (der Stocken et al., 2019a). The variation in barrier density will depend on the vertical complexity of the vegetation, including the root system and the position within the intertidal area (der Stocken et al., 2019a).

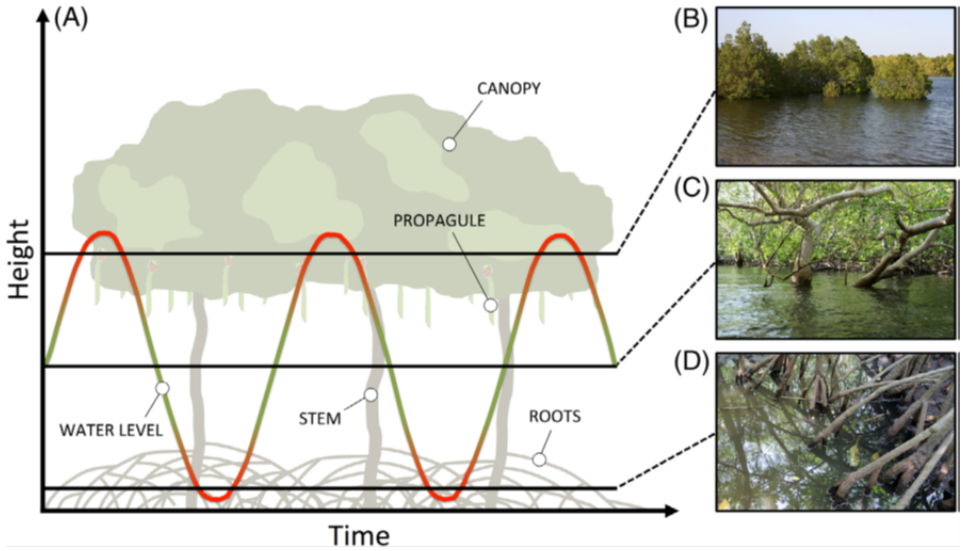

Figure 6.8: Schematic illustration of dispersal barrier density variation over a tidal cycle, temporal changes in water level may increase (red) or decrease (green) barrier density and hence the potential for dispersal. The physical barrier is particularly high in the canopy (B) or the root structure (D) and lower at the stems (C) (der Stocken et al., 2019a).

Furthermore, the influence of wind is large for the direction and speed of the floating propagules. In our NW monsoon model, the wind direction and speed is constant for the whole month and whole grid, in the SE monsoon a constant sea breeze is added every afternoon. In reality there are periods in time where the wind speed is lower or higher and local variations in wind in certain areas. For sediment pathways the small local changes in wind speed would not make a very significant difference, as wind effects are especially in the surface layer. Conversely, for propagules the small local changes could explain why some propagules remain in a different place.

6.3.5. Timing of Propagule Release

The timing (or phenology) of propagule release determines the moment that propagules become exposed to prevailing currents, which vary temporally in both strength and direction. Hence, the timing of propagule release significantly alters the pathways and resulting establishment area (Savage et al., 2010). Due to the complex environmental determinants that govern phenology in mangroves, the phenology of propagule release can be highly species and location specific (der Stocken et al., 2019a). In our study area one specie may release his propagules during the NW monsoon with landwards winds, whereas another specie may release his propagules during the SE monsoon with seaward winds. This research confirmed that this seasonal variability in propagule release could significantly influence the establishment area of propagules. In addition to seasonal variations, there are also variations in the time of the day a propagule is released. A propagule released for instance during flood is taking a slightly different trajectory, than one released during ebb. Although there is some research done on individual, seasonal and yearly variations in propagule release (subsection 2.1.3), there is hardly any knowledge on the timing of mangrove propagule release during the tidal (flood-ebb) cycle. As propagules are particles reproductively released by an organism that may germinate into another organisms, not only mangrove trees release propagules also marine animals such as barnacles and periwinkles release them to propagate. Barnacles were released in a rhythmic pattern coinciding with neap tides, when the speed of tidal currents was lowest, and there was no variation in propagule release in relation to flood–ebb tidal cycles. Periwinkles released propagules in a very irregular pattern, during periods of rough seas when onshore surface currents were expected to prevail, and the eggs were released from the propagules mostly during ebb tides (Bueno et al., 2010). The release pattern of mangrove propagules will definitely be different than marine animals, but the study of Bueno et al. (2010) shows that there may be variations during the tidal cycles.

Sensitivity tests for the timing of propagule release are therefore executed. For both the NW and SE monsoon propagules are released every 2 hours of one day, such that the sensitivity of release during one entire tidal cycle is tested. All the results of the sensitivity tests are shown in Appendix E. For the NW monsoon, there were barely any changes in the propagule pathways during a tidal cycle, as winds are landwards the propagules will be pushed towards the coast in any situation, even when they are released during ebb velocities. All propagules were thus still sticking at the coast and not floating away to offshore waters. For the SE monsoon, the differences are larger between the sensitivity simulations. The propagules experiencing seaward winds in the SE monsoon are much more dependent on the first hours of the simulation, because a particle will stick at the coast in the first day or it floats towards offshore waters in this first day. The flows in the first hours can therefore determine which of pathway of the two options it will be forced take. The sensitivity tests of the SE monsoon are thus analysed (Figure 6.9). Propagules released during the highest tidal water levels have a period of seaward velocities after their release, and thus the lowest probability to stick at the coast, most of them will be floating away. Whereas propagules released during the lowest tidal water levels have a period of landward velocities after their release, and thus a much larger probability to stick a the coast. This phenomenon is logical as as landward velocities promote establishment at the nearby coast and seaward velocities promote propagules to float away to offshore waters.. Although not all propagules are sticking at the coast of Demak and floating away to offshore waters, it must be taken into account that there is still a chance that these propagules stick at other coasts further away. der Stocken et al. (2019a) summarized different dispersal distance studies confirming that most *Avicennica marina* propagules are ending up within a few kilometers within their release location, but some propagules may establish more than 10 kilometers away (Appendix C). Sensitivity analysis thus show that it is likely for propagules released during ebb water levels to have a higher chance to successfully establish on the nearby coast than propagules released during flood water levels.

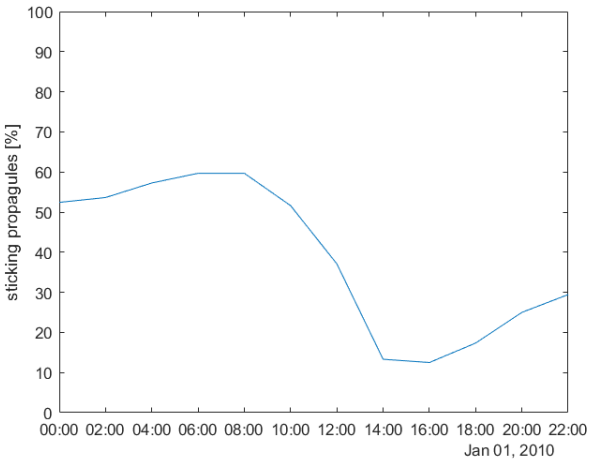

(a) Percentage of sticking propagules for the release during a certain point of the tidal cycle, in this case the release tests are done every two hours.

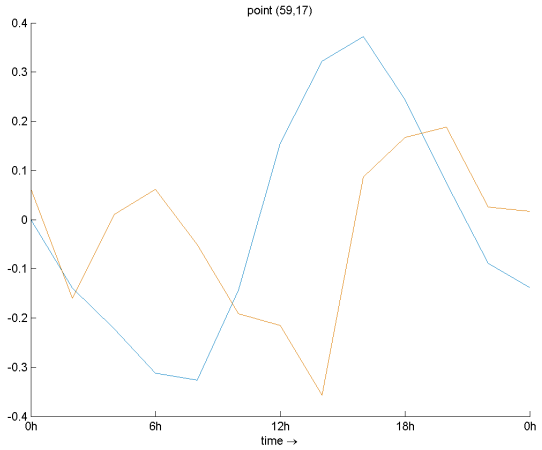

(b) Water levels (m) and depth-averaged flow velocities (m/s) during the tidal cycle at the intertidal basins of Timbulsloko, positive flow velocities are seaward and negative flow velocities are landward.

Figure 6.9: Sensitivity analysis of propagule release time during the SE monsoon.

6.3.6. Connectivity

The conceptual framework of connectivity is a structure for analyzing pathways. Although Pearson et al. (2020) applied this framework to extend the sediment pathway understanding, in principle it is possible to use this approach to determine the connectivity of any type of pathways. In this research it is therefore applied for both the sediment and propagule connectivity in the intertidal basins. For instance, high degree values mean that the node is connected to a large number of nodes and high strength values mean that the total transport in and out of a node is large. It is furthermore possible to plot your pathways in a unstructured manner, showing your results in a different way without the geographical information. The connectivity analysis was for this research not revealing really new insights into the pathways, but it confirmed the results and it helped in having a better understanding of the results. I would recommend to apply a connectivity analysis, because it is useful and allows you to look at the pathways with a different view, which is barely taking extra computational time as the pathways are already computed.

Many other type of connectivity analysis for sediment and propagule pathways may be useful to extend the understanding of the coastal system. Brockmann and Helbing (2013) for instance applied the 'effective distance' concept to predict the spreading of a diseases, in this analysis two nodes that are connected by a strong link (or the most 'popular' pathway between two nodes) are considered effectively close instead of two nodes with the shortest geographical absolute distance. This could also be applied for the spreading of sediment or propagules, because they do not necessarily take the shortest pathway from one node to another, they take the pathway that is forced by hydrodynamics and geographic features. Another example is the concept of 'effective borders', which Thiemann et al. (2010) applied for human traffic in the United States, and can reveal invisible barriers to transport in a system.

6.3.7. Plastic Transport

Areas with mangrove forests, such as Demak, often also have plastic pollution problems. Plastic waste enters the the sea due to a lack of waste collection and disposal services, even two-thirds of the global plastic waste enters ends up in the sea via the twenty most polluted rivers, all located in Asia (van Bijsterveldt et al., 2021). The similarities between the transport mechanisms of propagules and plastics provide another potential opportunity for applying the developed propagule module. Depending on the type of plastic, some adaptations may need to be done for the propagule module to model plastic. Relatively large plastics, such as drinking bottles float near the water surface similar to propagules and thus wind forcing will be important. Micro plastics are much smaller and are more distributed over the water column, but also for these plastic the propagule module can be applied by changing the forcing form the near-surface flow velocity to the depth-averaged velocity. In principle the flow

velocity of every layer in the water column can be used as forcing. Modelling the pathways of plastics using our propagule module may extend the understanding of where the plastics ends up and what type of measures will be effective against the pollution problems. This could provide a solution to prevent plastic from accumulating in mangrove forests, which thus may even help for the rehabilitation of mangroves.

6.4. Application

This research extends the physical and ecological understanding of the mangrove coastal system, especially of sediment and propagule pathways to improve rehabilitation strategies using Demak as study area. This knowledge could be applicable to other areas, taking into account local differences. For instance, larger swell waves are not present in the by islands surrounded Java Sea, which will be present at coasts facing the open ocean. The presence of higher (swell) waves inducing other erosion mechanisms or strong wave-driven currents may require a different approach. As well as coastlines near large rivers, because there is usually formation of sand banks, mud banks, chars and cheniers. Mangrove restoration using permeable structures trapping sediment is mainly proposed for coasts with a relatively high tidal range and sediment availability (Balke and Friess, 2016).

Two relevant examples of mangrove coasts are chosen to compare to Demak, due to their similar strong erosion (Deltares, 2022b). The coast of Guinea is an example of a place where this approach could be applied (Table 6.1). Although the tidal range is much larger in Guinea, other conditions are similar to Demak as it is a muddy low energetic environment influenced by wind- and tide-induced currents with some small rivers. Ghana, also located at the West coast of Africa, is facing more wave-dominated conditions, sandy sediments and two majors rivers. Since wave-driven currents and riverine processes will be more important, this approach is less suitable to apply. Much more sandy sediment is present here, strong wave-induced currents and two major rivers are determining for this area. Guinea is more suitable for mangrove restoration using structures than Ghana, as tidal ranges are larger. For both coasts sites exist where even mangrove forests are still well-developed, despite they are threatened by human interventions. From the four specific sites in Table 6.1 Kaback in Ghana is most similar to Demak, as mangroves along the coast are converted into rice fields, which are eroded and partly flooded now.

	Demak	**Guinea**	**Ghana**
sediment	muddy	muddy	sandy
environment	low energetic	low energetic	wave-dominated
tide	micro-meso tidal	meso-macro tidal	micro tidal
currents	wind and tide induced currents	wind and tide induced currents	strong wave induced currents
coastline	strong erosion	strong erosion	strong erosion
rivers	small rivers	small rivers	two large rivers
mangroves	both at open coast and along pond bunds	both at open coast and along tidal channel/creeks	not at open sea, along banks of tidal rivers
site status	mangrove converted to fish ponds, flooded and abandoned now	Kanfarandé: mangrove relatively untouched Kaback: mangrove converted to rice fields, partly flooded now	Anyanui: abundance of mangroves Anlo: mangroves underdeveloped due to human pressure

Table 6.1: Examples of two mangrove coasts at Guinea and Ghana (Deltares, 2022b).

Although the physical and ecological understanding of the system is essential for mangrove restoration, without social and economical understanding the modelling approach can not be applied successful. The coastline of Demak was almost completely deforested and excavated to build fish ponds. Ground water extraction resulted in large rates of land subsidence, and with this ongoing coastal erosion most ponds have been abandoned. Other mangrove coasts are facing similar problems due to human interventions, leading to detrimental effects for the local communities. Local communities and governments prioritize short-term economical development, and are unaware of the value of mangroves and long-term impact of ground water extraction (Gijón Mancheño, 2022). Without local awareness of the importance to protect mangroves, restoration is impossible. To restore the mangrove coastal system, cooperation between local communities and engineers is essential.

7

Conclusions & Recommendations

This chapter concludes the research questions and gives recommendations for further research.

7.1. Conclusions

The objective of this thesis is to extend the physical and ecological understanding of coastal mangrove systems, especially of currents, sediment pathways and propagule pathways, to improve mangrove rehabilitation using Demak as study area. This objective is represented by the main research question and corresponding sub-questions, the conclusions to these questions are summarized in this section.

7.1.1. Main Research Question

The main research question is:

What can we learn from modelling sediment and propagule pathways to improve mangrove rehabilitation strategies?

We can learn that sediment supplied by alongshore currents as well as riverine sediment could serve as source for the coastline. The protruding Wulan Delta in combination with the river plume confines the area for alongshore sediment pathways. The river plume behaves as barrier for sediment and propagule transport, because the stratification prevents mixing of the sea and river water. At the same time, the plume is thus obstructing as well as trapping sediment and propagules. However, sediments suspended near the bed could be transported underneath the river plume towards the coast by estuarine circulation. Although sand and mud particles may be suspended at the same location, the direction of movement of particles could thus differ depending on the height in the water column. Another lesson learnt is that sediment (suspended in the water column) and propagules (floating around the water surface) do not follow the same pathways, as for propagule dispersal the wind direction is of much larger influence than tidal currents. The simulations confirmed that the seasonal variability in wind direction could significantly influence the establishment area and availability of propagules, and old fish pond bunds can increase the establishment area for propagules. If winds are landward directed the probability for propagules to strand is high, while seaward winds lower this probability. Sensitivity analysis show that the timing of propagule release within one tidal cycle (flood-ebb) influences the probability to successfully establish on the nearby coast, this probability is higher for propagules released during ebb water levels than during flood water levels. Stormy seasons may increase the sediment availability, but the larger bed shear stresses may lower the survival of established propagules at certain locations. Therefore, a propagule module is developed which can determine the survival potential of a propagule based on the inundation-free period and maximum bed shear stress. Permeable dams would be recommended to add to the model in further research, because they could increase the survival of propagules by reducing bed shear stresses and increase the establishment of propagules by trapping them.

Altogether, tidal basins (in this case abandoned fish ponds) are a potentially good location for restoring mangroves, as under certain conditions the basins are a receptor for both sediment and propagules. Another favourable environment for mangrove restoration may be presented by the coastline behind by the river plume trapping riverine sediment, provided that local propagule sources are available. Although this modelling study is focusing on Demak, there are many other similar mangrove coasts around the world where a idealized model would enable to understand where the sediment and propagules are going and the travel time from source to sink. In conclusion, this research has made a start in counteracting coastal erosion and improving the success of mangrove forest rehabilitation by studying sediment and propagule pathways and developing a propagule survival module.

7.1.2. Phase A - Currents

The currents in the coastal system of Demak (Figure 7.1a) are influenced by the interaction of barotropic forcing (tidal flows, river discharge and wind), baroclinic forcing (salinity) and geometric features (protruding delta and tidal basins). During the NW monsoon (wet season), high Wulan river discharges are creating a freshwater plume along the coastline, and winds from offshore are enhancing this stratification. Residual alongshore currents coming from the southwest, are forced to flow around the plume and protruding delta. During the SE monsoon (dry season), low river discharges are hardly creating a freshwater plume and winds are coming from land. Residual alongshore currents are coming from the northeast, stay closer to the coast, as they are not obstructed by a plume. During both monsoons the tidal basins (abandoned fish ponds) are filled by flood currents and emptied by ebb currents.

7.1.3. Phase B - Sediment Pathways

The sediment pathways (Figure 7.1b) are influenced by the same factors as the currents (i.e. barotropic forcing, baroclinic forcing and topographic features). During the NW monsoon (wet season), the Wulan river, especially during flood events, as well as alongshore currents, are a potential sediment source. Sediment from the Wulan river is trapped in the coastal zone and is not lost to offshore waters, because the stratification prevents mixing of the sea and river water. Sediment carried by alongshore currents is not reaching the coastline behind as the plume behaves as a barrier. Part of the alongshore going sediment is settling offshore unable to pass the plume and protruding delta. The Wulan Delta in combination with the river plume thus confines the area for alongshore sediment pathways. So on the one hand, the river plume is a barrier for sediment transport, but on the other hand, coastal and riverine sediment is trapped inside the plume. The shallow part (above mean sea level) of the tidal basins (abandoned fish ponds) imports sediment, however, the deeper part (below mean sea level) is exporting sediment. Without accounting for interactions between the sandy and muddy particles in the bed or water column, sand is less mobile than mud. Therefore, more sand than mud is accumulating at the river mouth, which could explain the cheniers formed by sand around the delta. Sand suspended near the bed may be transported underneath the river plume towards the coast by estuarine circulation. Although sand and mud particles may be suspended at the same location, the direction of movement of particles could thus differ depending on the height in the water column. During the SE monsoon (dry season), there is almost no sediment transport due to the calm conditions, waves created by the wind from land are too weak to stir up sediment. Furthermore, the river discharge and thus the sediment source potential is low.

7.1.4. Phase C - Propagule Pathways

The propagule pathways (Figure 7.1c) are influenced by the same factors as the currents (i.e. barotropic forcing, baroclinic forcing and topographic features). During the NW monsoon (wet season), the local mangroves in the basins, along the coast and at the Delta, as well as the alongshore currents are a potential propagule source. Propagules from these sources are pushed landwards by the winds from offshore. The larger part of the propagules supplied from alongshore is able to enter the river plume, whereas a small part is obstructed by the plume in reaching land. During the SE monsoon (dry season), more propagules float away to offshore waters due to offshore directed winds. The main propagule receptors in this season are the tidal basins, where the old fish pond bunds increase the establishment area. The seasonal variability in wind direction thus significantly influences the establishment area and availability of propagules, as a consequence the propagule availability is larger in the NW than SE monsoon. Sensitivity analysis show that the timing of propagule release within one tidal cycle (flood-ebb) influences the probability to successfully establish on the nearby coast, this probability is higher for

propagules released during ebb water levels than during flood water levels. The survival of mangrove propagules at the establishment area is influenced by the 'Windows of Opportunity', for this a propagule module is developed to determine the survival based on the inundation-free period and maximum bed shear stress. Although the availability of propagules is much larger in the NW monsoon, survival of propagules during the stormy NW monsoon may be slightly lower due to higher bed shear stresses than during the calm SE monsoon.

Altogether, there are similarities and differences between the sediment and propagule pathways. Dispersal of the relatively large lightweight propagules floating around the water surface is more influenced by wind than of the smaller heavier sediment suspended in the water column relatively closer to the bed, hence they do not follow the same pathways. Furthermore, sediment is only in motion if flow velocities are high enough and propagules are floating around following flow velocities until they are able establish at a certain location.

7.2. Recommendations

This section elaborates the recommendations about SedTRAILS, permeable dams and the intertidal basins for further research.

7.2.1. SedTRAILS

The first recommendation is to include a mud transport formulation in SedTRAILS, because currently only a sand transport formulation is implemented in the model. Mud transport could be introduced by defining critical shear strengths for sedimentation and erosion. For instance, the method of Partheniades (1965) could be used as underlying formulation (Equation 2.2). In this research, mud is modelled as very fine sand or noncohesive silt, however, including the cohesive characteristics of mud would be more realistic. Instead of using SedTRAILS, another option is to compute the particle pathways using Delft3D-PART. This module is not developed for sediment in particular, however, it is a possibility to model sand and mud. Delft3D-PART can compute settling, but erosion processes can only be modelled with a simplified erosion formulation.

A small recommendation for the propagule module of SedTRAILS is to rename the sticky depth parameter. The underlying model was developed for coral larvae (Storlazzi et al., 2017) for which this parameter was named the sticky depth, however, it may be more appropriate to change the name of this parameter to a more mangrove-specific name, for instance establishment depth or rooting depth.

This research started a sensitivity analysis of propagule release time for one flood-ebb tidal cycle during the NW and SE monsoon. Many other factors may be influencing the sensitivity, hence it would be recommended to do a more in-depth analysis, for instance investigate the sensitivity of propagule release to the spring-neap tidal cycle, the variations in diurnal and semidiurnal tidal components and the sea breeze wind in the afternoon of the SE monsoon.

Lastly, the implementation of phase 1 and 2 of the windows of opportunity (Figure 2.3 (van Bijsterveldt et al., 2022; Balke et al., 2011)) in the propagule module of SedTRAILS could be more accurate, as the model is now mainly focusing on the propagule pathways and thus availability. Phase 1 and 2 are introduced into the module by defining two thresholds: a minimum inundation-free time and a maximum bed shear stress. The module compares the interpolated values and the thresholds at the location a propagule has stranded, to check whether the propagule will survive or not. Although a survival part of the propagule module is developed, our model is not optimal for the application of this part. The limitations of our model are the inaccurate inundation-free periods in the intertidal area and that waves are not penetrating into this intertidal area, which is exactly the area where propagules are sticking. It is thus recommended to increase the resolution of the model near the coastline and change the wave model from a stationary to non-stationary. In this case more accurate survival rates of sticking propagules can be computed and compared to observations. Another opportunity to improve the module is to implement phase 3 (bed erosion), by changing the model from morphostatic to morphodynamic and set a threshold for a maximum bed level change in a grid cell. Since a sediment imbalance may prevent establishment of propagules at intertidal areas and the early growth of planted mangroves, it would be interesting to investigate if bed erosion is the determining factor for propagule survival at this specific location.

7.2.2. Permeable Dams

Permeable dams made for example out of bamboo poles and brushwood filling, can enhance the trapping of fine sediments in the intertidal zone (Winterwerp et al., 2020). The intertidal basins at Timbulsloko and the coastline behind by the river plume (between Timbulsloko and the Wulan river) are identified here as most promising sites for the structures to improve mangrove rehabilitation in Demak. For the first site the main potential source is sediment supplied by the alongshore current and for the second site sediment supplied by the river. According to our model sediments are mainly imported to tidal areas above mean sea level, thus it is proposed to place the dams near and above the MSL line to retain the sediments.

Our results showed that the old pond bunds increase the amount of propagules able to stick, so dams may have the same effect and increase this amount even more. Especially during the SE monsoon (dry season), the dams could prevent the propagules from floating to offshore waters. Despite that most propagules float away, this season is biologically ideal for their establishment and growth as the hydrodynamic conditions are calm. Dams would therefore provide opportunities to capture propagules during the SE monsoon, however, with barely any sediment transport taking place during this season dams will not be able to trap sediment. During the NW monsoon (wet season) sediment is available to be trapped and propagules are already pushed by wind towards land, but the hydrodynamic conditions are slightly less favorable for the biological development of the propagules. The advantage of the dams is that they can reduce wave heights, currents and the resulting bed shear stresses, thereby providing more suitable conditions during the NW monsoon to survive the windows of opportunity threshold (van Bijsterveldt et al., 2022; Balke et al., 2011). To conclude, dams may thus be a solution for the establishment problems, because they could increase the survival of propagules by reducing bed shear stresses in the NW monsoon and increase the availability of propagules by trapping them in the SE monsoon. van Bijsterveldt et al. (2022) observed that the dams significantly increased the survival of already established mangrove seedlings compared to sites more exposed to waves. If enough propagules can successfully grow into mature mangrove trees, they can take over the function of the dams.

7.2.3. Intertidal Basins

The last recommendation is to look in more detail into the sediment and propagule pathways in the intertidal basins at Timbulsloko, because this area has large potential. Grid sizes have to be decreased locally. Delft3D-4 is not the ideal model for varying grid sizes, but it is an option to nest a smaller detailed grid inside the larger coarse grid. Delft3D-FM is more suitable for decreased grid size in certain area of interest. Decreased grid sizes enable to include more geograpical features of the basins, for instance the main and smaller pond bunds remaining from the abandoned fish ponds, mangrove patches and roads in the bathymetry. This more detailed bathymetry has to be determined by for example satellite derived bathymetry (SDB) techniques, as no data is available on this small-scale. The SDB approach can obtain bathymetric maps in the shallow water of coastal areas, but prior in-situ depth measurements are required, which limits the application area (Ma et al., 2020; Ashphaq et al., 2021). However, with the upcoming machnine learning algorithms, these in-situ measurements are not necessary anymore (Sagawa et al., 2019).

Smaller grid sizes also allow to have more accurate estimates of the inundation-free periods and bed shear stresses at the locations where propagules are stranding and thus whether they will survive. An additional possibility of the locally decreased grid size is to include the permeable dams in the model, to investigate how these dams are affecting the sediment and propagule pathways and to optimize the designs. The results would strongly depend on how the dams are schematized and if the SedTRAILS model can realistically reproduce this.

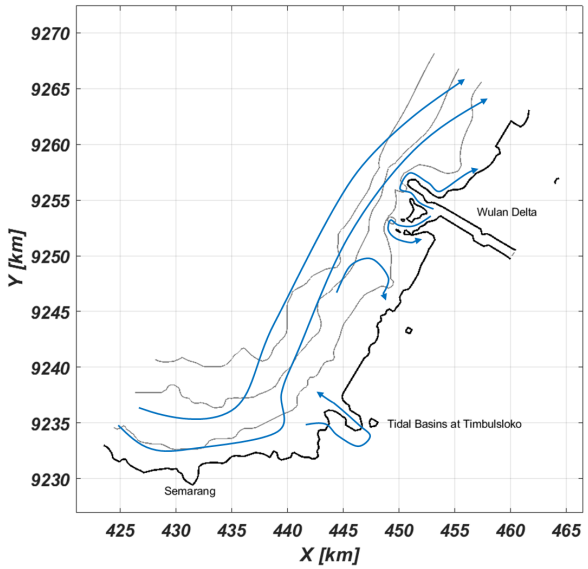

(a) Current pathways in the NW monsoon.

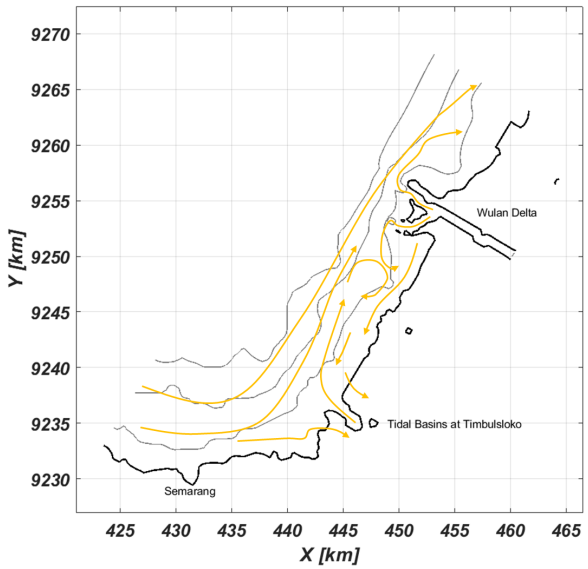

(b) Sediment pathways in the NW monsoon.

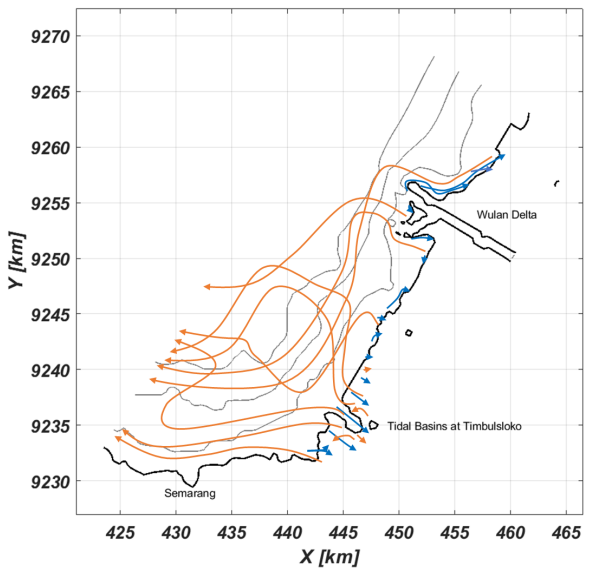

(c) Propagule pathways in the NW monsoon (blue) and SE monsoon (orange).

Figure 7.1: Conceptual summary of the pathways. The black depth contour is the coastline and the grey depth contours are each 5 meter deeper.

References

Alferink, M. (2022). Wave transmission through permeable structures in demak indonesia: A design study with the numerical model swash. Master's thesis, Delft University of Technology, Civil Engineering and Geosciences, Hydraulic Engineering.

Alleman, L. K. and Hester, M. W. (2011). Reproductive ecology of black mangrove (avicennia germinans) along the louisiana coast: Propagule production cycles, dispersal limitations, and establishment elevations. *Estuaries and Coasts*, 34:1068–1077.

Andreas, H., Abidin, H. Z., Gumilar, I., Sidiq, T. P., Sarsito, D. A., and Pradipta, D. (2018). Insight into the correlation between land subsidence and the floods in regions of indonesia. *Natural Hazards - Risk Assessment and Vulnerability Reduction*.

Ashphaq, M., Srivastava, P. K., and Mitra, D. (2021). Review of near-shore satellite derived bathymetry: Classification and account of five decades of coastal bathymetry research. *Journal of Ocean Engineering and Science*, 6:340–359.

Balke, T., Bouma, T. J., Horstman, E. M., Webb, E. L., Erftemeijer, P. L., and Herman, P. M. (2011). Windows of opportunity: Thresholds to mangrove seedling establishment on tidal flats. *Marine Ecology Progress Series*, 440:1–9.

Balke, T. and Friess, D. A. (2016). Geomorphic knowledge for mangrove restoration: a pan-tropical categorization. *Earth Surface Processes and Landforms*, 41:231–239.

Bariq, J. M. and Marfai, M. A. (2019). Distribution pattern of suspended sediments in wulan delta, demak, indonesia. page 36.

Bijsterveldt, C. E. V., van Wesenbeeck, B. K., van der Wal, D., Afiati, N., Pribadi, R., Brown, B., and Bouma, T. J. (2020). How to restore mangroves for greenbelt creation along eroding coasts with abandoned aquaculture ponds. *Estuarine, Coastal and Shelf Science*, 235.

BioManCO (2018). Bio-moprhodynamic modelling of mangrove-mud coasts. PhD research project.

Bisschop, F. (2018). Erosion of sand at high flow velocities: an experimental study.

Borsje, R. (2019). Wave-driven set-up of fluid mud: Demak, indonesia. Master's thesis, Delft University of Technology, Civil Engineering and Geosciences, Hydraulic Engineering.

Bosboom, J. and Stive, M. (2021). *Coastal Dynamics*. TU Delft.

Brockmann, D. and Helbing, D. (2013). The hidden geometry of complex, network-driven contagion phenomena. *Science*, 342(6164):1337–1342.

Bueno, M., Moser, G., Tocci, B., and Flores, A. (2010). Retention-favorable timing of propagule release in barnacles and periwinkles. *Marine Ecology Progress Series*, 414:155.

Cavanaugh, K. C., Kellner, J. R., Forde, A. J., Gruner, D. S., Parker, J. D., Rodriguez, W., and Feller, I. C. (2014). Poleward expansion of mangroves is a threshold response to decreased frequency of extreme cold events. *Proceedings of the National Academy of Sciences of the United States of America*, 111:723–727.

Clarke, P. J. (1993). Dispersal of grey mangrove (avicennia marina) propagules in southeastern australia. *Aquatic Botany*, 45:195–204.

Clarke, P. J., Kerrigan, R. A., and Westphal, C. J. (2001). Dispersal potential and early growth in 14 tropical mangroves: do early life history traits correlate with patterns of adult distribution? *Journal of Ecology*, 89:648–659.

Clarke, P. J. and Myerscough, P. J. (1991). Buoyancy of avicennia marina propagules in south-eastern australia. *Australian Journal of Botany*, 39:77–83.

Codiga, D. L. (2011). Unified tidal analysis and prediction using the utide matlab functions. page 59.

Cowen, R. K. and Sponaugle, S. (2008). Larval dispersal and marine population connectivity.

Cuong, C. and Brown, S. (2012). Coastal rehabilitation and mangrove restoration using melaleuca fences: Practical experience form kien giang province.

Damastuti, E., Groot, R. D., Debrot, A. O., and Silvius, M. J. (2022). Effectiveness of community-based mangrove management for biodiversity conservation: A case study from central java, indonesia. *Trees, Forests and People*, 7:100202.

Deltares (2020). Effectiveness of ecosystem-based adaptation measures subject to sea level rise land subsidence. Technical Report 1220476-004-ZKS-011.

Deltares (2022a). Delft3d 4 suite (structured) - deltares.

Deltares (2022b). Mangroves as a protection from erosion and coastal flooding in selected west african coastal countries. Technical Report 11205569-000-ZKS-0003.

der Stocken, T. V., Carroll, D., Menemenlis, D., Simard, M., and Koedam, N. (2019a). Global-scale dispersal and connectivity in mangroves. *Proceedings of the National Academy of Sciences of the United States of America*, 116:915–922.

der Stocken, T. V., López-Portillo, J., and Koedam, N. (2017). Seasonal release of propagules in mangroves – assessment of current data. *Aquatic Botany*, 138:92–99.

der Stocken, T. V. and Menemenlis, D. (2017). Modelling mangrove propagule dispersal trajectories using high-resolution estimates of ocean surface winds and currents. *Biotropica*, 49:472–481.

der Stocken, T. V., Wee, A. K., Ryck, D. J. D., Vanschoenwinkel, B., Friess, D. A., Dahdouh-Guebas, F., Simard, M., Koedam, N., and Webb, E. L. (2019b). A general framework for propagule dispersal in mangroves. *Biological Reviews*, 94:1547–1575.

Donato, D. C., Kauffman, J. B., Murdiyarso, D., Kurnianto, S., Stidham, M., and Kanninen, M. (2011). Mangroves among the most carbon-rich forests in the tropics. *Nature Geoscience 2011 4:5*, 4:293–297.

Drexler, J. Z. (2001). Maximum longevities of rhizophora apiculata and r. mucronata propagules. *Pacific Science*, 55:17–22.

EcoShape (2015). Building with nature indonesia securing eroding delta coastlines design and engineering plan towards a district level masterplan.

Eisma, D. (1986). Flocculation and de-flocculation of suspended matter in estuaries. *Netherlands Journal of Sea Research*, 20(2):183–199.

Ervita, K., Marfai, M. A., Ervita, K., and Marfai, M. A. (2017). Shoreline change analysis in demak, indonesia. *Journal of Environmental Protection*, 8:940–955.

Fadlillah, L. N., Sunarto, Widyastuti, M., and Marfai, M. A. (2018). The impact of human activities in the wulan delta estuary, indonesia. *IOP Conference Series: Earth and Environmental Science*, 148.

Fadlillah, L. N., Widyastuti, M., Geottongsong, T., Sunarto, and Marfai, M. A. (2019). Hydrological characteristics of estuary in wulan delta in demak regency, indonesia. *Water Resources*, 46:832–843.

FAO (2007). The world's mangroves 1980-2005. a thematic study prepared in the framework of the global forest resources assessment 2005.

Flanders Marine Institute (VLIZ) and Intergovernmental Oceanographic Commission (IOC) (2021). Sea level station monitoring facility.

Foreman, M. G. and Henry, R. F. (1989). The harmonic analysis of tidal model time series. *Advances in Water Resources*, 12:109–120.

Friedrichs, C. T. and Madsen, O. S. (1992). Nonlinear diffusion of the tidal signal in frictionally dominated embayments. *Journal of Geophysical Research: Oceans*, 97:5637–5650.

Gedan, K. B., Kirwan, M. L., Wolanski, E., Barbier, E. B., and Silliman, B. R. (2011). The present and future role of coastal wetland vegetation in protecting shorelines: Answering recent challenges to the paradigm. *Climatic Change*, 106:7–29.

Gijón Mancheño, A. (2022). Restoring mangroves with structures: Improving the mangrove habitat using local materials.

Gijón Mancheño, A., Jansen, W., Uijttewaal, W. S., Reniers, A. J., van Rooijen, A. A., Suzuki, T., Etminan, V., and Winterwerp, J. C. (2021). Wave transmission and drag coefficients through dense cylinder arrays: Implications for designing structures for mangrove restoration. *Ecological Engineering*, 165:106231.

Giri, C., Ochieng, E., Tieszen, L. L., Zhu, Z., Singh, A., Loveland, T., Masek, J., and Duke, N. (2011). Status and distribution of mangrove forests of the world using earth observation satellite data. *Global Ecology and Biogeography*, 20:154–159.

Gray, A. B., Warrick, J. A., Pasternack, G. B., Watson, E. B., and Goñi, M. A. (2014). Suspended sediment behavior in a coastal dry-summer subtropical catchment: Effects of hydrologic preconditions. *Geomorphology*, 214:485–501.

Guo, C., He, Q., Guo, L., and Winterwerp, J. C. (2017). A study of in-situ sediment flocculation in the turbidity maxima of the yangtze estuary. *Estuarine, Coastal and Shelf Science*, 191:1–9.

Guppy, H. B. (1906). *Observations of a naturalist in the Pacific between 1896 and 1899: plant-dispersal*, volume 2. Macmillan and Company, limited.

Haurwitz, B. (1947). Comments on the Sea-Breeze Circulation. *Journal of Atmospheric Sciences*, 4(1):1–8.

Heckmann, T., Schwanghart, W., and Phillips, J. D. (2015). Graph theory—recent developments of its application in geomorphology. *Geomorphology*, 243:130–146.

Hendriks, H. C., van Prooijen, B. C., Aarninkhof, S. G., and Winterwerp, J. C. (2020). How human activities affect the fine sediment distribution in the dutch coastal zone seabed. *Geomorphology*, 367:107314.

Hir, P. L., Roberts, W., Cazaillet, O., Christie, M., Bassoullet, P., and Bacher, C. (2000). Characterization of intertidal flat hydrodynamics. *Continental Shelf Research*, 20:1433–1459.

HK., B. T., Gernowo, R., H., S. W. B., and J., I. (2008). Rainfall distribution over the year in semarang. Presented at the International Symposium on Equatorial Monsoon System, Yogyakarta, Indonesia.

Irsadi, A., Kartijono, N. E., Partaya, P., Abdullah, M., Hadiyanti, L. N., and Aji, H. S. (2022). Carbon stock profiling of mangrove ecosystem in the semarang-demak coastal area for global warming mitigation. *International Journal of Environmental Research*, 16:1–12.

Ismanto, A., Zainuri, M., Hutabarat, S., Sugianto, D. N., Widada, S., and Wirasatriya, A. (2017). Sediment transport model in sayung district, demak. *IOP Conference Series: Earth and Environmental Science*, 55:012007.

Kerssens, P. (1980). New developments in suspended sediment research.

Kitamura, S. and for Mangrove Ecosystems., I. S. (1997). *Handbook of mangroves in indonesia : Bali lombok*. Saritaksu.

Kjerfve, B. and Magill, K. E. (1989). Geographic and hydrodynamic characteristics of shallow coastal lagoons. *Marine Geology*, 88:187–199.

KOICA (2012). Coastal protection and management policy addressing climate change impact in indonesia. Technical report.

Kuitenbrouwer, D., Reniers, A., MacMahan, J., and Roth, M. K. (2018). Coastal protection by a small scale river plume against oil spills in the northern gulf of mexico. *Continental Shelf Research*, 163:1–11.

Kusumaningrum, P. B. and Haryono, E. (2020). The potential of delta ecosystem in north coast of java in reducing co2 emissions. *IOP Conference Series: Earth and Environmental Science*, 451.

Latiff, A. and Faridah-Hanum, I. (2014). Mangrove ecosystem of malaysia: Status, challenges and management strategies. *Mangrove Ecosystems of Asia: Status, Challenges and Management Strategies*, pages 1–22.

Lesser, G. R., Roelvink, J. A., van Kester, J. A., and Stelling, G. S. (2004). Development and validation of a three-dimensional morphological model. *Coastal Engineering*, 51:883–915.

Lewis, R. R. (2005). Ecological engineering for successful management and restoration of mangrove forests. *Ecological Engineering*, 24:403–418.

Lieth, H. and of Biological Sciences., A. I. (1974). *Phenology and seasonality modeling.* Springer-Verlag.

Longuet-Higgins, M. S. (1953). Mass transport in water waves. *Philosophical Transactions of the Royal Society of London. Series A, Mathematical and Physical Sciences*, 245(903):535–581.

Ma, Y., Xu, N., Liu, Z., Yang, B., Yang, F., Wang, X. H., and Li, S. (2020). Satellite-derived bathymetry using the icesat-2 lidar and sentinel-2 imagery datasets. *Remote Sensing of Environment*, 250:112047.

Maanen, B. V., Coco, G., and Bryan, K. R. (2015). On the ecogeomorphological feedbacks that control tidal channel network evolution in a sandy mangrove setting. *Proceedings of the Royal Society A: Mathematical, Physical and Engineering Sciences*, 471.

Many, G., de Madron, X. D., Verney, R., Bourrin, F., Renosh, P. R., Jourdin, F., and Gangloff, A. (2019). Geometry, fractal dimension and settling velocity of flocs during flooding conditions in the rhône rofi. *Estuarine, Coastal and Shelf Science*, 219:1–13.

Marfai, M. A. (2011). The hazards of coastal erosion in central java, indonesia: An overview.

Marfai, M. A. and King, L. (2007). Monitoring land subsidence in semarang, indonesia. *Environmental Geology*, 53:651–659.

Marfai, M. A., Tyas, D. W., Nugraha, I., Fitriatul'Ulya, A., Riasasi, W., Marfai, M. A., Tyas, D. W., Nugraha, I., Fitriatul'Ulya, A., and Riasasi, W. (2016). The morphodynamics of wulan delta and its impacts on the coastal community in wedung subdistrict, demak regency, indonesia. *Journal of Environmental Protection*, 7:60–71.

Mariotti, G. and Fagherazzi, S. (2010). A numerical model for the coupled long-term evolution of salt marshes and tidal flats. *Journal of Geophysical Research: Earth Surface*, 115.

Maulina, N. (2010). Shoreline change analysis and prediction; an application of remote sensing and gis. Master's thesis, Geography Faculty, Gadjah Mada University, Yogyakarta, Indonesia.

Michel, J. (2014). Oil spills in mangroves; planning response considerations. Technical report.

MMAF (2012). Oceanography condition in coastal of sayung sub-district, district of demak province of central java. Technical report, Ministry of Marine Affairs and Fisheries, Republic of Indonesia.

Moore, G. E. (2009). *Community-Based Mangrove Restoration Management Woburn Bay Marine Protected Area, Grenada, West Indies Mangrove Seed Preparation Guidelines*. University of New Hampshire, Department of Biological Sciences.

Murray, S. P. and Young, M. (1985). The nearshore current along a high-rainfall, trade-wind coast-nicaragua. *Estuarine, Coastal and Shelf Science*, 21:687–699.

Naidoo, G. (2016). Mangrove propagule size and oil contamination effects: Does size matter? *Marine Pollution Bulletin*, 110:362–370.

Nielsen, P. (2009). *Coastal and estuarine processes*. World Scientific Publishing Co.

Nitto, D. D., Erftemeijer, P. L. A., Beek, J. K. L. V., Dahdouh-Guebas, F., Higazi, L., Quisthoudt, K., Jayatissa, L. P., and Koedam, N. (2013). Climate of the past geoscientific instrumentation methods and data systems modelling drivers of mangrove propagule dispersal and restoration of abandoned shrimp farms. *Biogeosciences*, 10:5095–5113.

Oh, R. R., Friess, D. A., and Brown, B. M. (2017). The role of surface elevation in the rehabilitation of abandoned aquaculture ponds to mangrove forests, sulawesi, indonesia. *Ecological Engineering*, 100:325–334.

Partheniades, E. (1965). Erosion and deposition of cohesive soils. *Journal of the Hydraulics Division*, 91(1):105–139.

Pascolo, S., Petti, M., and Bosa, S. (2018). On the wave bottom shear stress in shallow depths: The role of wave period and bed roughness. *Water 2018, Vol. 10, Page 1348*, 10:1348.

Pearson, S., Elias, E., van Ormondt, M., Roelvink, F. E., Lambregts, P., Wang, Z., and van Prooijen, B. (2021a). Lagrangian sediment transport modelling as a tool for investigating coastal connectivity. Coastal Dynamics 2021 Conference.

Pearson, S. G. (2021). Sedtrails development.

Pearson, S. G., van Prooijen, B. C., Elias, E. P., Vitousek, S., and Wang, Z. B. (2020). Sediment connectivity: A framework for analyzing coastal sediment transport pathways. *Journal of Geophysical Research: Earth Surface*, 125:e2020JF005595.

Pearson, S. G. A., Verney, R. ., Prooijen, B. C. V., Tran, D. ., Hendriks, E. C. M., Jacquet, M. ., and Wang, Z. B. (2021b). Characterizing the composition of sand and mud suspensions in coastal and estuarine environments using combined optical and acoustic measurements. *Journal of Geophysical Research: Oceans*, 126.

Peel, M. C., Finlayson, B. L., and McMahon, T. A. (2007). Updated world map of the köppen-geiger climate classification. *Hydrology and Earth System Sciences*, 11(5):1633–1644.

Prasetyo, Y., Bashit, N., and Setianingsih, W. (2019). Iop conference series: Earth and environmental science impact of land subsidence and sea level rise influence shoreline change in the coastal area of demak. *IOP Conf. Ser.: Earth Environ. Sci*, 280:12006.

Primavera, J. H. and Esteban, J. M. (2008). A review of mangrove rehabilitation in the philippines: Successes, failures and future prospects. *Wetlands Ecology and Management*, 16:345–358.

Pritchard, D., Hogg, A. J., and Roberts, W. (2002). Morphological modelling of intertidal mudflats: the role of cross-shore tidal currents. *Continental Shelf Research*, 22:1887–1895.

Pugh, D. (1987). *Tides, Surges and Mean Sea-Level*. Wiley.

Rabinowitz, D. (1978). Dispersal properties of mangrove propagules. *Biotropica*, 10(1):47–57.

Robertson, A. and Alongi, D. (1992). *Tropical Mangrove Ecosystems*. Coastal and Estuarine Studies. Wiley.

Rönnbäck, P. (1999). The ecological basis for economic value of seafood production supported by mangrove ecosystems. *Ecological Economics*, 29:235–252.

Sagawa, T., Yamashita, Y., Okumura, T., and Yamanokuchi, T. (2019). Satellite derived bathymetry using machine learning and multi-temporal satellite images. *Remote Sensing 2019, Vol. 11, Page 1155*, 11:1155.

Saintilan, N., Khan, N. S., Ashe, E., Kelleway, J. J., Rogers, K., Woodroffe, C. D., and Horton, B. P. (2020). Thresholds of mangrove survival under rapid sea level rise. *Science*, 368:1118–1121.

Saintilan, N., Wilson, N. C., Rogers, K., Rajkaran, A., and Krauss, K. W. (2014). Mangrove expansion and salt marsh decline at mangrove poleward limits. *Global Change Biology*, 20:147–157.

Sasekumar, A., Chong, V. C., Leh, M. U., and D'Cruz, R. (1992). Mangroves as a habitat for fish and prawns. *The Ecology of Mangrove and Related Ecosystems*, pages 195–207.

Savage, D., Barbetti, M. J., MacLeod, W. J., Salam, M. U., and Renton, M. (2010). Timing of propagule release significantly alters the deposition area of resulting aerial dispersal. *Diversity and Distributions*, 16:288–299.

Selvam, V. and Karunagaran, V. (2019). *Ecology and Biology of Mangroves Orientation Guide*.

Septiangga, B. and Mutaqin, B. (2021). Spatio-temporal analysis of wulan delta in indonesia: Characteristics, evolution, and controlling factors. *Geographia Technica*, 16:43–55.

Sidik, F., Kusuma, D. W., Priyono, B., Proisy, C., and Lovelock, C. E. (2021). Managing sediment dynamics through reintroduction of tidal flow for mangrove restoration in abandoned aquaculture ponds. *Dynamic Sedimentary Environments of Mangrove Coasts*, pages 563–582.

Smits, B. P. (2016). Morphodynamic optimisation study of the design of semi-permeable dams for rehabilitation of a mangrove-mud coast: A case study of the building-with-nature project in demak, indonesia. Master's thesis, Delft University of Technology, Civil Engineering and Geosciences, Hydraulic Engineering.

Soulsby, R. (1997). *Dynamics of marine sands*. Thomas Telford Publishing.

Soulsby, R. L., Mead, C. T., Wild, B. R., and Wood, M. J. (2011). A lagrangian model for simulating the dispersal of sand-sized particles in coastal waters hrpp 492. *Journal of Waterway, Port, Coastal, and Ocean Engineering*, 137.

Soulsby, R. L. and Whitehouse, R. (1997). Threshold of sediment motion in coastal environments.

Stanley, O. D. and Lewis, R. R. (2009). Strategies for mangrove rehabilitation in an eroded coastline of selangor, peninsular malaysia.

Stocken, T. V. D., Ryck, D. J. D., Balke, T., Bouma, T. J., Dahdouh-Guebas, F., and Koedam, N. (2013). The role of wind in hydrochorous mangrove propagule dispersal. *Biogeosciences*, 10:3635–3647.

Stocken, T. V. D., Ryck, D. J. D., Vanschoenwinkel, B., Deboelpaep, E., Bouma, T. J., Dahdouh-Guebas, F., and Koedam, N. (2015a). Impact of landscape structure on propagule dispersal in mangrove forests. *Marine Ecology Progress Series*, 524:95–106.

Stocken, T. V. D., Vanschoenwinkel, B., Ryck, D. J. D., Bouma, T. J., Dahdouh-Guebas, F., and Koedam, N. (2015b). Interaction between water and wind as a driver of passive dispersal in mangroves. *PLOS ONE*, 10:e0121593.

Storlazzi, C. D., van Ormondt, M., Chen, Y. L., and Elias, E. P. (2017). Modeling fine-scale coral larval dispersal and interisland connectivity to help designate mutually-supporting coral reef marine protected areas: Insights from maui nui, hawaii. *Frontiers in Marine Science*, 4:381.

Sugianto, D. N., Rochaddi, B., Wulandari, Y., Subardjo, P., Anugroho, A., Suryoputro, D., Atmodjo, W., Satriadi, A., Suryono, C. A., and Soenardjo, N. (2017). Current characteristics in demak waters based on acoustic measurement. *International Journal of Civil Engineering and Technology*, 8:749–760.

Sunarto, S. (2004). *Geomorphic changes in coastal area surround Muria Volcano*. PhD thesis, Dissertation, Gadjah Mada University Yogyakarta (in Indonesian).

Swart, D. H. (1974). Offshore sediment transport and equilibrium beach profiles.

Tas, S. (2022). Chenier dynamics.

Tas, S., Mancheño, A. G., Herman, P., Reniers, A., Uijttewaal, W., and Winterwerp, H. (2017). Wave transformation on the mangrove-mud coast of demak, indonesia. *Abstract from INTERCOH 2017*, pages 39–40.

Tas, S. A., van Maren, D. S., Helmi, M., and Reniers, A. J. (2022). Drivers of cross-shore chenier dynamics off a drowning coastal plain. *Marine Geology*, 445:106753.

Tas, S. A., van Maren, D. S., and Reniers, A. J. (2020). Observations of cross-shore chenier dynamics in demak, indonesia. *Journal of Marine Science and Engineering*, 8:1–18.

Thampanya, U., Vermaat, J. E., Sinsakul, S., and Panapitukkul, N. (2006). Coastal erosion and mangrove progradation of southern thailand. *Estuarine, Coastal and Shelf Science*, 68:75–85.

Thiemann, C., Theis, F., Grady, D., Brune, R., and Brockmann, D. (2010). The structure of borders in a small world. *PLOS ONE*, 5(11):1–7.

Thongjoo, C., Choosak, S., and Chaichana, R. (2018). Soil fertility improvement from commercial monospecific mangrove forests (rhizophora apiculata) at yeesarn village, samut songkram province, thailand. *Tropical Ecology*, 59:91–97.

Triest, L., Hasan, S., Mitro, P. R., Ryck, D. J. D., and der Stocken, T. V. (2018). Geographical distance and large rivers shape genetic structure of avicennia officinalis in the highly dynamic sundarbans mangrove forest and ganges delta region. *Estuaries and Coasts*, 41:908–920.

Turner, R. and Lewis, R. (1997). Hydrologic restoration of coastal wetlands. *pp*, 65:72.

van Bijsterveldt, C. E., Debrot, A. O., Bouma, T. J., Maulana, M. B., Pribadi, R., Schop, J., Tonneijck, F. H., and van Wesenbeeck, B. K. (2022). To plant or not to plant: When can planting facilitate mangrove restoration? *Frontiers in Environmental Science*, 9:762.

van Bijsterveldt, C. E., van Wesenbeeck, B. K., Ramadhani, S., Raven, O. V., van Gool, F. E., Pribadi, R., and Bouma, T. J. (2021). Does plastic waste kill mangroves? a field experiment to assess the impact of macro plastics on mangrove growth, stress response and survival. *Science of The Total Environment*, 756:143826.

Van Domburg, T. (2018). Identifying windows of opportunity for mangrove establishment on a mud coast: A case study for the biomanco project in demak, indonesia. Master's thesis, Delft University of Technology, Civil Engineering and Geosciences, Hydraulic Engineering.

van Eekelen, E. and Bouw, M. (2020). Building with nature : creating, implementing and upscaling nature-based solutions.

van Ledden, M., van Kesteren, W. G. M., and Winterwerp, J. C. (2004). A conceptual framework for the erosion behaviour of sand-mud mixtures. 24(1):1–11.

van Prooijen, B. (2021). Sediment dynamics: Transport modes and erosion rates. Lecture slides.

van Rijn, L. C. (2020). Erodibility of mud–sand bed mixtures. *Journal of Hydraulic Engineering*, 146(1):04019050.

van Sebille, E., Griffies, S. M., Abernathey, R., Adams, T. P., Berloff, P., Biastoch, A., Blanke, B., Chassignet, E. P., Cheng, Y., Cotter, C. J., Deleersnijder, E., Döös, K., Drake, H. F., Drijfhout, S., Gary, S. F., Heemink, A. W., Kjellsson, J., Koszalka, I. M., Lange, M., Lique, C., MacGilchrist, G. A., Marsh, R., Adame, C. G. M., McAdam, R., Nencioli, F., Paris, C. B., Piggott, M. D., Polton, J. A., Rühs, S., Shah, S. H., Thomas, M. D., Wang, J., Wolfram, P. J., Zanna, L., and Zika, J. D. (2018). Lagrangian ocean analysis: Fundamentals and practices. *Ocean Modelling*, 121:49–75.

Verschure, S. (2013). Applying hybrid engineering to restore a muddy coast in north java, indonesia experiences based on a four month field work, timbul sloko, sayung, demak.

Walters, B. B., nnbä ck, P. R., Kovacs, J. M., Crona, B., Hussain, S. A., Badola, R., Primavera, J. H., Barbier, E., and Dahdouh-Guebas, F. (2008). Ethnobiology, socio-economics and management of mangrove forests: A review.

Wattayakorn, G., Wolanski, E., and Kjerfve, B. (1990). Mixing, trapping and outwelling in the klong ngao mangrove swamp, thailand. *Estuarine, Coastal and Shelf Science*, 31:667–688.

Wells, J. T. and Kemp, G. P. (1986). Interaction of surface waves and cohesive sediments: Field observations and geologic significance. In Mehta, A. J., editor, *Estuarine Cohesive Sediment Dynamics*, pages 43–65, New York, NY. Springer New York.

Wells, S. and Ravilious, C. (2006). *In the front line: shoreline protection and other ecosystem services from mangroves and coral reefs*. Number 24. UNEP/Earthprint.

Wilms, T., der Groot, F. V., Tonneijk, F., Nurhabni, F., and Sembiring, L. (2020). Building with nature to restore eroding tropical muddy coasts.

Winterwerp, H., Wesenbeeck, B. V., Dalfsen, J. V., Tonneijck, F., Astra, A., Verschure, S., and Eijk, P. V. (2014). A sustainable solution for massive coastal erosion in central java towards regional scale application of hybrid engineering discussion paper.

Winterwerp, J. C., Albers, T., Anthony, E. J., Friess, D., Mancheño, A. G., Moseley, K., Muhari, A., Naipal, S., Noordermeer, J., Oost, A., Saengsupavanich, C., Tas, S. A. J., Tonneijck, F. H., Wilms, T., Bijsterveldt, C. V., Eijk, P. V., Lavieren, E. V., and Wesenbeeck, B. K. V. (2020). Managing erosion of mangrove-mud coasts with permeable dams-lessons learned.

Winterwerp, J. C., Borst, W. G., and Vries, M. B. D. (2005). Pilot study on the erosion and rehabilitation of a mangrove mud coast. *Journal of Coastal Research*, 21:223–230.

Winterwerp, J. C., Erftemeijer, P. L., Suryadiputra, N., Eijk, P. V., and Zhang, L. (2013). Defining eco-morphodynamic requirements for rehabilitating eroding mangrove-mud coasts. *Wetlands*, 33:515–526.

Winterwerp, P. H., Wilms, T., Siri, H., Vries, J. T. V., Noor, Y., Wesenbeeck, B. V., Cronin, K., Eijk, P. V., and Tonneijck, F. (2016). Building with nature: Sustainable protection of mangrove coasts. *Terra et Agua*.

Wisha, U. J. and Ondara, K. (2017). Total suspended solid (tss) distributed by tidal currents during low to high tide phase in the waters of sayung, demak: Its relations to water quality parameters. *Journal of Marine and Aquatic Sciences*, 3:154.

Wolanski, E. (1992). Hydrodynamics of mangrove swamps and their coastal waters. *Hydrobiologia 1992 247:1*, 247:141–161.

Woodroffe, C. D., Rogers, K., McKee, K. L., Lovelock, C. E., Mendelssohn, I. A., and Saintilan, N. (2016). Mangrove sedimentation and response to relative sea-level rise. *http://dx.doi.org/10.1146/annurev-marine-122414-034025*, 8:243–266.

Wyrtki, K. (1961). *Physical Oceanography of the Southeast Asian Waters*. Naga report. University of California, Scripps Institution of Oceanography.

A

Tidal Variations

This appendix shows the seasonal tidal variations over a year in Semarang. The months March, April, September and October have much larger semi-diurnal components in their tidal signal, which is approximately during the transition in between the monsoons (Appendix A). Tidal constituents of the month January are therefore applied in this model, as this month has representative constituents for the NW en SE monsoon period.

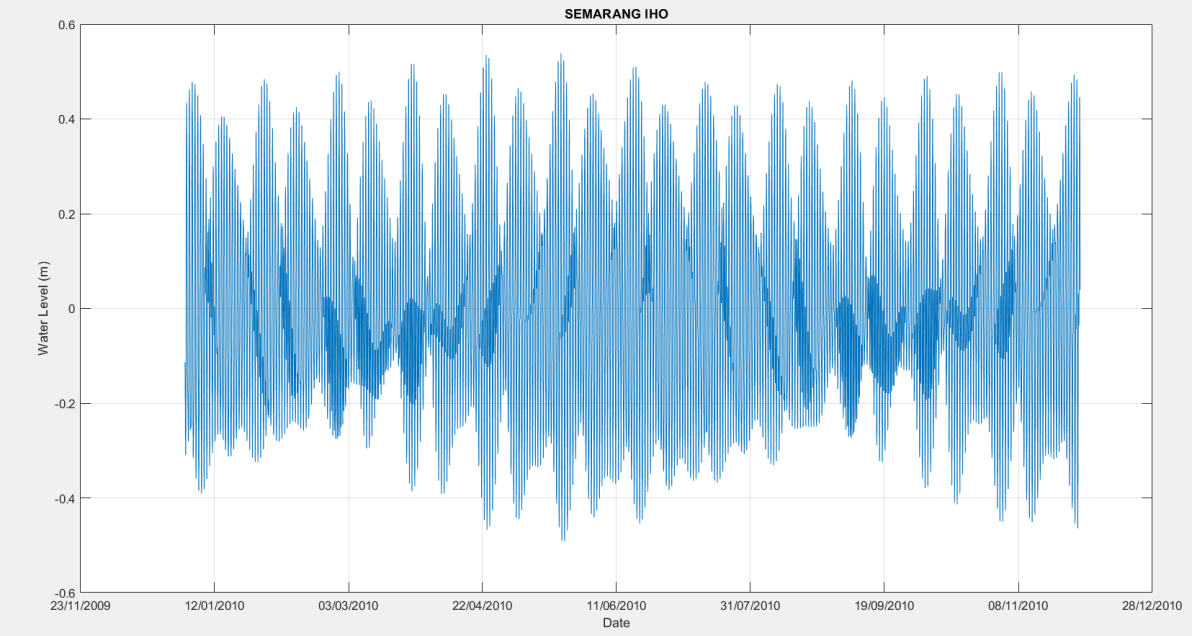

Figure A.1: One year of water level measurements in Semarang IHO Station (downloaded from DelftDashboard).

B

Sediment Measurements

This appendix consists of the set-up of the sediment measurements along two transects (Van Domburg, 2018) corresponding to the grain sizes shown in Table 4.1, these measurements are used for this research to determine the sediment characteristics (D_{50}) of the area.

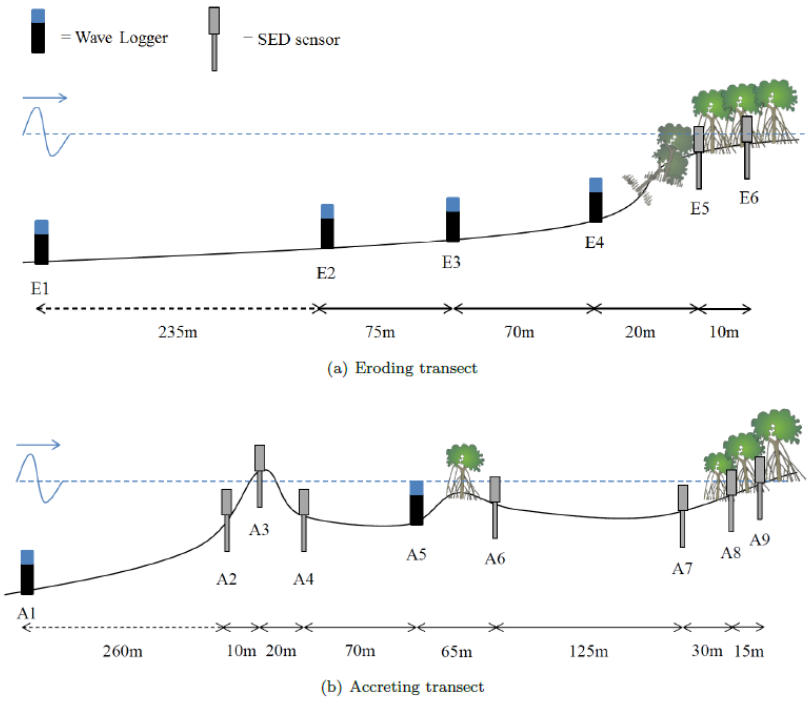

Figure B.1: Schematization of the experimental set-up during sediment measurements, note that figure is not on scale.

C

Propagule Dispersal

This appendix shows two tables with propagule characteristics, the first table consist of buoyancy and viability and the second one of the dispersal distances from the two main mangrove species at Demak

Species	Salinity	Predominant buoyancy pattern	Refloat	BP (days)	Buoyant after reported BP (%)	VP (days)	Viable after reported VP (%)	ODP (days)	Reference
Avicennia marina	F	Floater	Yes	15	ca. 80	—	—	—	Clarke et al. (2001)
Avicennia marina	S	—	No	A few days	—	240	ca. 5	ca. 7	Clarke (1993)
Avicennia marina	S	Floater	Yes	15	100	—	—	4 §	Clarke et al. (2001)
Avicennia marina	S	Sinker	No	2	5 to 10	—	—	—	Clarke & Myerscough (1991)
Avicennia marina	S	Sinker	Yes	ca. 6	ca. 40	—	—	—	Clarke & Myerscough (1991)
Avicennia marina	S (10%)	Sinker	Yes	ca. 6	ca. 35	—	—	—	Clarke & Myerscough (1991)
Avicennia marina	S (12%)	Sinker	Yes	2	ca. 45	—	—	—	Clarke & Myerscough (1991)
Rhizophora mucronata	S	—	—	87	60	—	—	—	Guppy (1906, p. 459)
Rhizophora mucronata	S (35–36 ppt)	—	—	150	ca. 1	150	ca. 1	—	Drexler (2001)

Table C.1: Buoyancy and viability characteristics of propagules from the two main mangrove species at Demak. Typically, dispersal experiments are conducted using sea water (S), fresh water (F), or river water (R). Although some studies report minimum, median and mean values for the buoyancy period (BP) and viability period (VP), we here only considered maximum values for these propagule traits. Obligate dispersal period (ODP) refers to the post-abscission period during which a propagule is yet to initiate root growth (der Stocken et al., 2019a).

Species or Ecosystem	Dispersal distance	Methodological approach	Reference
Avicennia marina	≤ 3 km; a few recoveries at 5 km, 12 km, and 24 km; max. 700 km	R	Steinke & Ward (2003)
Avicennia marina	Multiple kilometers	R	Gunn & Dennis (1973)
Avicennia marina	Close to the parent tree parent; some >20 km: max. 50 km	R	Clarke & Myerscough (1991)
Avicennia marina	Most <1 km; very few >10 km	R	Clarke (1993)
Avicennia marina	Up to 60 m	R	Breitfuss et al. (2003)
Rhizophora mucronata	<20 m; a few >50 m	R	Chan & Husin (1985)
Rhizophora mucronata	68% <300 m; max. 1210 m downstream; max. 485 m upstream	R	Komiyama et al. (1992)
Rhizophora mucronata	Max. 60 m	R	De Ryck et al. (2012)
Rhizophora mucronata	Short-distance dispersal	M	Di Nitto et al. (2013)
Rhizophora mucronata	Max. 2783 m	R	Van der Stocken et al. (2013)
Rhizophora mucronata	<50 m; max. <150 m	R	Van der Stocken et al. (2015a)

Table C.2: Dispersal distance characteristics of propagules from the two main mangrove species at Demak and methods used to obtain these values. Different methodological approaches were used to measure dispersal in mangroves, each allowing information to be obtained at different spatial scales. Typically, the applicability of release–recapture (R) experiments is restricted to the landscape scale (10^2 – 10^3 m), while phylogenetic and population genetic studies (G), and dispersal simulation models (M) allow studying dispersal and connectivity at landscape (10^2 – 10^3 m), regional (10^3 – 10^5 m), and biogeographic (10^5 – 10^7 m) spatial scales (der Stocken et al., 2019a).

D

Currents SE monsoon

This appendix shows the large-scale surface currents in the SE monsoon (Wyrtki, 1961), the modelled average current pattern and salinity pattern (3D) over a month in the SE monsoon. The modelled current pattern (Figure D.2) in the Demak area is compared to the large-scale current pattern in the Java Sea (Wyrtki, 1961), which is showed in Figure D.1. The large-scale current in the Se monsoon is from East to West, which corresponds to the alongshore current from NE to SW in our specific modelling area. When comparing the NW monsoon surface salinity of Figure 5.2 to SE monsoon salinity of Figure D.3, it seems that due to a much smaller Wulan river discharge in the SE monsoon, hardly any fresh water plume is created.

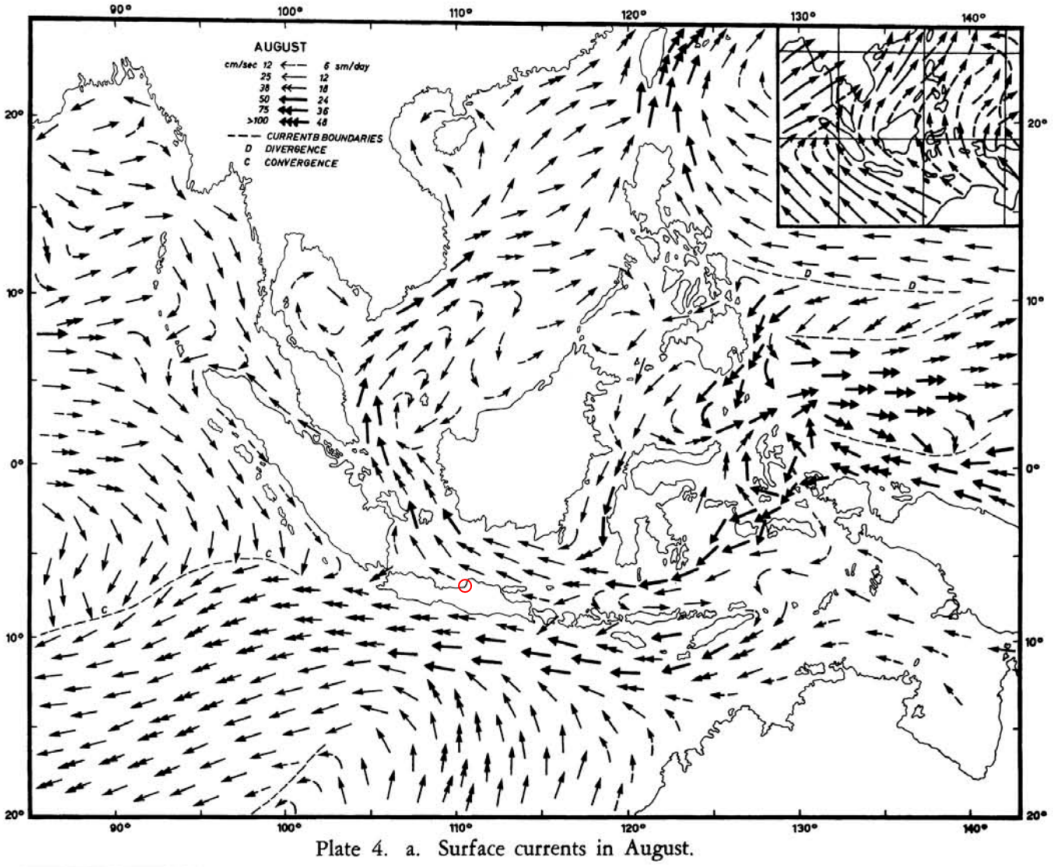

Plate 4. a. Surface currents in August.

Figure D.1: Large-scale surface currents in the SE monsoon, Demak is highlighted by a small red circle (Wyrtki, 1961).

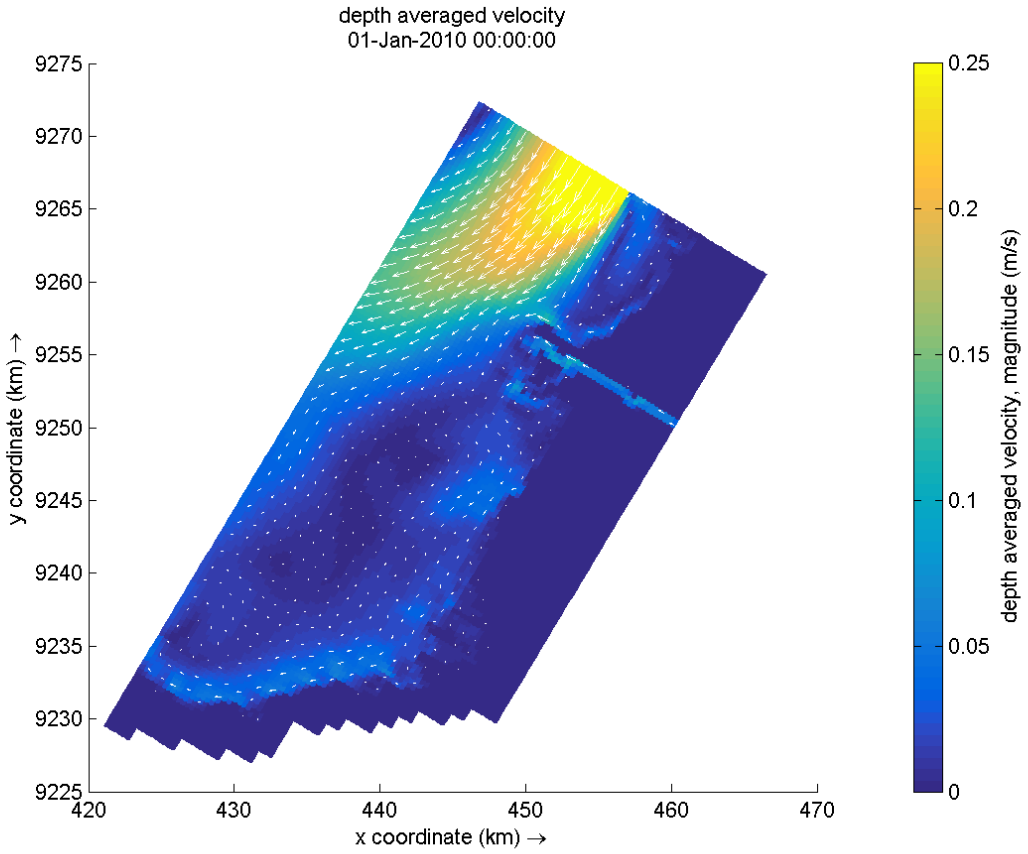

Figure D.2: Average current patterns for a month in the SE monsoon (wet season), including baroclinic forcing.

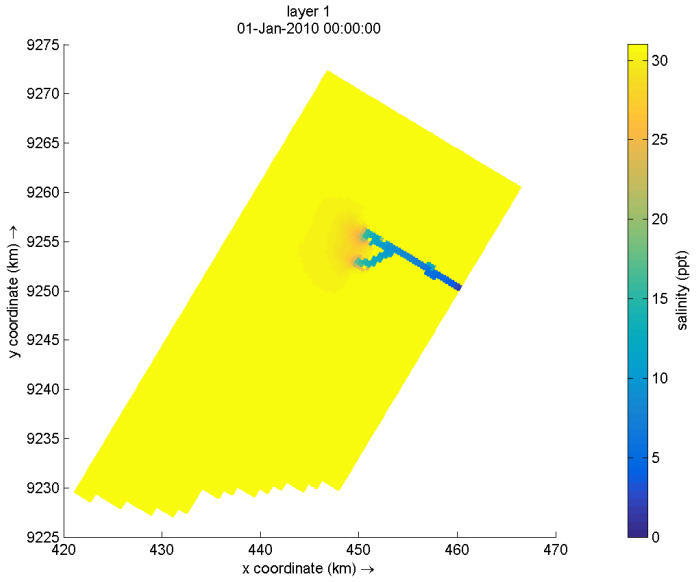

Figure D.3: Average salinity pattern for a month in the SE monsoon (wet season), including baroclinic forcing.

E

Sensitivity Analysis Propagules Release

This appendix shows the results of the sensitivity analysis of the timing of propagule release for the NW monsoon as well as the SE monsoon. Propagules are released every 2 hours of a day, such that the sensitivity of release during one entire tidal cycle is tested.

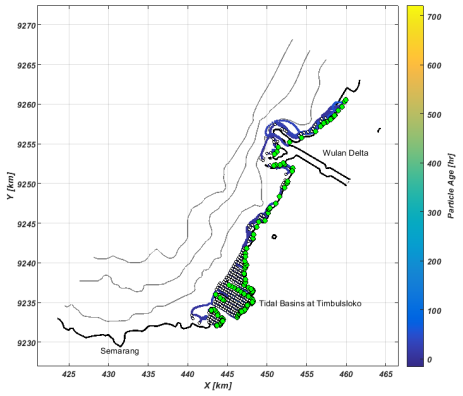

(a) NW monsoon +0 hours (simulation showed in results).

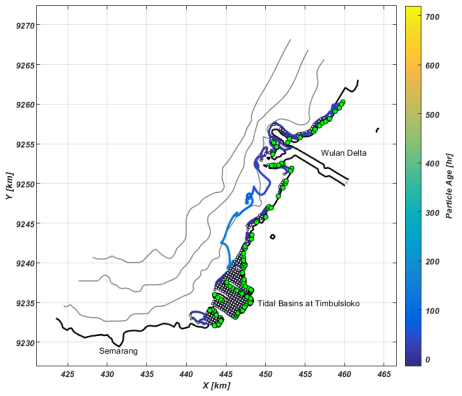

(b) NW monsoon +2 hours.

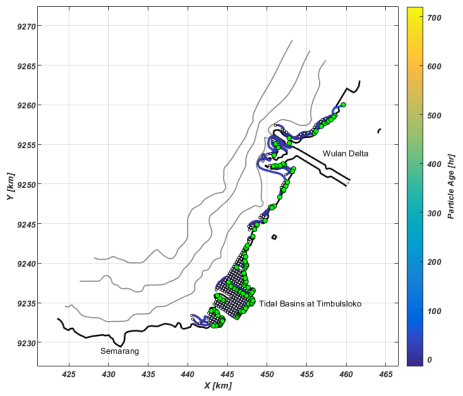

(c) NW monsoon +4 hours.

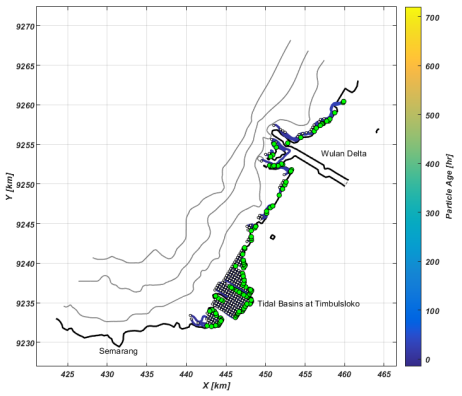

(d) NW monsoon +6 hours.

Figure E.1: Sensitivity analysis of the timing of propagule release for the NW monsoon.

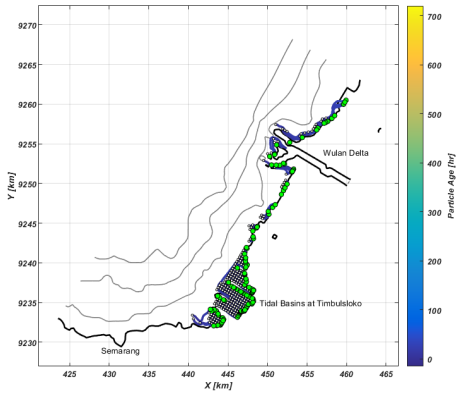

(e) NW monsoon +8 hours.

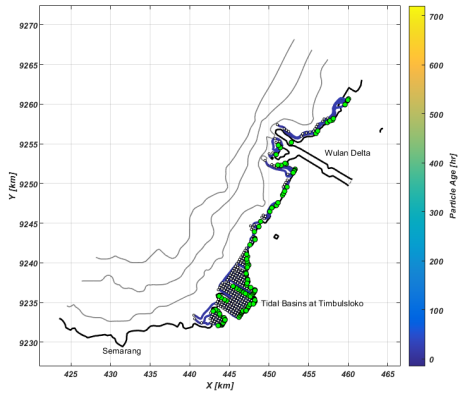

(f) NW monsoon +10 hours.

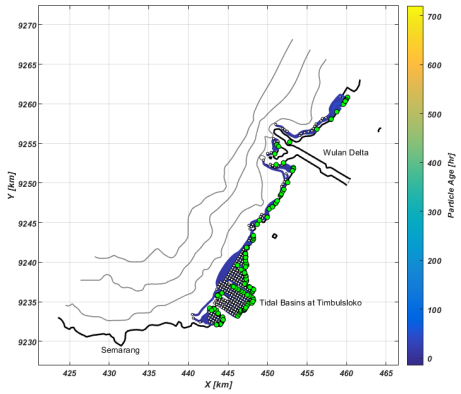

(g) NW monsoon +12 hours.

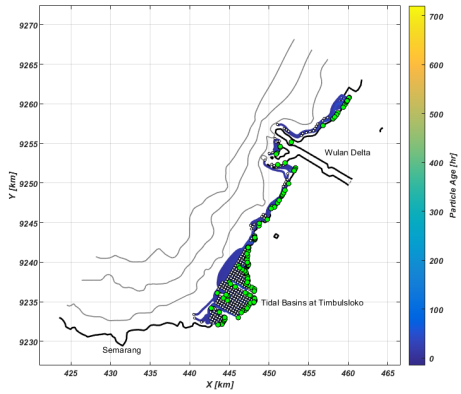

(h) NW monsoon +14 hours.

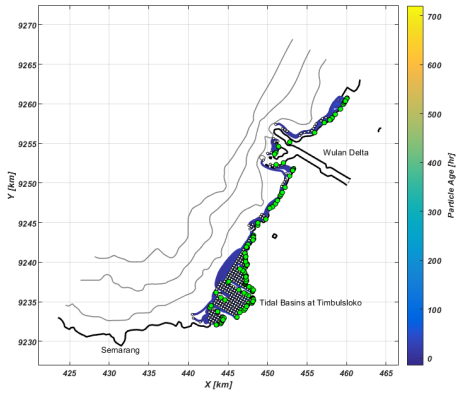

(i) NW monsoon +16 hours.

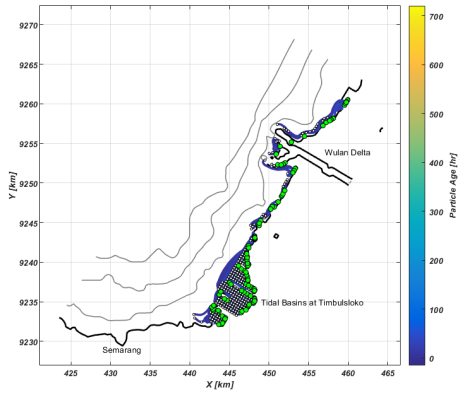

(j) NW monsoon +18 hours.

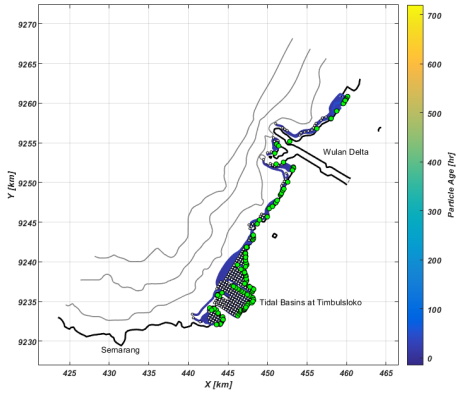

(k) NW monsoon +20 hours.

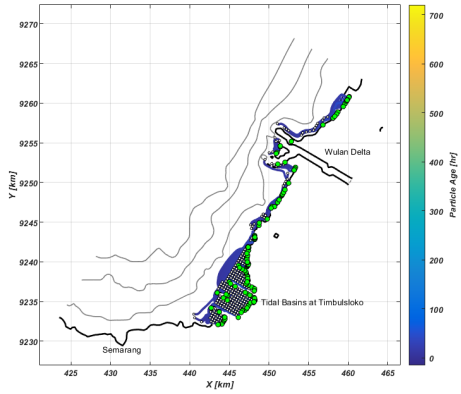

(l) NW monsoon +22 hours.

Figure E.1: Sensitivity analysis of the timing of propagule release for the NW monsoon.

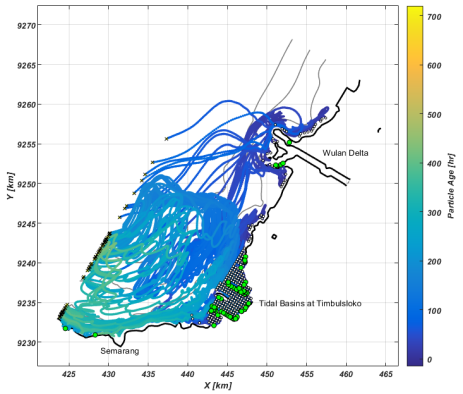

(a) SE monsoon +0 hours (simulation showed in results).

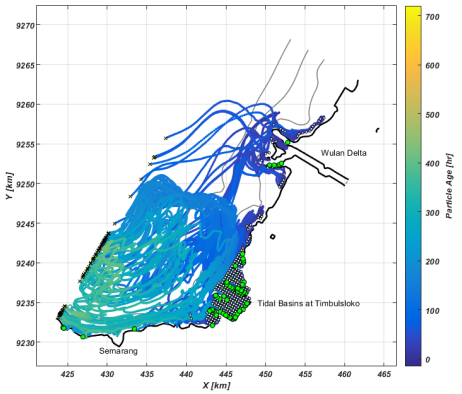

(b) SE monsoon +2 hours.

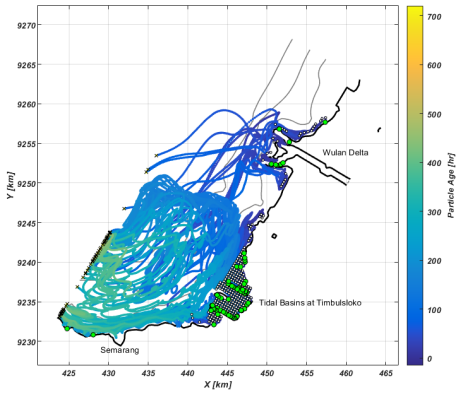

(c) SE monsoon +4 hours.

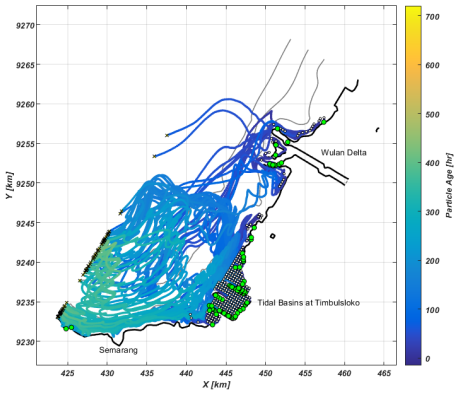

(d) SE monsoon +6 hours.

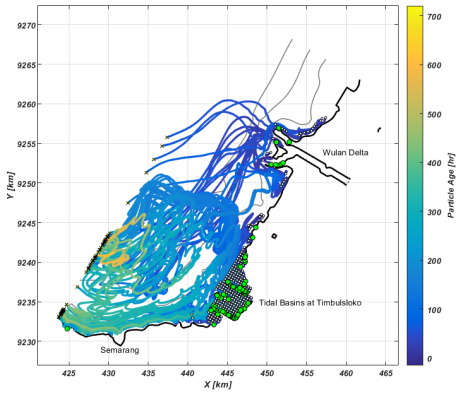

(e) SE monsoon +8 hours.

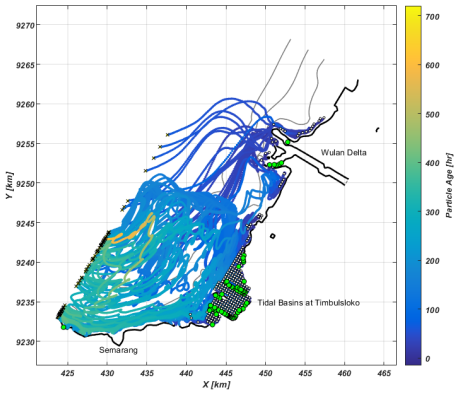

(f) SE monsoon +10 hours.

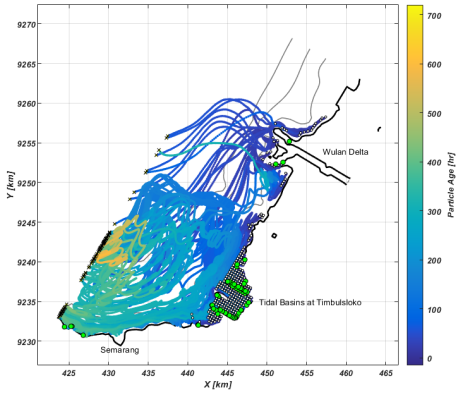

(g) SE monsoon +12 hours.

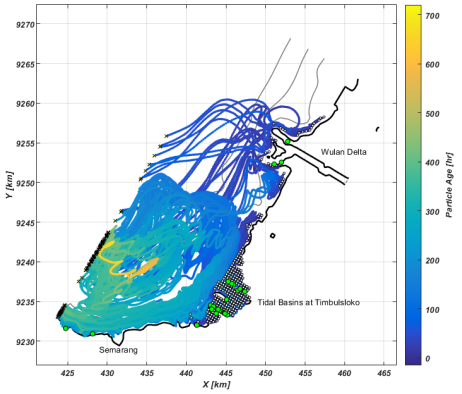

(h) SE monsoon +14 hours.

Figure E.2: Sensitivity analysis of the timing of propagule release for the SE monsoon.

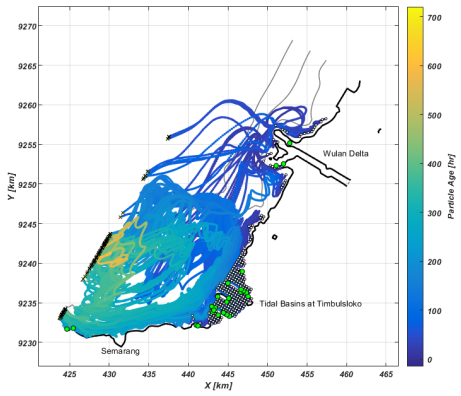

(i) SE monsoon +16 hours.

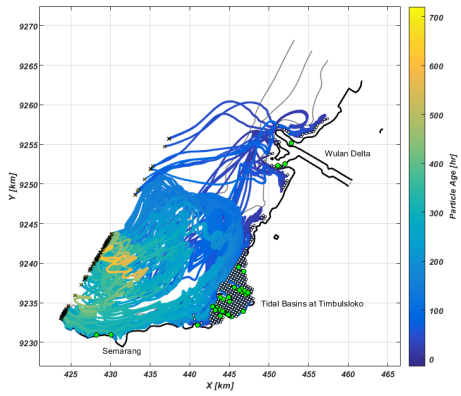

(j) SE monsoon +18 hours.

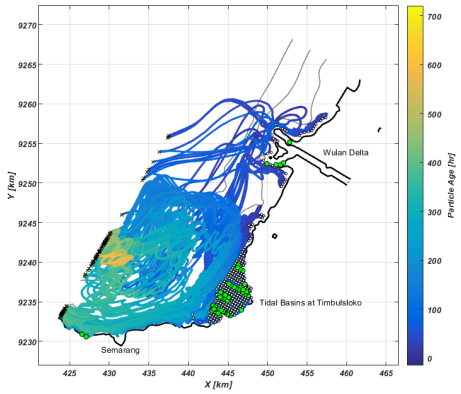

(k) SE monsoon +20 hours.

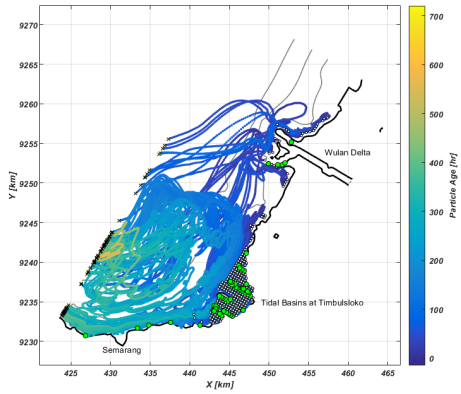

(l) SE monsoon +22 hours.

Figure E.2: Sensitivity analysis of the timing of propagule release for the SE monsoon.